ผลของอัตราส่วน Si/Al และการเติมโพแทสเซียมต่อการผลิตกรดอะคริลิคจากกรดแลคติกบนตัวเร่งปฏิกิริยาซีโอไลต์วายที่ผสมด้วยอะลูมินา

นายณัฐพงษ์ สถิตย์ภูมิ

วิทยานิพนธ์นี้เป็นส่วนหนึ่งของการศึกษาตามหลักสูตรปริญญาวิศวกรรมศาสตรมหาบัณฑิต
สาขาวิชาวิศวกรรมเคมี ภาควิชาวิศวกรรมเคมี
คณะวิศวกรรมศาสตร์ จุฬาลงกรณ์มหาวิทยาลัย
ปีการศึกษา 2559

EFFECT OF Si/Al RATIOS AND POTASSIUM ADDITION ON ACRYLIC ACID PRODUCTION FROM LACTIC ACID ON Y-ZEOLITE CATALYSTS MIXED WITH ALUMINA

Mr. Natthapong Satitpoom

A Thesis Submitted in Partial Fulfillment of the Requirements
for the Degree of Master of Engineering Program in Chemical Engineering
Department of Chemical Engineering
Faculty of Engineering
Chulalongkorn University
Academic Year 2016

Thesis Title	EFFECT OF Si/Al RATIOS AND POTASSIUM ADDITION ON ACRYLIC ACID PRODUCTION FROM LACTIC ACID ON Y-ZEOLITE CATALYSTS MIXED WITH ALUMINA
By	Mr. Natthapong Satitpoom
Field of Study	Chemical Engineering
Thesis Advisor	Assistant Professor Suphot Phatanasri, D.Eng.

Accepted by the Faculty of Engineering, Chulalongkorn University in Partial Fulfillment of the Requirements for the Master's Degree

.....Dean of the Faculty of Engineering
(Associate Professor Supot Teachavorasinskun, D.Eng.)

THESIS COMMITTEE

.....Chairman
(Associate Professor Joongjai Panpranot, Ph.D.)

.....Thesis Advisor
(Assistant Professor Suphot Phatanasri, D.Eng.)

.....Examiner
(Palang Bumroongsakulsawat, Ph.D.)

.....External Examiner
(Assistant Professor Soipatta Soisuwan, D.Eng.)

ณัฐพงษ์ สถิตย์ภูมิ : ผลของอัตราส่วน Si/Al และการเติมโพแทสเซียมต่อการผลิตกรดอะคริลิคจากกรดแลคติกบนตัวเร่งปฏิกิริยาซีโอไลต์วายที่ผสมด้วยอะลูมินา (EFFECT OF Si/Al RATIOS AND POTASSIUM ADDITION ON ACRYLIC ACID PRODUCTION FROM LACTIC ACID ON Y-ZEOLITE CATALYSTS MIXED WITH ALUMINA) อ.ที่ปรึกษาวิทยานิพนธ์หลัก: ผศ. ดร. สุพจน์ พัฒนะศรี, 94 หน้า.

ในงานวิจัยนี้ได้ทำการศึกษาผลของการเติมโพแทสเซียมในปริมาณที่แตกต่างกันลงบนซีโอไลต์Y ที่อัตราส่วน 0, 2, 4, 6 และ 8 เปอร์เซ็นต์ โดยน้ำหนัก ที่ถูกเตรียมโดยวิธีการเคลือบฝังแบบเปียก นอกจากนี้ยังศึกษาผลของอัตราส่วนซิลิกาต่ออะลูมินา (15, 100 และ 500) ของซีโอไลต์Y ที่ถูกปรับปรุงด้วยโพแทสเซียมที่อัตราส่วน 6 เปอร์เซ็นต์ โดยน้ำหนัก และยังศึกษาผลของอัตราส่วนของตัวรองรับอะลูมินาและซีโอไลต์Y ที่ถูกปรับปรุงด้วยโพแทสเซียมที่อัตราส่วน 6 เปอร์เซ็นต์ โดยน้ำหนัก ด้วยอัตราส่วนของตัวรองรับดังนี้ 3:1, 1:1 และ 1:3 ซึ่งตัวเร่งปฏิกิริยาทั้งหมดถูกทดสอบในปฏิกิริยาดีไฮเดรชันของกรดแลคติกที่อุณหภูมิ 340 องศาเซลเซียสภายใต้ความดันบรรยากาศและวิเคราะห์คุณลักษณะด้วยเทคนิคต่างๆ จากผลการทดลองพบว่าซีโอไลต์Y ที่ถูกปรับปรุงด้วยโพแทสเซียมที่อัตราส่วนแตกต่างกัน และอัตราส่วนซิลิกาต่ออะลูมินาของซีโอไลต์Y และอัตราส่วนของตัวรองรับอะลูมินาต่อซีโอไลต์Y มีผลต่อความสามารถในการเร่งปฏิกิริยาดีไฮเดรชันของกรดแลคติก ในบรรดาตัวเร่งปฏิกิริยาทั้งหมด ซีโอไลต์Y ที่มีอัตราส่วนซิลิกาต่ออะลูมินาเท่ากับ 100 และถูกปรับปรุงด้วยโพแทสเซียมที่อัตราส่วน 6 เปอร์เซ็นต์ โดยน้ำหนัก แสดงประสิทธิภาพการเร่งปฏิกิริยาดีไฮเดรชันของกรดแลคติกได้ดีที่สุด คือ 100 เปอร์เซ็นต์การเปลี่ยนแปลงกรดแลคติกและ 45.5 เปอร์เซ็นต์การเลือกเกิดกรดอะคริลิคและจะมีเปอร์เซ็นต์การเลือกเกิดอะซิทัลดีไฮด์ที่ต่ำที่สุดเพราะว่าตัวเร่งปฏิกิริยานี้มีปริมาณความเป็นกรดและความเป็นเบสที่เหมาะสมในการเกิดปฏิกิริยา อย่างไรก็ตามตัวเร่งปฏิกิริยาที่มีปริมาณอะลูมินาที่สูงจะมีแนวโน้มให้เกิดการทำลายต่อโครงสร้างผลึกของตัวเร่งปฏิกิริยาและทำให้มีปริมาณกรดแก่มาก ซึ่งทำให้มีความสามารถในการเร่งปฏิกิริยาต่ำ และจากผลการทดลองแสดงให้เห็นว่าการเติมโพแทสเซียมช่วยปรับปรุงการเลือกเกิดกรดอะคริลิคและช่วยลดการเลือกเกิดอะซิทัลดีไฮด์

ภาควิชา วิศวกรรมเคมี ลายมือชื่อนิสิต .....

สาขาวิชา วิศวกรรมเคมี ลายมือชื่อ อ.ที่ปรึกษาหลัก .....

ปีการศึกษา 2559

5770167721 : MAJOR CHEMICAL ENGINEERING
KEYWORDS: LACTIC ACID DEHYDRATION / HY ZEOLITE CATALYST / AL2O3-HY ZEOLITE CATALYST / SI/AL MOLAR RATIO / POTASSIUM

NATTHAPONG SATITPOOM: EFFECT OF Si/Al RATIOS AND POTASSIUM ADDITION ON ACRYLIC ACID PRODUCTION FROM LACTIC ACID ON Y-ZEOLITE CATALYSTS MIXED WITH ALUMINA. ADVISOR: ASST. PROF. SUPHOT PHATANASRI, D.Eng., 94 pp.

In this research, the effect of different potassium loading over HY100 zeolite catalysts at 0, 2, 4, 6 and 8 wt.% prepared by incipient wetness impregnation method was studied. In addition, the effect of Si/Al molar ratios (15, 100 and 500) of HY zeolite modified with potassium at 6 wt.% was also investigated. Furthermore, the effect of support ratios of Al_2O_3 and HY zeolite modified with potassium 6 wt.% was studied as follows: 3:1, 1:1 and 1:3. All catalysts were tested in lactic acid dehydration reaction at 340 °C of reaction temperature under atmospheric pressure and characterized by various techniques. From the results, it was found that HY zeolite modified with different potassium loading, Si/Al molar ratios of HY zeolite and support ratios of Al_2O_3 and HY zeolite affected the catalytic activity in lactic acid dehydration reaction, evidenced by characterization results. Among all the catalysts, the HY zeolite with Si/Al molar ratios of 100 and modified with potassium at 6 wt.% represented the best catalyst for lactic acid dehydration with 100% conversion and 45.5% selectivity for acrylic acid as well as the lowest acetaldehyde selectivity due to the suitability of total acidity and basicity of the catalyst. However, the catalyst with too high Al_2O_3 content caused the structural collapse, high strong acid sites and high coke deposition resulting in the lowest catalytic performance. The catalytic results indicated that potassium modification of HY zeolite could improve acrylic acid selectivity and reduce acetaldehyde selectivity.

Department: Chemical Engineering Student's Signature .....
Field of Study: Chemical Engineering Advisor's Signature .....
Academic Year: 2016

ACKNOWLEDGEMENTS

The first, I would like to express my gratefulness and appreciation to my adviser, Assistant Professor Dr. Suphot Phatanasri for his best suggestion, useful discussion and knowledge for this research. This thesis would not have been completed without all the support and guidance that the author have always received from his. I would also like to thank Associate Professor Dr. Joongjai Panpranot, as the chairman of committee of this thesis, Dr. Palang Bumroongsakulsawat and Assistance Professor Dr. Soipatta Soisuwan, as member of committee of this thesis.

Most of all, I would like to thank my parents for support and suggestion all the time and to all my friends in Center of Excellence on Catalysis and Catalytic Reaction Engineering for their useful help, advice and suggestion.

Lastly, many thanks are given to Thailand Research Fund and Chulalongkorn University for financial support to this work.

CONTENTS

Page

Page

Page

Page

TABLE CONTENTS

FIGURE CONTENTS

Page

CHAPTER I
INTRODUCTION

1.1 General introduction

Acrylic acid (AA) and its esters are produced from petrochemical industry by two-step gas phase partial oxidation of propylene [1] and acrylic acid (AA) and its esters are widely used in the manufacture of adhesives, paint additives, textile, leather treating agents, raw materials for polymers, drugs and other products [2, 3]. Recently, the partial oxidation of propane to AA through a one-step process has been more attention [4-7]. Despite that multicomponent metal oxides are catalytically active for one-step process but metal oxides are sensitive to preparation and not efficient enough for practical application. In addition, both propylene and propane are produced from non-sustainable sources in the petrochemical industry. With the ever rising demand for petroleum, it has been costly to use propylene as feedstock. As a sustainable, alternative route, acrylic acid (AA) can be synthesized by dehydration of lactic acid (LA), which is one of the mass fermentation products. However, the dehydration of LA to produce AA is also accompanied by other competing reactions such as condensation, decarboxylation and reduction, are showed in Figure 1.1 [8].

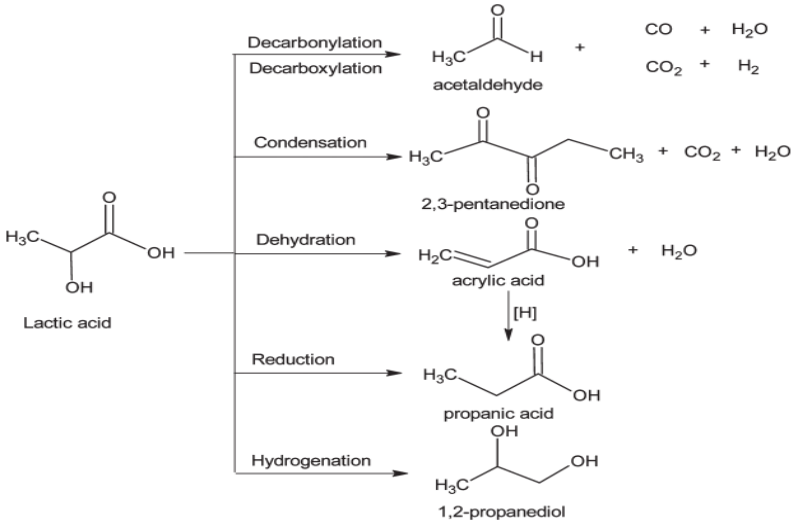

Figure 1.1 Reaction pathways for LA conversion [8].

The decarboxylation of LA to acetaldehyde (AD) is one of the key side reactions and should take main responsibility for the low selectivity for AA. The selective conversion of LA to AA in the gas phase requires the usage of suitable catalyst by means of which the side reactions can be inhibited kinetically.

Typical inorganic salt catalysts have been the focus of research into the conversion of LA such as phosphates, silicates, carbonates, nitrates and sulfates [9-11]. However, the research and development of suitable catalysts for the industrials of AA production by the dehydration of LA is still important. However, zeolites are a solid acid/base properties, can be used as catalysts for biorenewable molecular transformation such as dehydration, hydronenolysis and hydrogenoration [12-14]. Recently, NaY zeolites based catalysts with unique acid/base characteristics and widely used in industrial processes have been investigated and used in the dehydration of LA to AA [15, 16]. It have been found that modification by alkaline or rare earth metal to NaY zeolites could improve catalytic performance, especially the selectivity to acrylic acid. Generally, dehydration over zeolites has always been considered to be a process catalyzed by acidic sites, which could be modified by surface cations. Alumina (Al_2O_3) widely used in the dehydration process. This beneficial effect is ascribed to the dilution of the strong acid sites of zeolite in the alumina matrix [17].

In this research, we focused on the effect of different potassium loading over HY zeolite catalysts were prepared by incipient wetness impregnation method and the HY zeolites with different Si/Al ratios and the effect of Al_2O_3 and HY zeolite ratios were prepared by sol-gel method and the modification of HY zeolite and Al_2O_3-HY zeolite catalysts by potassium. The catalysts have been characterized by various techniques, and the catalytic performance for the dehydration of lactic acid to acrylic acid were investigated.

1.2 Research objectives

1.2.1 To study the effect of different potassium loading over HY zeolite catalysts to compare with unmodified on the catalytic performances and acidity/basicity for lactic acid dehydration.

1.2.2 To study the effects of Si/Al molar ratio on acidity/basicity and catalytic performances of HY zeolite catalysts for lactic acid dehydration.

1.2.3 To investigate the effect of Al_2O_3 and HY zeolite ratios on catalytic performance for lactic acid dehydration.

1.3 Research scopes

1.3.1 Preparation of HY zeolite catalysts modified with different potassium loading at 0, 2, 4, 6 and 8 wt.% by incipient wetness impregnation method.

1.3.2 Preparation of HY zeolites catalysts with different Si/Al ratio (15, 100 and 500) and modified with potassium at the best percent loading from the 1.3.1.

1.3.2 Preparation of Al_2O_3-HY zeolite with ratios of 3:1, 1:1, and 1:3 by sol-gel method and modified with potassium at the best percent loading from the 1.3.1.

1.3.3 Characterization of Al_2O_3, HY zeolite and Al_2O_3-HY zeolite catalysts modified with potassium by using various techniques:

- Nitrogen physisorption to determine BET surface area, pore size and pore volume.
- X-ray diffractometry (XRD) to determine crystallite phase.
- Ammonia temperature program desorption (NH_3-TPD) to determine acidity of catalysts.
- Carbon dioxide temperature program desorption (CO_2-TPD) to determine basicity of catalysts.
- Scanning Electron Microscopy (SEM-EDX) to study morphology of catalysts.
- Thermogravimetric analysis (TGA) to study carbon deposition on spent catalyst.

1.3.4 Investigation the catalytic performances of HY zeolite modified with different potassium loading and HY zeolites catalysts with different Si/Al ratio and Al_2O_3-HY zeolite ratios modified with potassium for lactic acid dehydration reaction under temperature 340 °C and atmospheric pressure. The products were analyzed by GC equipped with a DB-WAX UL column and FID detector.

1.4 Research methodology

1.4.1 Part I: Investigate the effect HY zeolite catalysts modified with different potassium loading at 0, 2, 4, 6 and 8 wt.% by incipient wetness impregnation method.

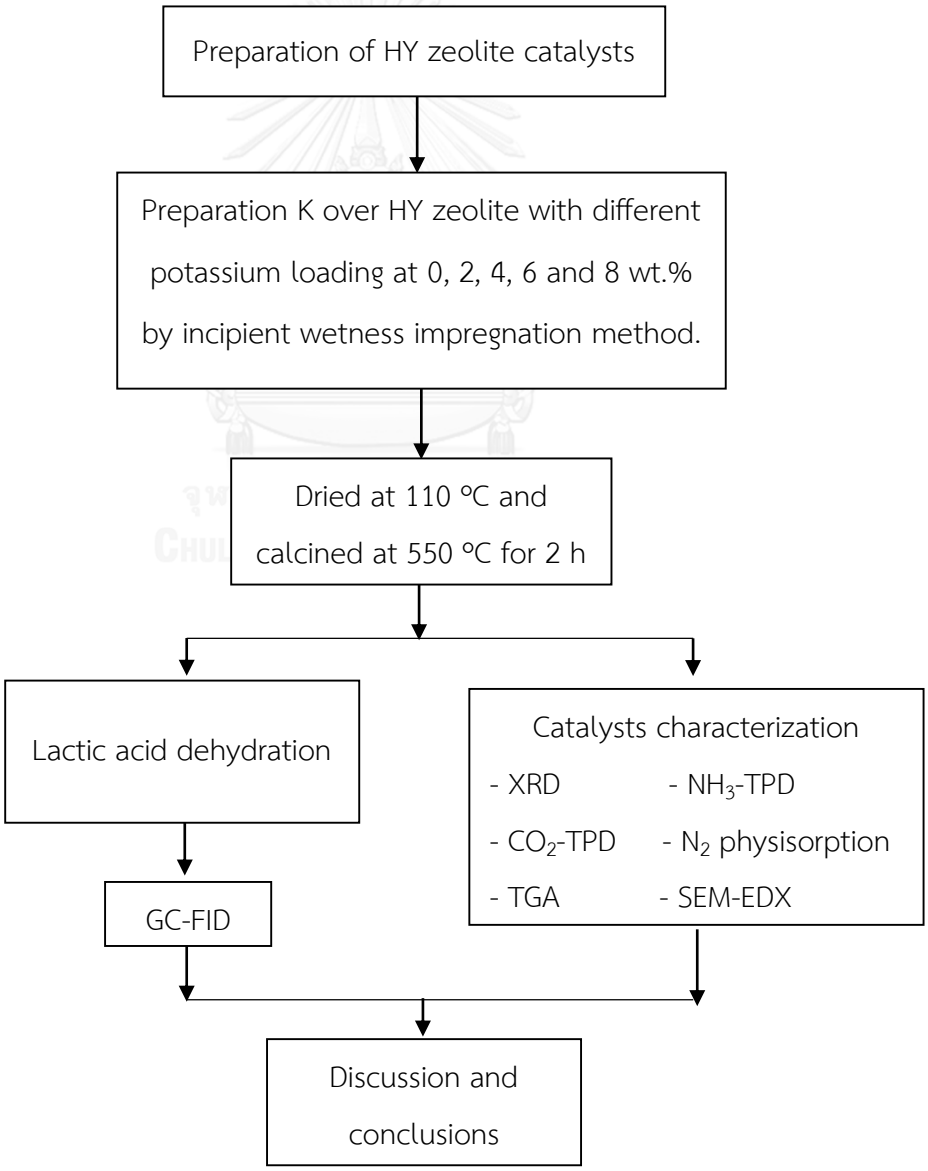

1.4.2 <u>Part II</u>: Comparative HY zeolite catalysts with different Si/Al molar ratio of 15, 100, and 500 and modified with potassium.

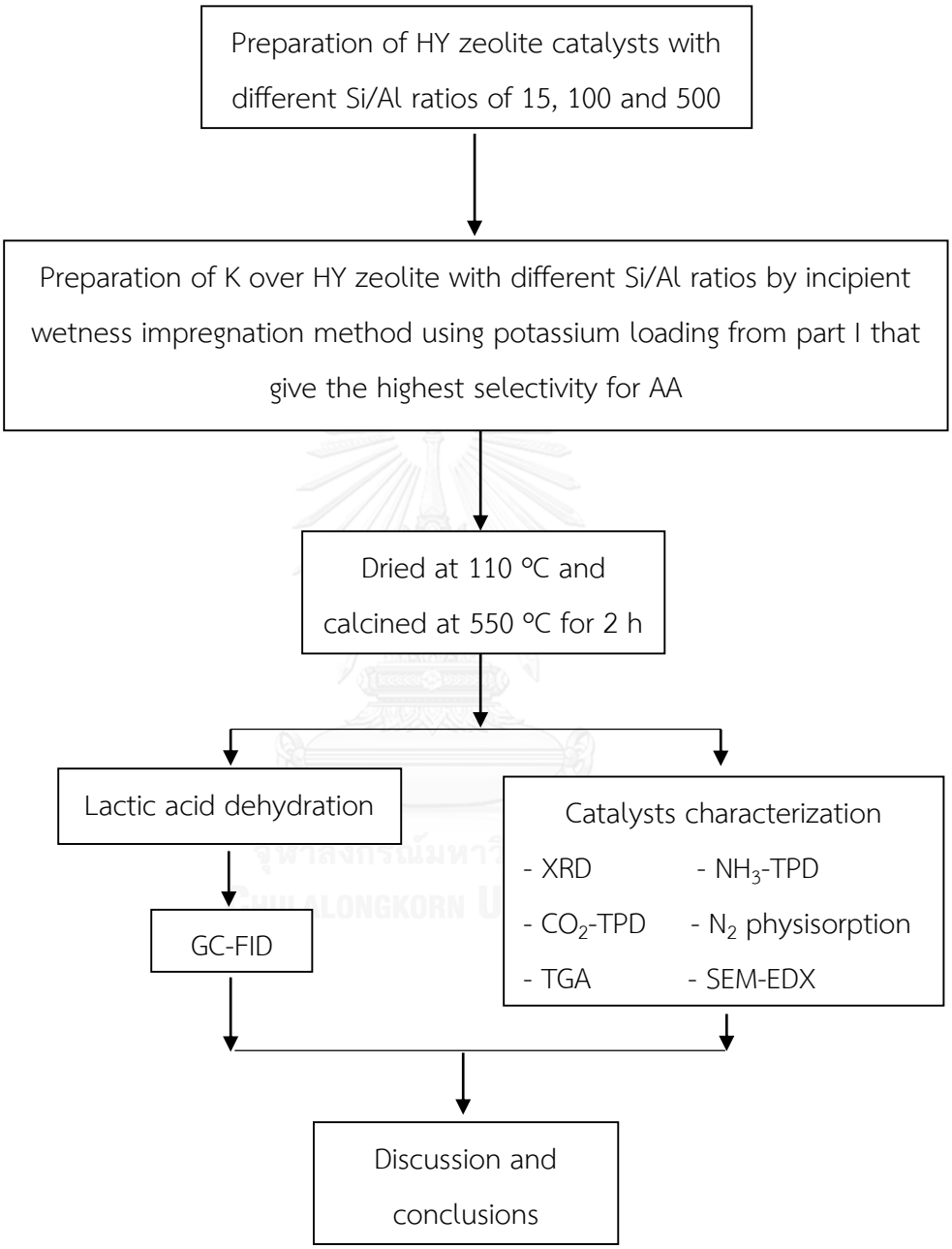

1.4.3 <u>Part III</u>: Investigate the effect of Al_2O_3-HY zeolite with ratios of 3:1, 1:1, and 1:3 by sol-gel method and modified with potassium.

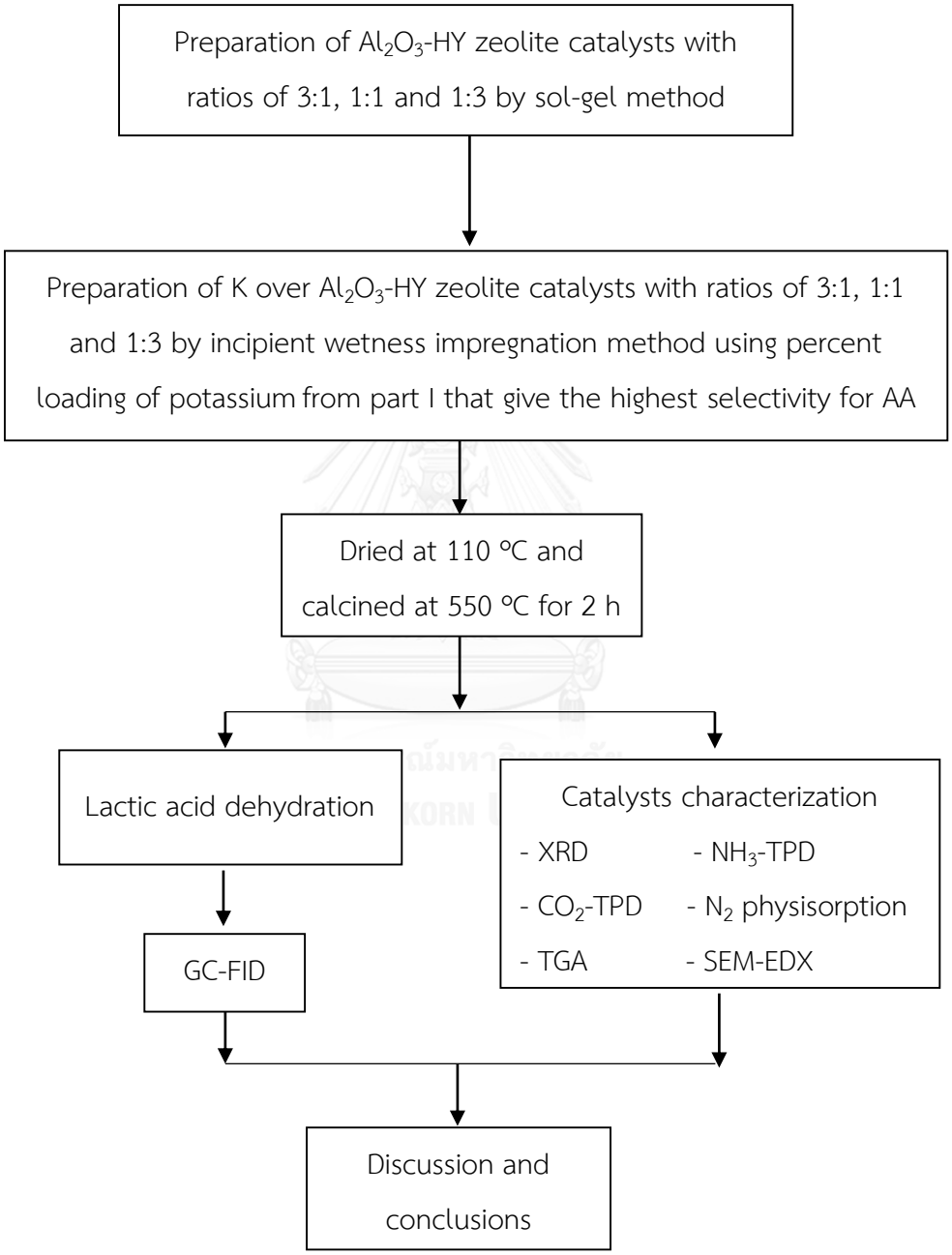

CHAPTER II
THEORY AND LITERATURE REVIEWS

2.1 Theoretical

2.1.1 Acrylic acid production

Acrylic acid (AA), an important monomer of synthetic resin, is a versatile compound for organic synthesis. It has been widely used to fabricate a variety of functional materials such as water absorbent polymer, adhesives and textile-treatment agents [18]. Acrylic acid is typically produced through a two-stage propylene-based oxidation process using acrolein as a fast-acting intermediate. The first step is the oxidation of propylene to acrolein and the second step is itself oxidized to acrylic acid, as depicted below in Eq.1 and Eq.2 [19].

$$H_2C{=}CHCH_3 + O_2 \longrightarrow H_2C{=}CHCHO + H_2O \quad ; \Delta H = -340 \text{ kJ/mol} \quad \text{.....(Eq.1)}$$

$$H_2C{=}CHCHO + 0.5O_2 \longrightarrow H_2C{=}CHCOOH \quad ; \Delta H = -254.1 \text{ kJ/mol} \quad \text{.....(Eq.2)}$$

However, due to the high demands for fossil fuel and the relative low reserves of oil, the prices of propylene and its downstream products go up dramatically, leading to increasing pressure to the production line of AA from propylene. What is more, it is challenging to solve the issues of groundwater pollution and air pollution caused by extraction. In 1958, Holmen first demonstrated that AA could be synthesized by the dehydration of lactic acid in Eq.3. They are using a mixture of sodium sulfate and calcium sulfate as catalysts. Therefore, dehydration of LA provides a promising and environmentally friendly route to produce AA product [20].

$$CH_3CHOHCOOH \xrightarrow{\text{Dehydration}} H_2C{=}CHCOOH + H_2O \quad \text{.....(Eq.3)}$$

2.1.2 Lactic acid dehydration

With both hydroxyl and carboxylic acid functions, lactic acid offers novel routes to a variety of commodity chemicals (Fig. 2.1) through the reactions of dehydration, dehydrogenation, condensation, reduction, decarbonylation, esterification and polymerization [21].

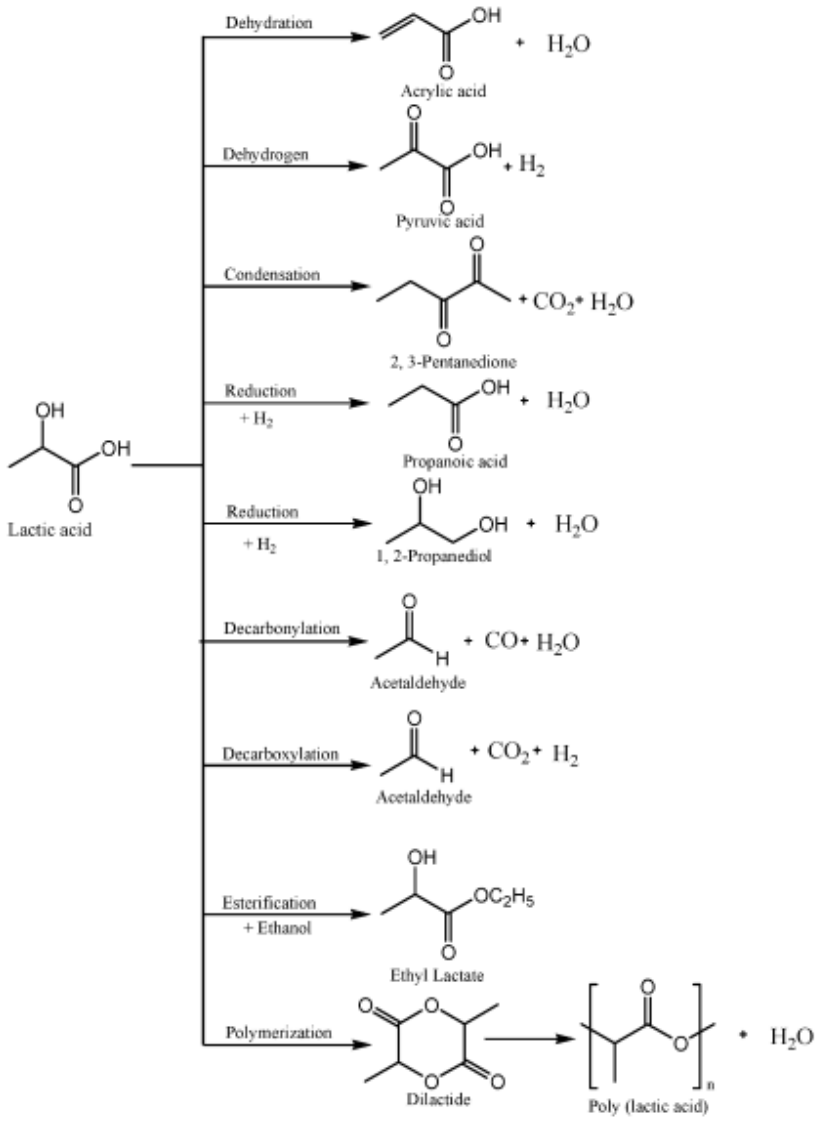

Figure 2.1 Lactic acid conversion pathways [21].

- **Lactic acid conversion to acrylic acid**

The first intramolecular reaction mechanism they considered involved an internal attack on a ß-hydrogen by a basic group, together with the loss of the **α**-OH group via an E2 elimination mechanism (Fig. 2.2). During the elimination, the carboxyl proton may be transferred to the departing hydroxyl, thereby making it a better leaving group [22].

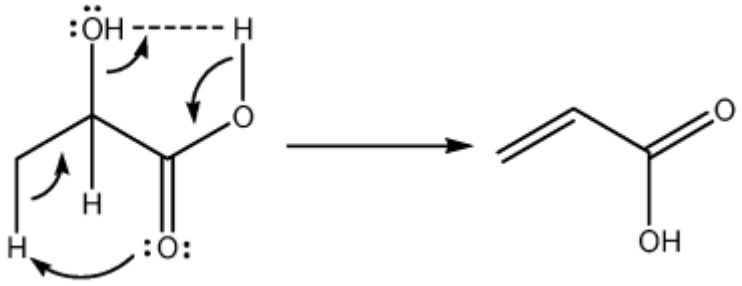

Figure 2.2 Elimination mechanism for dehydration of lactic acid in supercritical water [22].

- **Lactic acid conversion to pyruvic acid**

This method requires two additional processes besides the oxidative dehydrogenation process, that is, esterification of lactic acid and hydrolysis of produced alkyl pyruvate. It is naturally favorable to produce pyruvic acid by an oxidative dehydrogenation process only, are showed in Eq.4. However, it still seemed to be difficult to obtain pyruvic acid directly from lactic acid, because the major part of lactic acid is converted to form acetaldehyde and CO_2 by the oxidative C-C bond fission rather than to form pyruvic acid by oxidative dehydrogenation over $V_2O_5^-$ or MoO_3^- based mixed oxide catalysts, are showed in Eq.5 [23].

$$CH_3\text{-}CH(OH)\text{-}COOH + 0.5O_2 \longrightarrow CH_3\text{-}CO\text{-}COOH + H_2O \quad .....(Eq.4)$$

$$CH_3\text{-}CH(OH)\text{-}COOH + 0.5O_2 \longrightarrow CH_3\text{-}CHO + CO_2 + H_2O \quad .....(Eq.5)$$

- **Lactic acid conversion to 2,3-Pentanedione**

The discovery of this pathway came about because the reactions were conducted at higher pressure (0.5 MPa) and lower temperatures (280–320 °C). The possibility was tested that pentanedione might arise via a condensation between these fragments, with loss of water because propanoic acid and acetaldehyde are both products of lactic acid conversion (Fig. 2.3). Alternatively, pentanedione might be the primary product, which gives rise to the two low-molecular-weight species via hydrolytic fragmentation [24].

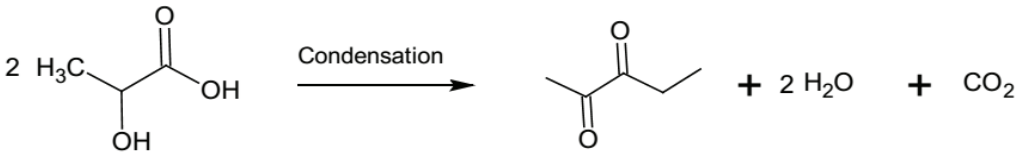

Figure 2.3 Condensation reaction of lactic acid to 2,3-pentanedione [24].

- **Lactic acid conversion to propanoic acid**

The reduction of the lactic acid with hydrogen provides the propionic acid. The propanoic acid may also be formed by hydrogenation of acrylic acid. The decarboxylation of lactic acid to acetaldehyde induces the formation of hydrogen which the hydrogen can turn to react with the lactic acid and / or acrylic acid to produce propanoic acid (Fig. 2.4) [25].

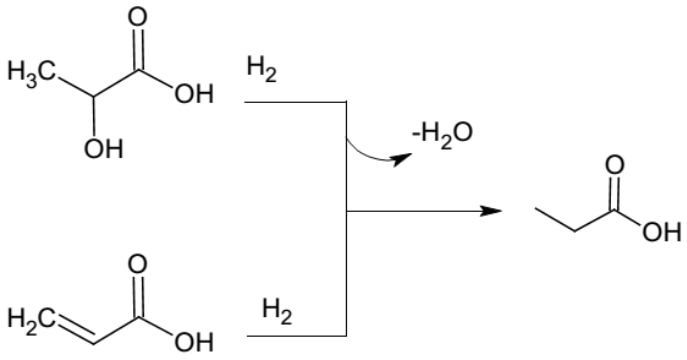

Figure 2.4 Hydrogenation reaction of LA and acrylic acid to propanoic acid [25].

- **Lactic acid conversion to 1,2-Propanediol**

The proposed direct hydrogenation of lactic acid would provide an alternative green process for the production of 1, 2-propanediol from feedstocks, not from oil. The production of 1,2-propanediol from lactic acid required hydrogenation of the carboxyl group to an alcohol without removal of the α-hydroxyl group, while reduction of the α-hydroxyl group resulted in the formation of propionic acid (Fig. 2.5). The first propanediol formation from lactate was described in the 1930s and 1940s, in which converted pure ethyl lactate to propanediol over Raney Ni with yield of exceeding 80% at very high pressures (> 25 MPa) [26].

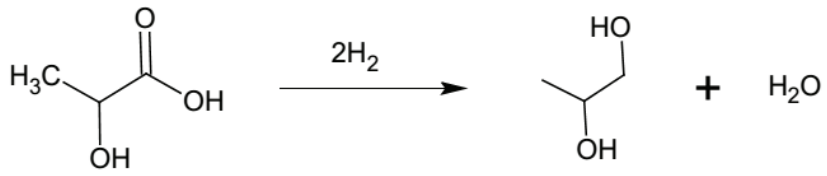

Figure 2.5 Hydrogenation reaction of lactic acid to 1,2-Propanediol [26].

- **Lactic acid conversion to acetaldehyde**

Lactic acid can be converted into acetaldehyde via two mechanisms of the decarboxylation (1) and the decarbonylation (2) to present below (Fig. 2.6) [27].

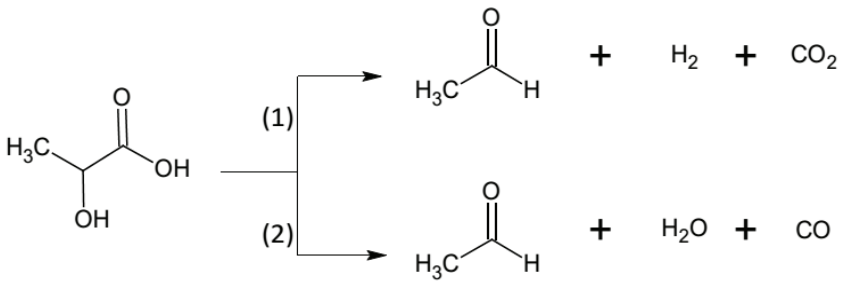

Figure 2.6 decarboxylation (1) and the decarbonylation (2) of lactic acid to acetaldehyde [27].

The formation of acetaldehyde is the main reaction in competition with the dehydration. It is done on acid sites [27]. Gunter et al. showed by a test on silica-alumina as the main lactic acid decomposition product is acetaldehyde but the addition of phosphate salts inhibit very strongly the reaction [9]. Therefore, as it was reported by Sawicki et al. and Mok et al., the decarbonylation reaction can be avoided on less acidic catalysts [22].

- **Lactic acid conversion to Poly (Lactic Acid)**

Polymerization of lactic acid to high molecular weight PLA can be achieved in two ways (Fig. 2.7). First (i), direct condensation which involves solvents under high vacuum and temperatures for the removal of water produced in the condensation. Secondly (ii), formation of the cyclic dimer intermediate (lactide) which is solvent free. It is produced and purified by distillation. Catalytic ring-opening polymerization of the lactide intermediate results in PLA with controlled molecular weight [28, 29]. By controlling residence time and temperatures in combination with catalyst type and concentration.

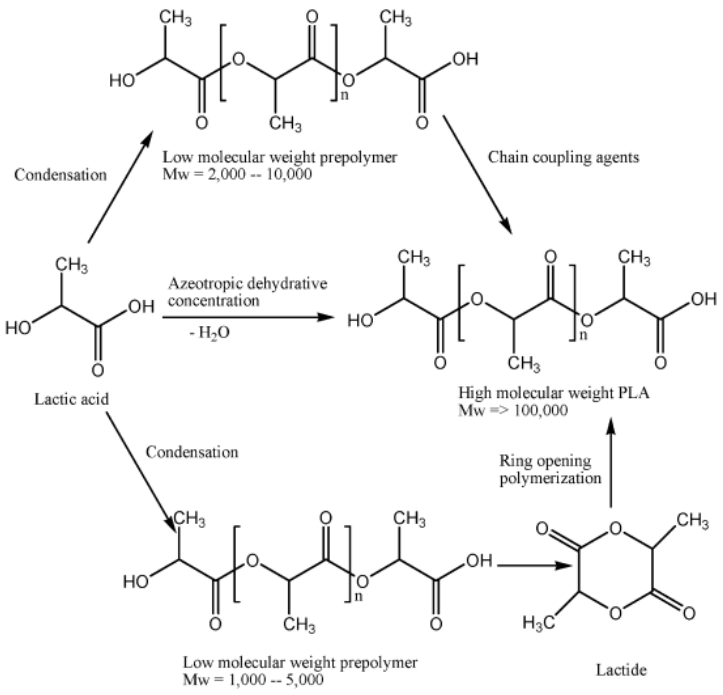

Figure 2.7 Synthesis of polylactic acid [28, 29]

2.1.3 Alumina catalyst (Al_2O_3)

Alumina or aluminum oxide is a chemical compound of aluminium (Al) and oxygen (O) with the chemical formula Al_2O_3. It is the most commonly occurring of several aluminum oxides and specifically identified as aluminium (III) oxide. It is commonly called alumina and may also be called aloxide, aloxite, or alundum depending on particular forms or applications.

The structure of Aluminum Oxide has two types of sites, hexagonal and octahedral in which it holds the atoms. Hexagonal sites are the corner atoms in the cell while the octahedral sites are present between two layers of vertical stacking. Aluminum cations are in 2/3 of the octahedral sites, and oxygen anions are in 1/3 of the octahedral sites. Each oxygen is shared between four octahedra. The oxygen presence in octahedral sites permits strong bonding and, therefore, gives rise to the characteristics of the properties of alumina [30].

The crystal structures, physical and chemical properties of alumna depend on preparation, purity, dehydration and thermal treatment history. From different crystalline structure, there are many forms of Al_2O_3 such as beta phase (γ-Al_2O_3), gamma phase (γ-Al_2O_3), alpha phase (α-Al_2O_3), theta phase (Θ-Al_2O_3), kappa phase (κ-Al_2O_3), chi phase (χ-Al_2O_3), eta phase (η-Al_2O_3) and delta phase (δ-Al_2O_3) [31]. Alumina phases, present as a function of temperature, are illustrated in Fig. 2.8, and the structure and properties of alumina at different calcination temperature are listed in Table 2.1 [31].

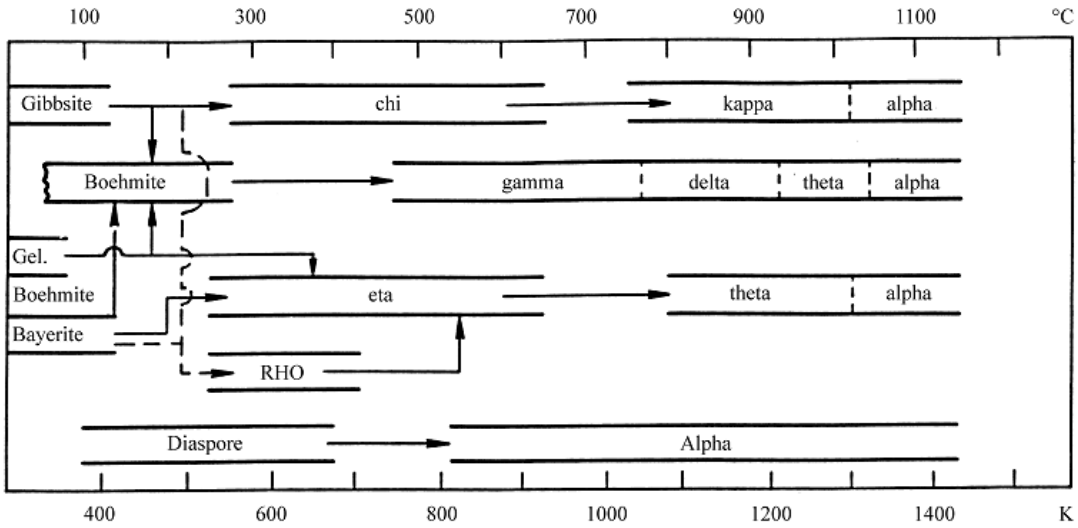

Figure 2.8 The structure transformation of alumina and aluminum hydroxides [31].

Table 2.1 Physical and structural characteristic of common aluminum oxides.

Calcination temperature (°C)	Alumina phase	Surface area (m^2/g)	Pore volume (cm^3/g)	Pore diameter (nm)
250	pseudoboehmite	390	0.50	5.2
450	γ-alumina	335	0.53	6.4
650	γ-alumina	226	0.55	9.8
850	γ-alumina	167	0.58	14
950	δ-alumina	120	0.50	16.6
1050	θ-alumina	50	0.50	28
1200	α-alumina	1-5	-	-

2.1.4 Y-Zeolite

Zeolites are microporous, aluminosilicate minerals commonly used as commercial adsorbents and catalysts. About 40 natural zeolites have been identified during the past 200 years; the most common are analcime, chabazite, clinoptilolite, erionite, ferrierite, heulandite, laumontite, mordenite, and phillipsite. More than 150 zeolites have been synthesized; the most common are zeolites A, X, Y, and ZMS-5. Natural and synthetic zeolites are used commercially because of their unique adsorption, ion-exchange, molecular sieve, and catalytic properties [32].

Y-Zeolite (Faujasite) is a mineral group in the zeolite family of silicate minerals. The group consists of faujasite-Na, faujasite-Mg and faujasite-Ca. They all share the same basic formula: $(Na_2,Ca,Mg)_{3.5}[Al_7Si_{17}O_{48}]\cdot 32(H_2O)$ by varying the amounts of sodium (Na), magnesium (Mg) and calcium (Ca). The faujasite framework consists of sodalite cages which are connected through hexagonal prisms. The pores are arranged perpendicular to each other. The pore, which is formed by a 12-membered ring, has a relatively large diameter of 7.4 Å. The inner cavity has a diameter of 12 Å and is surrounded by 10 sodalite cages. The unit cell is cubic which having lattice constant 24.7 Å [33].

Zeolites are solid acids effective for the catalytic dehydration of alcohols and hydroxy-carboxylate acids/esters [34]. It is believed that due to enrichment of reactant in the channels of zeolites, there is enhancement of reactivity. The FAU topology and supercage structure of Y zeolite are beneficial for molecule accessibility and diffusion, showing high selectivity to small molecule product [35].

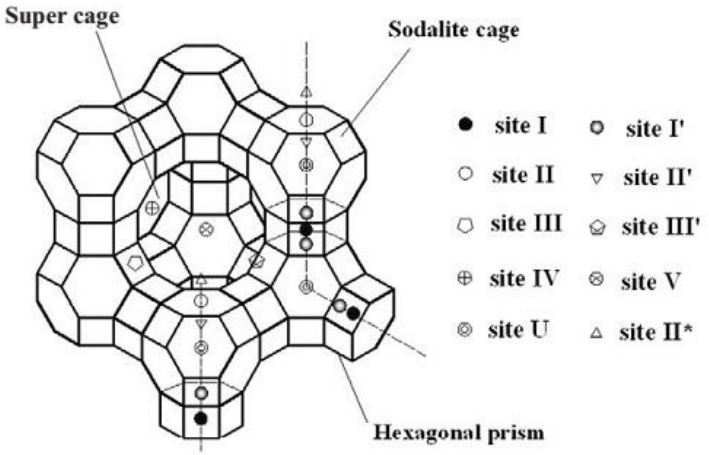

Figure 2.9 The different cation sites in the faujasite structure [36].

The diffusion efficiency of the reactants in the conversion of LA to AA is also an important factor that affects the reaction in addition to the characteristics of the surface cation clusters mentioned above. The diffusion resistance for LA and AA depends on the channel size (super cage < sodalite cage < hexagonal prism) and the location of the cations over the zeolites. A diagram of the different cation sites in the faujasite structure is shown in Fig. 2.9 [36].

2.1.5 Potassium (K)

Neutral potassium atoms have 19 electrons, one more than the extremely stable configuration of the noble gas argon. Because of this and its low first ionization energy of 418.8 kJ/mol, the potassium atom is much more likely to lose the last electron and acquire a positive charge than to gain one and acquire a negative charge (though negatively charged alkalide K^- ions are not impossible) [37].

Peng Sun et al. [38] introduced various potassium salts into NaY zeolites to study the effect of counteranions on the catalytic performance of NaY zeolites.

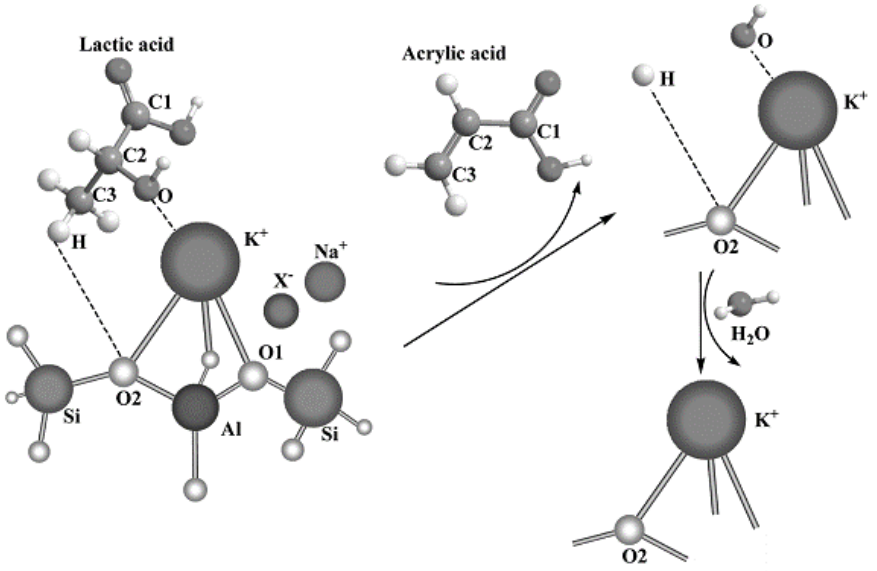

Figure 2.10 Mechanism proposed for dehydration of lactic acid to acrylic acid over the KX-modified NaY zeolites [38].

As illustrated in Fig 2.10, NaY zeolites formed a cyclic transition state with the C2 and C3 atoms of the lactic acid molecule. The introduced halogen anions with strong electronegativity could reduce the electron density and promote the basicity of the framework oxygen atoms that interacted with hydrogen at C3 atoms of the lactic acid molecule and the replacement of Na+ with K+ could reduce the acidity of NaY zeolites could restrain the formation of acetaldehyde and coke deposits and maintain the high selectivity for acrylic acid.

Physical Properties

Table 2.2 Physical properties of Potassium.

Parameters	Value
Name	Potassium
Symbol	K
Phase	solid
Atomic number	19
Atomic mass	39.0983 g/mol
Density	0.862 g/cm^3
Melting point	336.7 K
Boiling point	1032 K
Heat of fusion	2.33 kJ/mol
Heat of vaporization	76.9 kJ/mol
Molar heat capacity	29.6 J/(mol.K)

2.1.5 Sol-gel method

The sol-gel process is a formation of an oxide network through polycondensation reactions of a molecular precursor in a liquid. The advantages of sol-gel processing include precise control of chemistry and structure at the molecular level, nano-sized porosity, and use of lower processing temperatures resulting in unique structures and lower associated costs [39].

A sol is a stable dispersion of colloidal particles or polymers in a solvent. The particles may be amorphous or crystalline. An aerosol is particles in a gas phase, while a sol is particles in a liquid.

A gel consists of a three dimensional continuous network, which encloses a liquid phase in a colloidal gel, the network is built from agglomeration of colloidal particles. In a polymer gel the particles have a polymeric sub-structure made by aggregates of sub-colloidal particles. Generally, the sol particles may interact by van der Waals forces or hydrogen bonds. A gel may also be formed from linking polymer chains. In most gel systems used for materials synthesis, the interactions are of a covalent nature and the gel process is irreversible [40].

Sol-gel synthesis may be used to prepare materials with a variety of shapes, such as porous structures, thin fibers, dense powders and thin films, are illustrated in Fig. 2.11.

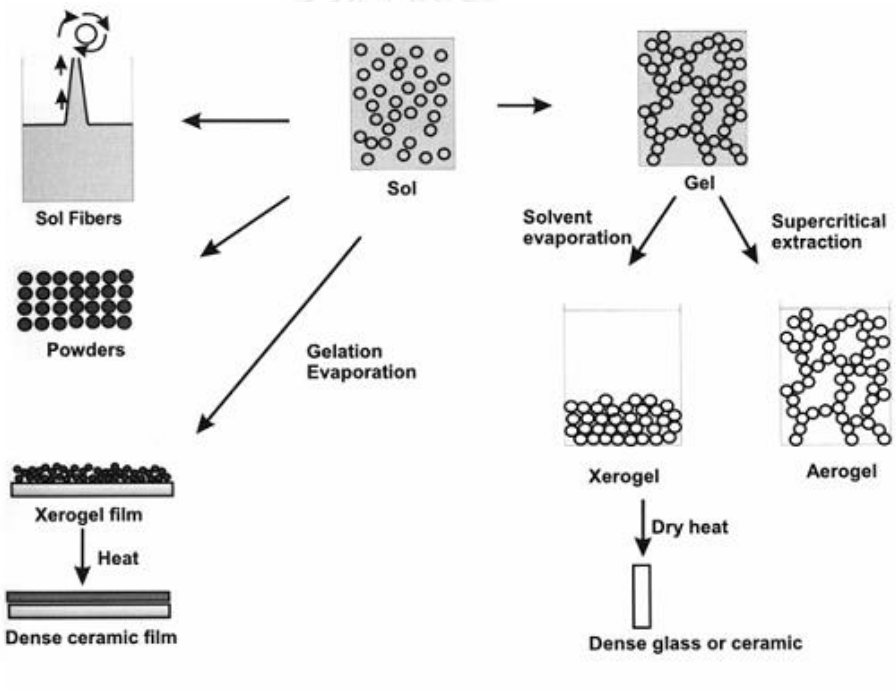

Figure 2.11 Sol-gel processing options [40].

If the gel is dried by evaporation, then the capillary forces will result in shrinkage, the gel network will collapse, and a xerogel is formed. If drying is performed under supercritical conditions, the network structure may be retained and a gel with large pores may be formed. This is called an aerogel, and the density will be very low about 0.005 g/cm^3 [40].

2.2 Literature reviews

2.2.1 Y zeolites catalyst for lactic acid dehydration reaction.

Hongjuan Wang et al. (2008) [41] studied catalytic dehydration performance of lactic acid to acrylic acid over NaY zeolites modified by rare earth metals (lanthanum, cerium, samarium, and europium) to compare with unmodified NaY catalyst. The catalytic performance results showed that La was the most effective modifying ion and the optimum addition amount was 2 wt%. The structure characterization results showed that the addition of lanthanum ion had changed catalyst physical performance such as decreased surface acidity density, increased specific surface area, enlarged pore size and changed the charge effect of lanthanum ion specific location (solidate cage), which might induce the improved coke resistance and restrain the side reaction.

Peng Sun et al. (2009) [42] were investigated potassium modification significantly improved the selectivity and durability of NaY zeolites during lactic acid dehydration reaction. The results showed that the selectivity of 2.8 K/NaY zeolites improved from 14.8% to 50.0% over NaY catalyst because potassium modification could impair the acidity of NaY zeolites. A carbenium ion mechanism is proposed for the formation of acetaldehyde under acidic condition. The acidic sites in Y zeolites are induced for carbenium ion formation, further facilitate the decarbonylation to acetaldehyde. Adding potassium also increase catalyst life. After 22 h the acrylic acid selectivity of NaY zeolites reduced to less than 10% while that of 3.5K/NaY retained 35.6% due to the weaker adsorptive strength between lactic acid/acrylic acid and K/NaY surface could reduce side reaction and coke formation. The changed chemical adsorption between adsorbate and K/NaY surface because of potassium electronic promoter effect. The presence of K^+ with less electronegativity that decreases the electron field induced by the cations and weaken the interactions of the adsorbate with the electron field.

YAN Jie et al. (2010) [43] studied the NaY zeolites modified by two kinds of metals. In our study, a series of La^{3+} and Ba^{3+} modified NaY zeolites were synthesized through different impregnation procedures. Lactic acid dehydration to acrylic acid was selected as a probe reaction to test the catalytic performance of these zeolites synthesized. The effects of synthesis details on their pore structures and surface acid/base properties were investigated by means of techniques such as N_2 sorption, NH_3–TPD and CO_2–TPD. The characterization results demonstrated that the samples synthesized by two-step impregnation had more medium acid and base sites inducing better catalytic performance. Moreover, compared with successive impregnations, calcination between two impregnations could endow the NaY zeolites with much more acid amount. Additionally, the special surface properties resulted in the improvement of selectivity to acrylic acid during lactic acid dehydration.

Dinghua Yu et al. (2010) [38] reported the NaY zeolite catalyst with and without potassium salt modifications were studied lactic acid dehydration to acrylic acid. The selectivity for acrylic acid could be enhanced by modification of the NaY catalysts with potassium salts. The KI-modified NaY catalyst exhibited the best catalytic performance for lactic acid dehydration reaction, over which 97.6% conversion and 67.9% acrylic acid selectivity could be gained at 598 K because the halogen anions with strong electronegativity could reduce the electron density and promote the basicity of the framework oxygen atoms that interacted with beta-hydrogen at C3 atoms of the lactic acid molecule. As illustrated in our previous paper, the replacement of Na^+ with K^+ could reduce the acidity of NaY zeolites. Hence, both increased basicity and decreased acidity of KX-modified NaY zeolites could restrain the formation of acetaldehyde and coke deposits and maintain the high selectivity for acrylic acid.

YAN jie et al. (2011) [36] investigated various NaY zeolites modified by alkaline earth metals (Mg, Ca, Sr and Ba). They were synthesized and used as catalysts for the dehydration of lactic acid to acrylic acid to investigate the effects of cationic species on the structure and surface acid/base distribution of the NaY zeolites catalyst. The yields of acrylic acid were found to increase as follows: 2%Mg/NaY < 2%Ca/NaY < 2%BaNaY. This order is consistent with the basicity of the respective cation clusters and the amount of medium basic sites on the catalysts. The yield of acetaldehyde gave the following sequence: 2%Ba/NaY > NaY > 2%Ca/NaY > 2%Sr/NaY > 2%Mg/NaY. This is similar to the amount of medium acidic sites on the catalysts. Moreover, the sequence for the yields of acrylic acid over the Ba/NaY zeolites containing various amounts of Ba was similar to that of the amount of medium basic sites. The higher amount of Ba can inhibit the formation of acetaldehyde because the generation of acetaldehyde can be affected by the acidic sites. Among the studied catalysts, 2%Ba/NaY gave the highest yield of acrylic acid at up to 44.6% because it contained the most medium basic sites and a suitable Ba^{2+} cluster character.

2.2.2 Others Catalyst for lactic acid dehydration reaction.

Junfeng Zhang et al. (2013) [44] investigated the catalytic conversion of lactic acid to acrylic acid and 2,3-pentanedione over sodium nitrate supported mesoporous SBA-15 and fumed silica was studied. The yields of acrylic acid, 2,3-pentanedione and acetaldehyde are 44.8%, 25.1% and 13.3% respectively, over the 23%$NaNO_3$/SBA-15 catalyst. The performance of the catalysts is strongly affected by $NaNO_3$ loading, catalyst texture and porosity and product diffusion efficiency. A proper control of $NaNO_3$ loading can result in modification catalyst structure and tune the size of mesopores for improvement of 2,3-pentanedione selectivity. The three-dimensional pore texture of the $NaNO_3$/FS catalyst may favor AA diffusion and hence suppress AA post-disintegration. The result of IR investigation revealed that $NaNO_3$-silica interaction

is weak and under certain working conditions the surface $NaNO_3$ can readily transform to sodium lactate that functions as active component to catalyze the target reactions.

Congming Tang et al. (2013) [45] studied dehydration of lactic acid to acrylic acid was carried out over the barium phosphate catalysts at various conditions. Barium phosphate catalysts were prepared by a precipitation method. The catalysts were calcined at 500 ºC for 6 h in air atmosphere. The dibarium pyrophosphate catalyst was found to have the best catalytic performance, ascribing to weak acidity on the surface. Under the optimal reaction conditions, 99.7% of the lactic acid conversion and 76.0% of the selectivity to acrylic acid were achieved over the dibarium pyrophosphate catalyst. It is not astonishing that the highest selectivity to propionic acid was observed from $Ba_3(PO_4)_2$. The reason is that the alkalinity of catalyst favors for the hydrogenation reaction and under the steam atmosphere $Ba_3(PO_4)_2$ has the strongest alkalinity. Therefore, $Ba_2P_2O_7$ is an excellent catalyst for formation of acrylic acid from dehydration reaction of lactic acid although plenty of acetaldehyde was also produced in the catalytic process.

E. Blanco et al. (2013) [46] investigated gas phase dehydration of lactic acid over alkaline-earth phosphates were prepared by co-precipitation method using sodium free or sodium containing precursors. After checking the stability of catalysts under feed, it was shown that selectivity to acrylic acid strongly depended on reaction temperature but not on contact time. At temperature of 380 °C, values ranging from 19 to 49% were measured for the different prepared catalysts. In optimized conditions, the highest conversions were measured for hydroxyapatites, which exhibited the highest surface areas whereas the best AA selectivities (40–50%) were obtained for ortho and pyrophosphates. The highest value was reached with $Ba_3(PO_4)_2$ (55% for C3 products) but selectivity rather close were obtained with different other phosphates suggesting kinetic limitation. Acid–base properties measurements revealed that alkaline-earth phosphates exhibited high proportion of acidic and basic sites with same

weak strength. Furthermore, correlation between acrylic selectivity of alkaline earth phosphates and the acid–base balance were clearly established for the first time: selectivity was 50% for balance close to 1 and decreased by factor two increasing this parameter to 2. Finally, FTIR spectra of spent catalysts showed alkaline-earth lactates adsorbed over the catalysts which could be reaction intermediates for dehydration of lactic acid.

Yumiko Matsuura et al. (2013) [47] prepared substituted hydroxyapatite catalysts such as $Ca_{10}(PO_4)_6(OH)_2$, $Sr_{10}(PO_4)_6(OH)_2$, $Pb_{10}(PO_4)_6(OH)_2$, $Ca_{10}(VO_4)_6(OH)_2$ and $Sr_{10}(VO_4)_6(OH)_2$ and carried out conversions of lactic acid over the prepared catalysts. The hydroxyapatite catalysts had stabilities for the reaction media under flowing gas including lactic acid and water at 623K. The catalytic activities of prepared hydroxyapatite catalysts scarcely decreased during time on stream for 6 h. The hydroxyapatite catalysts exhibited markedly higher acrylic acid yields than those of P_2O_5/SiO_2 and MgO catalysts. In the lactic acid conversions, the relatively acidic catalysts such as P_2O_5/SiO_2, $Ca_{10}(VO_4)_6(OH)_2$ and $Sr_{10}(VO_4)_6(OH)_2$ catalysts, accelerated the formations of acetaldehyde and propionic acid, whereas the relatively basic catalysts, such as MgO and $Pb_{10}(PO_4)_6(OH)_2$ catalysts, gave large amounts of unidentified products. On the other hand, the moderate acid–base catalysts, such as $Ca_{10}(PO_4)_6(OH)_2$ and $Sr_{10}(PO_4)_6(OH)_2$ catalysts, selectively accelerated the dehydration of lactic acid into acrylic acid.

Chuan Yuan et al. (2015) [48] investigated the effect of cationic species on the structures and surface acid-base distribution of the lactic acid dehydration over ZSM-5 zeolites modified with alkali metals (Li, Na, K, Rb and Cs) were prepared using ion-exchange. The catalysts were used to enhance the catalytic dehydration of lactic acid (LA) to acrylic acid (AA). The results show that the acid-base sites that are adjusted by alkali-metal species, particularly weak acid-base sites, are mainly responsible for the formation of AA. The KZSM-5 catalyst, in particular, significantly improved LA conversion and AA selectivity because of the synergistic effect of weak acid-base sites

and increase in the number of Lewis acid sites, which was caused by metal-cation modification of ZSM-5, was beneficial to LA dehydration to AA. The KZSM-5 zeolite had excellent stability in catalytic LA dehydration because of its shape selectivity and the absence of strong acidity and three-dimensional supercages. The reaction was conducted at different reaction temperatures and liquid hourly space velocities (LHSVs) to understand the catalyst selectivity for AA and trends in byproduct formation. Approximately 98% LA conversion and 77% AA selectivity were achieved using the KZSM-5 catalyst under the optimum conditions (40 wt% LA, aqueous solution, 365 °C and LHSV = 2 h^{-1}).

CHAPTER III
EXPERIMENTAL

This chapter describes about the experimental procedures which consists of three sections. The first, support and catalysts were prepared. Second, catalysts were characterized by various techniques. Finally, the lactic acid dehydration reaction was studied and analyzed by gas chromatograph equipped with DB-WAX UL column and flame ionization detector (FID).

3.1 Catalyst preparation

3.1.1 Chemicals

- HY zeolites (Si/Al ratio = 15, 100 and 500, from TOSOH)
- Alumina isoproproxide (>98%, from Sigma-Aldrich)
- Ethanol (99%, from Merck)
- Hydrochloric acid (37.7 %, from RCI Labscan)
- Potassium nitrate (KNO_3, from Sigma-Aldrich)
- Distilled water
- Lactic acid (analytical grade, from Sigma-Aldrich)

3.1.2 The preparation of Al_2O_3 catalysts by sol-gel method

Alumina isoproproxide (AIP) and ethanol were used as a precursor and organic solvent, respectively. Firstly, alumina isoproproxide was dissolved in a mixture of deionized water and ethanol with volume ratio of 1:1 and stirring at 80 ºC for 1 h. Then, increased the temperature of solution to 90 ºC. After that, hydrochloric acid was dropped to adjust pH value of the solution equal to 2.5 and aged with stirring at 90

°C, until eliminating solvent. After this step the sol was became so viscous. The formed gel was dried overnight at 110 °C and calcined under air flow at 550 °C for 2 h.

3.1.3 The preparation of Al_2O_3-HY zeolite catalysts by sol-gel method

Alumina isoproproxide (AIP) and ethanol were used as a precursor and organic solvent, respectively. Firstly, alumina isoproproxide was dissolved in a mixture of deionized water and ethanol with volume ratio of 1:1 and stirring at 80 °C for 1 h. Then, increased the temperature of solution to 90 °C and added HY zeolite into the solution with varied compositions of Al_2O_3-NaY zeolite weight ratio 1:3, 1:1 and 3:1. Finally, hydrochloric acid was dropped to adjust pH value of the solution equal to 2.5 and aged with stirring at 90 °C, until eliminating solvent. After this step the sol was became so viscous. The formed gel was dried overnight at 110 °C and calcined under air flow at 550 °C for 2 h.

3.1.4 The preparation of catalysts by incipient wetness impregnation method

The K/HY zeolite and K/Al_2O_3-HY zeolite catalysts of all ratios were prepared by the incipient wetness impregnation method using KNO_3 as metal precursors with different potassium loading of 2, 4, 6 and 8 wt.%. First of all, KNO_3 was dissolved in deionized water in equal volume to pore volume of the support. An aqueous solution of KNO_3 was dropped to the support. After that, the impregnated catalysts were kept at room temperature for 4 h to assure adequate distribution of metal complete. Finally, the catalysts were dried overnight at 110 °C and calcined under air flow at 550 °C for 2 h.

3.2 Catalyst characterization

3.2.1 X-ray diffraction (XRD)

X-ray diffraction (XRD) analysis were characterized to determine the crystallite phase of the catalyst by using X-ray diffractometer SIEMENS D 5000. It was connected to a personal computer with Diffract AT version 3.3 program for fully control of XRD analyzer. The XRD analysis was conducted to Cu-Kα radiation between 20° and 80° with a generator voltage and current of 30 kV and 30 mA, respectively. The scan step was 0.04°.

3.2.2 Temperature programed desorption of ammonia (NH_3-TPD)

The acid properties of catalysts were observed by Ammonia Temperature Programmed Desorption (NH_3-TPD) using Micromeritics chemisorp 2750 Pulse Chemisorption System. 0.1 g of the sample was conducted in a quartz U-tube and pretreated in a helium flow at 500 °C for 1 h and then ammonia was introduced with helium about 1 h. The sample was heated from 40 °C to 600 °C with a heating rate of 10 °C/min. The desorbed ammonia was measured as a function of temperature using TCD.

3.2.3 Temperature programed desorption of carbon dioxide (CO_2-TPD)

The basicity of the catalysts were measured by temperature programmed desorption of carbon dioxide (CO_2-TPD) equipment by using Micromeritics Chemisorp 2750 Pulse Chemisorption System instrument. 0.1 g of the sample was conducted in a quartz U-tube and pretreated in a helium flow at 500 °C for 1 h and then carbon dioxide was introduced with helium about 1 h. The sample was heated from 40 °C to

600 °C with a heating rate of 10 °C/min. The desorbed carbon dioxide was measured as a function of temperature using TCD.

3.2.4 Nitrogen physisorption (BET)

Brunauer–Emmett–Teller (BET) method is used to determine specific surface area of the catalysts, and Barret-Joyner-Halenda (BJH) method is used to examine pore diameter and pore volume of the prepared catalysts. 0.1 grams of each samples were measured by N2 adsorption-desorption isotherm using Micromeritics ASAP 2020 at liquid nitrogen temperature of -196 °C. Prior to the analysis, samples were dried to eliminate moisture in the sample.

3.2.5 Scanning electron microscopy (SEM) and energy x-ray spectroscopy (EDX)

The morphology and elemental dispersion over the catalysts surface were determined by scanning electron microscope (SEM) and energy X-ray spectroscopy (EDX), respectively. The SEM model is JEOL mode JSM-5800LV and Link Isis Series 300 program was performed for EDX.

3.2.6 Thermogravimetric analysis (TGA)

Thermal gravimetric analysis (TGA) was used to study the thermal decomposition of catalyst under the temperature range of room temperature to 1000 °C with a heating rate of 10 °C /min in nitrogen atmosphere using an STD analyzer model Q600 from TA instrument.

3.3 Lactic acid catalytic dehydration test

In this research, the catalytic activity of all catalyst was investigated by using the experimental set-up apparatus as show in Figure 3.1.

3.3.1 Chemicals and reactants

- Ultra high purity nitrogen gas (99.999%) (TIG)
- Lactic acid (>85%) (Sigma-Aidrich)

3.3.2 Instruments and apparatus

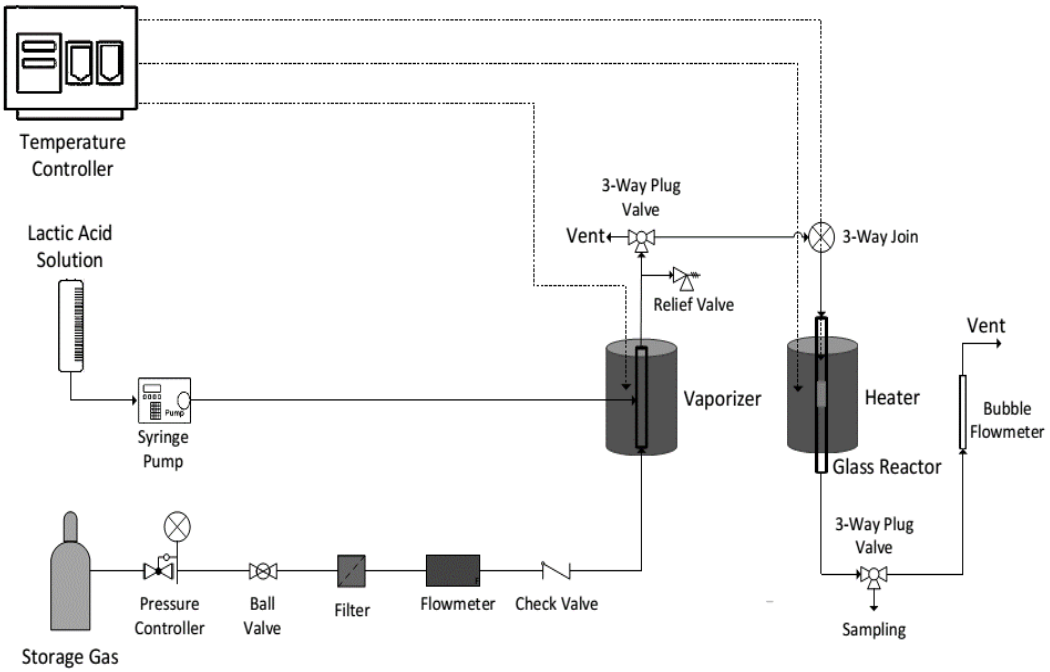

Figure 3.1 Experimental set-up for reaction test.

From Figure 3.1, the Experimental set-up for reaction tests consists of:

a) *Reactor*: The reactor is made from glass tube and inner diameter of 9 mm.

b) *Vaporizer*: The vaporizer is equipment to vaporize lactic acid from liquid phase to vapor phase. It is operated at temperature of 230 °C at atmospheric pressure. This

temperature is higher than the boiling point of lactic acid (218 °C), thus lactic acid can be vaporized.

c) *Syringe pump*: The syringe pump is used to inject lactic acid into vaporizer at fixed rate of 1 ml/h.

d) *Furnace*: The furnace is heated to the catalyst fixed-bed reactor tube. The temperature of the furnace is controlled by temperature controller.

e) *Temperature controller*: - At furnace, the temperature of furnace is set at temperatures in 340 °C.

- At vaporizer, the temperature is set at 230 °C. (Above the boiling point of lactic acid)

f) *Gas system*: Nitrogen is a carrier gas, which is used to carry lactic acid vapor into the reactor or catalyst bed. The flow rate of carrier gas is controlled by mass flow controller.

g) *Sampling*: The sample is collected at sampling with 1.0 ml of product to analyze by GC.

h) *Gas chromatography (GC)*: A Gas chromatography is used for investigating lactic acid conversion and product selectivity. It equipped (Shimadzu GC-14B) with flame ionization detector (FID) with DB-WAX UL column.

The operating condition for gas chromatography is reported;

- Detector: FID
- Capillary column: DB-WAX
- Carrier gas: Nitrogen (99.99 vol. %)
- Column temperature
    - Initial: 230 °C
    - Final: 230 °C
- Injector temperature: 230 °C
- Detector temperature: 230 °C

- Time analysis: 10 min
- Analyzed gas: lactic acid, acrylic acid, acetaldehyde, propanoic acid, and 2-3-pentanedione

3.3.3 Lactic acid dehydration reaction procedure

The lactic acid dehydration to acrylic acid over the catalysts was carried out in a fixed-bed reactor with 9 mm inner diameter. The catalyst of 0.1 g was placed in the middle of glass tube and quartz wool was placed in both ends. The catalyst was preheated at required reaction temperature at 340 ºC for 0.5 h under high purity N_2 (40 ml/min) before catalytic evaluation. The feedstock of 34% by volume (11% by mole) of lactic acid was pumped into the preheating zone and driven through the catalyst bed by nitrogen. The concentration of lactic acid after vaporization and balance with nitrogen are 2% by mole. The products were analyzed by GC equipped with a DB-WAX UL column and FID detector.

CHAPTER IV
Results and discussion

In this chapter consists of three parts. The first part studies the effect of different percent loading of K over HY zeolite catalysts at 0, 2, 4, 6 and 8 wt.% of potassium. The second part investigates the effect of different Si/Al molar ratio of HY zeolite (15, 100 and 500) on K over HY zeolite catalysts. The final part investigates the effect of support ratio of Al_2O_3 and HY zeolite on K over Al_2O_3-HY zeolite catalysts. Support ratio of Al_2O_3 and HY zeolite are as follows: 3:1, 1:1 and 1:3. All three part shows the characterization of catalysts by X-ray diffraction (XRD), N_2 physisorption, scanning electron microscope and energy dispersive X-ray spectroscopy (SEM-EDX) , ammonia temperature-programmed desorption (NH_3-TPD), temperature programed desorption of carbon dioxide (CO_2-TPD), thermogravimetric analysis (TGA), and activity in lactic acid dehydration reaction.

4.1 The effect of different potassium loading over HY zeolite catalysts at 0, 2, 4, 6 and 8 wt.%.

The catalyst nomenclatures are represent as below:

HY100 zeolite represents the HY zeolite having Si/Al molar ratio of 100

2%K/HY100 represents the catalyst which have 2 wt.% K over HY zeolite with HY zeolite having Si/Al molar ratio of 100

4%K/HY100 represents the catalyst which have 4 wt.% K over HY zeolite with HY zeolite having Si/Al molar ratio of 100

6%K/HY100 represents the catalyst which have 6 wt.% K over HY zeolite with HY zeolite having Si/Al molar ratio of 100

8%K/HY100 represents the catalyst which have 8 wt.% K over HY zeolite with HY zeolite having Si/Al molar ratio of 100

4.1.1 Catalyst characterization

4.1.1.1 X-Ray diffraction (XRD)

The X-ray diffraction (XRD) patterns of HY100 zeolite and HY100 zeolite modified with potassium at 2, 4, 6 and 8 wt.% are shown in Figure 4.1. XRD was performed regarding the crystallite phases of the samples. The XRD patterns of HY100 zeolite and HY100 zeolite modified with potassium at 2, 4, 6 and 8 wt.% were observed at 2θ = 20.3°, 23.7°, 27.0°, 31.8°, 34.2°, 38.4° and 54.6° which are typical of zeolite faujasite [49]. Neither potassium nor any unidentified phase was observed on the XRD patterns of HY100 zeolite modified with potassium. The identical XRD patterns of these samples and the parent zeolites indicated that the large surface area of the HY zeolites might contribute to good dispersion of potassium on HY100 zeolite. But, it is also obvious that the intensities of peaks decrease dramatically with the increase of potassium loading from 2, 4, 6 and 8 wt.%, respectively, indicating that the extent of damage to the structure becomes severe. In Figure 4.1, showing that the potassium at high percent loading seriously destroys HY100 zeolite structure.

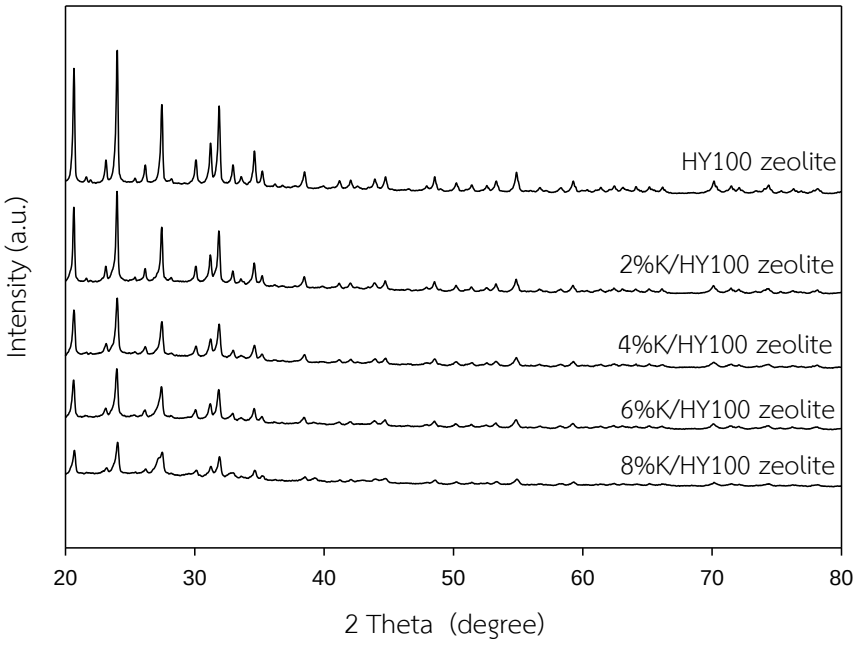

Figure 4.1 XRD patterns of HY100 zeolite and HY100 zeolite modified with potassium at 2, 4, 6 and 8 wt.%.

4.1.1.2 Nitrogen adsorption-desorption

The textural properties of catalysts were investigated by nitrogen adsorption-desorption technique using Brunauer-Emmett-Teller (BET) method and Barret-Joyner-Halenda (BJH) method. The BET surface area, pore volume and pore size were summarized in Table 4.1. The BET surface area of HY100 zeolite was 675 m^2/g, while the BET surface area of HY100 zeolite modified with potassium at 2, 4, 6 and 8 wt.% were ranged between 513-604 m^2/g. The BET surface area of HY100 zeolite catalysts modified with potassium decreased significantly with increasing potassium content from 2, 4, 6 and 8 wt.%, respectively. The pore volume of catalysts were range 0.16-0.26 cm^3/g. The decrease of BET surface area and pore volume may be due to the pores of HY zeolite filled with potassium species, so that the pore may be blocked by the metal [8]. The pore size of HY100 zeolite and HY100 zeolite modified with potassium at 2, 4 and 6 wt.% were range 6.1-6.9 nm that it had no significant change, while that of 8%K/HY100 zeolite was 8.9 nm because the potassium at high percent loading seriously destroys HY100 zeolite structure, consistent with the XRD investigation.

Table 4.1 The physiochemical properties of HY100 zeolite and HY100 zeolite modified with potassium at 2, 4, 6 and 8 wt.%

Catalysts	BET surface area (m^2/g)	Pore volume [a] (cm^3/g)	Pore size [a] (nm)
HY100 zeolite	675	0.26	6.1
2%K/HY100 zeolite	604	0.26	6.4
4%K/HY100 zeolite	541	0.21	6.7
6%K/HY100 zeolite	527	0.23	6.9
8%K/HY100 zeolite	513	0.16	8.9

[a] Determined from the Barret-Joyner-Halenda (BJH) desorption method.

The N_2 adsorption-desorption isotherm of HY100 zeolite and HY100 zeolite modified with potassium at 2, 4, 6 and 8 wt.% are provided in Figure 4.2. The isotherms

of all catalyst can be classified as a type IV isotherm with H3-shaped hysteresis loops that are implied the mesoporous structures [50].

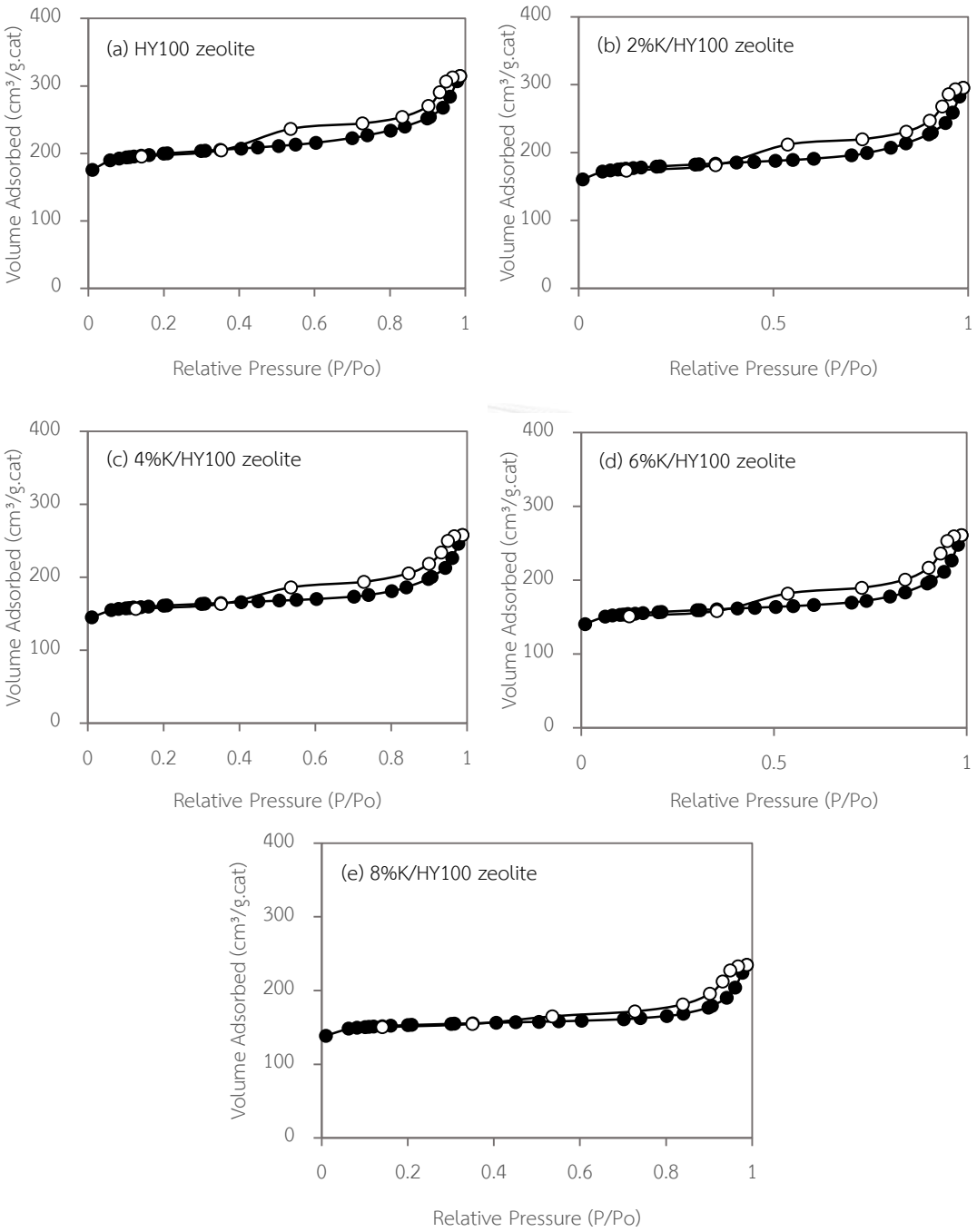

Figure 4.2 N_2 adsorption-desorption isotherm of HY100 zeolite and HY100 zeolite modified with potassium at 2, 4, 6 and 8 wt.%.

4.1.1.3 Ammonia temperature program desorption (NH_3-TPD)

Ammonia temperature program desorption (NH_3-TPD) was used for evaluating the acidity on surface of HY100 zeolite and HY100 zeolite modified with potassium at 2, 4, 6 and 8 wt.%. The amount of desorbed ammonia corresponds to the total surface acidity of the catalyst. In addition, the desorption temperature of desorbed ammonia corresponds to the acid strength on surface of the catalysts.

NH_3-TPD profiles of HY100 zeolite and HY100 zeolite modified with potassium at 2, 4, 6 and 8 wt.% are shown in Figure 4.3. The temperature ranges of regions I (100-200 °C), II (200-400 °C) and III (400-600 °C) represent weak, medium and strong acid sites, respectively [36]. Previous studies have shown that the surface acidity and basicity of catalysts play key roles in lactic acid dehydration reaction [51]. The HY100 zeolite catalyst show higher acid strengths than HY zeolite modified with potassium in view of the NH_3-desorption temperatures in Figure 4.3. There is a tendency that the surface acidity and the fractions of medium and strong acid sites of HY100 zeolite decrease with increasing potassium content from 2, 4, 8 and 6 wt.%, respectively. The basic sites that were induced by the alkali cations species play a positive role in the formation of acrylic acid. The surface basicity induced by cations has always been explained using the trimer cluster model. The cations are sorted as trimer cationic clusters and interact with the zeolite framework oxygen [38]. The framework oxygen nearest the cation provides a basic site for catalyzing lactic acid dehydration to acrylic acid.

The total acidity of different samples were quantified based on the area of NH_3 desorption peaks in the TPD profiles, and the results are shown in Table 4.2. The total acidity of catalysts decreased in the following order: HY100 zeolite > 2%K/HY100 zeolite > 4%K/HY100 zeolite > 8%K/HY100 zeolite > 6%K/HY100 zeolite. The results shown that total acidity decreased with increasing potassium content from 2, 4 and 6 wt.%, while the total acidity of 8%K/HY100 zeolite was 5.46 mmol NH_3/g.cat because the potassium at high percent loading destroys HY100 zeolite structure. It is known that the catalysts with high surface acidities can catalyze lactic acid dehydration to undesirable products such as acetaldehyde.

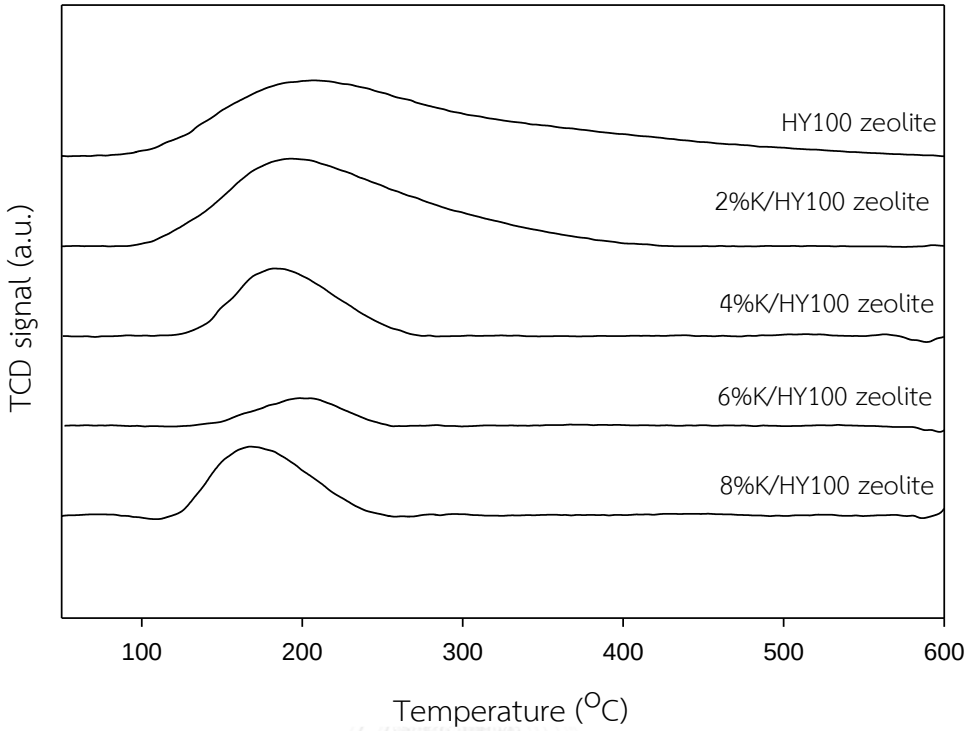

Figure 4.3 NH_3-TPD profiles of HY100 zeolite and HY100 zeolite modified with potassium at 2, 4, 6 and 8 wt.%.

Table 4.2 Total acidity of HY100 zeolite and HY100 zeolite modified with potassium at 2, 4, 6 and 8 wt.%.

Catalysts	Total acidity (mmol NH_3/g.cat)
HY100 zeolite	17.95
2%K/HY100 zeolite	14.42
4%K/HY100 zeolite	5.73
6%K/HY100 zeolite	2.01
8%K/HY100 zeolite	5.46

4.1.1.4 Carbon dioxide temperature program desorption (CO_2-TPD)

Carbon dioxide temperature program desorption (CO_2-TPD) was used for evaluating the basicity on surface of HY100 zeolite and HY100 zeolite modified with potassium at 2, 4, 6 and 8 wt.%. The amount of desorbed carbon dioxide corresponds to the total surface basicity of the catalyst. In addition, the desorption temperature of desorbed carbon dioxide corresponds to the base strength on surface of the catalysts.

CO_2-TPD profiles of HY100 zeolite and HY100 zeolite modified with potassium at 2, 4, 6 and 8 wt.% are shown in Figure 4.4. HY100 zeolite modified with potassium have one large peak at around 100 °C ascribed to the weak basic sites of the catalysts. The HY100 zeolite modified with potassium show higher basic sites than HY100 zeolite catalyst in view of the CO_2-desorption temperatures in Figure 4.4. There is a tendency that the surface basicity of HY100 zeolite increase with increasing potassium content from 2, 4, 8 and 6 wt.%, respectively. The total basicity of different samples were quantified based on the area of CO_2 desorption peaks in the TPD profiles, and the results are shown in Table 4.3. The total basicity of catalysts increased in the following order: HY100 zeolite < 2%K/HY100 zeolite < 4%K/HY100 zeolite < 8%K/HY100 zeolite < 6%K/HY100 zeolite. 6%K/HY100 zeolite catalyst had a higher total basicity than the other catalysts, which might be the reason for the higher selectivity to AA over it.

Table 4.3 Total basicity of HY100 zeolite and HY100 zeolite modified with potassium at 2, 4, 6 and 8 wt.%.

Catalysts	Total basicity (μmol CO_2/g.cat)
HY100 zeolite	0.01
2%K/HY100 zeolite	3.97
4%K/HY100 zeolite	4.81
6%K/HY100 zeolite	5.18
8%K/HY100 zeolite	5.14

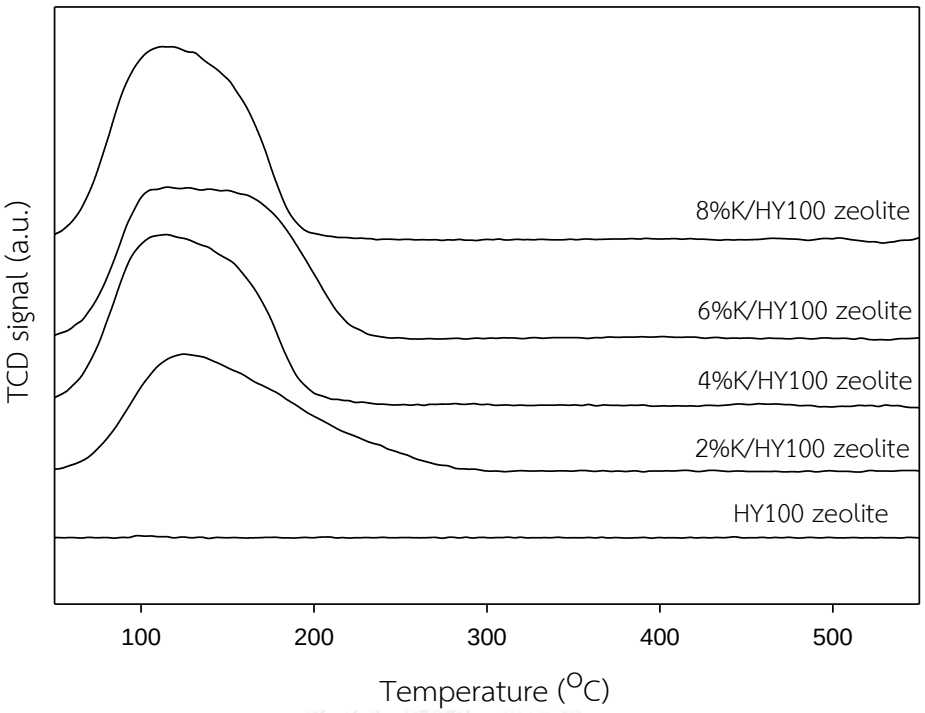

Figure 4.4 CO_2-TPD profiles of HY100 zeolite and HY100 zeolite modified with potassium at 2, 4, 6 and 8 wt.%.

4.1.1.5 Scanning electron microscope and energy dispersive X-ray spectroscopy (SEM-EDX)

The morphology of HY100 zeolite and HY100 zeolite modified with potassium at 2, 4, 6 and 8 wt.% studied by Scanning Electron Microscopy (SEM) are shown in Figure 4.5. All catalysts have similar surface morphology and uniform in size distribution. It was found that potassium over HY100 zeolite did not affect the morphology of catalysts.

The elements and potassium dispersion over the HY100 zeolite catalysts surface were determined by energy dispersive X-ray spectroscopy (EDX) in Table 4.4 and Figure 4.6. The results show that 8%K/HY100 zeolite catalyst had a highest potassium content with 7.76 wt.% and all catalyst have a good dispersion of potassium on the surface of HY100 zeolite catalyst, consistent with the XRD investigation. The

HY100 zeolite modified with potassium from EDX results shown higher amount of potassium than initial loading because EDX can detect only the surface of catalysts.

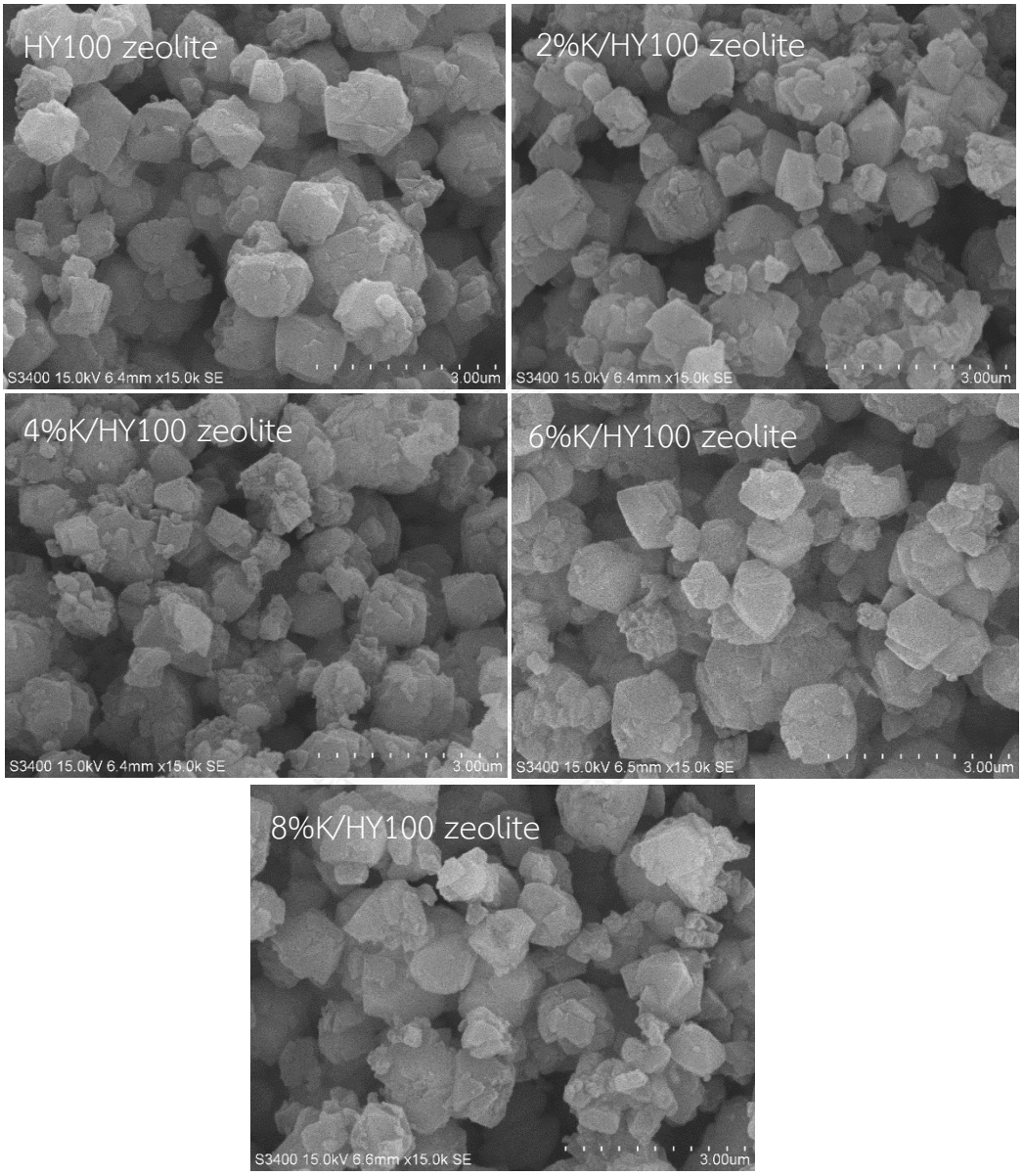

Figure 4.5 SEM images of HY100 zeolite and HY100 zeolite modified with potassium at 2, 4, 6 and 8 wt.%.

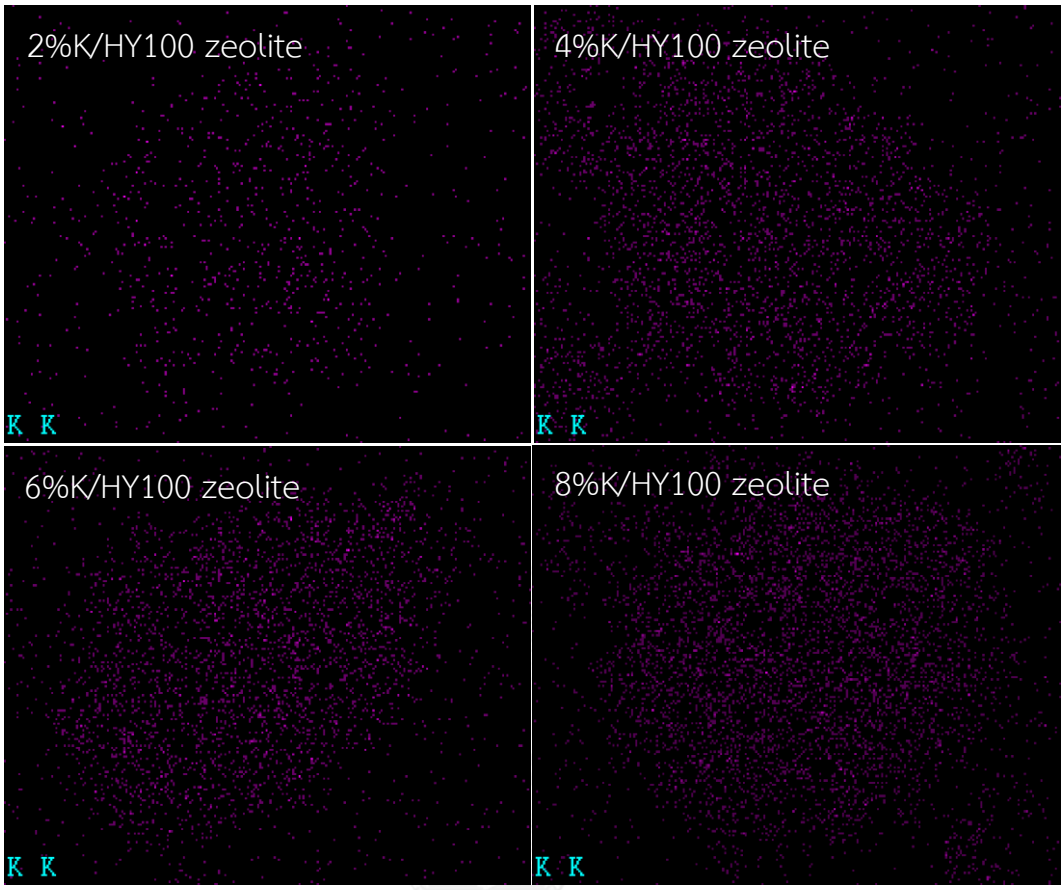

Figure 4.6 EDX images of potassium on the surface of HY100 zeolite catalysts modified with potassium at 2, 4, 6 and 8 wt.%.

Table 4.4 The elemental dispersion over the surface of HY zeolite catalyst modified with potassium at 2, 4, 6 and 8 wt.%.

Catalysts	Percent by weight (wt.%)			
	O	Al	Si	K
HY100 zeolite	42.20	1.26	56.54	0
2%K/HY100 zeolite	47.02	1.17	49.40	2.41
4%K/HY100 zeolite	43.46	1.13	51.07	4.34
6%K/HY100 zeolite	46.95	1.18	45.55	6.32
8%K/HY100 zeolite	44.99	0.96	46.29	7.76

4.1.1.6 Thermogravimetric analysis (TGA)

Thermogravimetric analysis (TGA) was used for study carbon deposition of the spent catalysts are investigated in Figure 4.7. The slightly weight loss of all spent catalyst around 100 ℃ could be assigned to the evaporation of moisture in catalysts. Figure 4.7, the weight loss were observed at around 300-400 ℃ in the following order: 8%K/HY100 zeolite > 4%K/HY100 zeolite > 6%K/HY100 zeolite > 2%K/HY100 zeolite > HY100 zeolite which should be attributed to the carbon deposits over spent catalyst [52]. These results demonstrated that potassium modification affect to increase of carbon deposits. The 6%K/HY100 zeolite catalyst had a lower carbon deposition than the 4%K/HY100 zeolite and 8%K/HY100 zeolite, respectively, which might be the reason for the higher selectivity to acrylic acid over it.

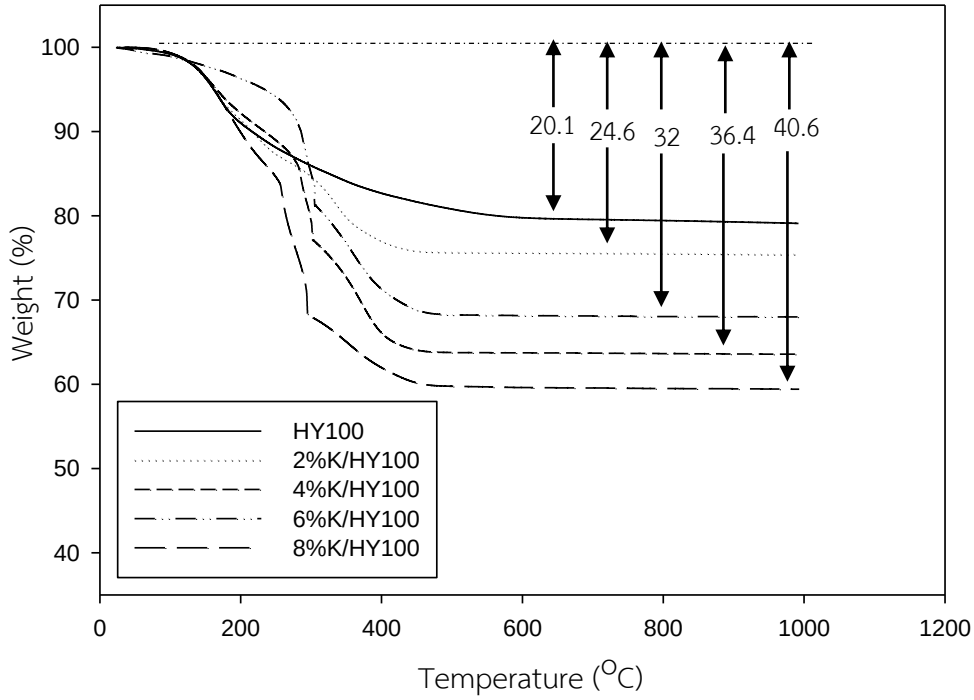

Figure 4.7 TGA results of spent HY100 zeolite and HY100 zeolite modified with potassium at 2, 4, 6 and 8 wt.% after 180 min of reaction.

4.1.2 Activity in lactic acid dehydration reaction

The activity of HY100 zeolite and HY100 zeolite modified with potassium at 2, 4, 6 and 8 wt.% were test in lactic acid dehydration reaction. The catalyst 0.1 g was packed in glass reactor with quartz wool and preheated at 340 ℃ for 30 min. After that, the lactic acid solution with concentration 34%volume were injected into the vaporizer at flow rate 1 ml/h and the vapor was carried through the catalyst bed by nitrogen. The gas products were analyzed by GC with a DB-WAX capillary column and FID detector.

The lactic acid conversion and product selectivity in lactic acid dehydration reaction at reaction temperature 340 ℃ and 90 min are shown in Figure 4.8 and Table 4.5. The lactic acid conversion of HY100 zeolite and HY100 zeolite modified with potassium at 2, 4, 6 and 8 wt.% were shown 100% and acrylic acid selectivity were ranged between 0-45.5%. Acetaldehyde is the main byproduct competing with acrylic acid over HY100 zeolite without modification, while all the HY100 zeolite modified with potassium could result in an increase in selectivity for acrylic acid, indicating that the potassium played an essential role [48]. The 6%K/HY100 zeolite catalyst was the best for lactic acid dehydration with 100% conversion and 45.5% selectivity for acrylic acid. From table 4.5, it also seen that with increasing the potassium loading from 2 wt.% to 6 wt.%, the formation of acetaldehyde is obviously suppressed with its selectivity decreasing from 100% to 49.5% and AA selectivity increasing from 0% to 45.5%. The decline of acetaldehyde selectivity should be ascribed to decrease of total acidity of HY100 zeolite as shown in NH_3-TPD result since the formation of acetaldehyde from lactic acid reactant is preferred over acidic catalysts. However, the catalysts with high surface basicity can catalyze lactic acid dehydration to propionic acid via reduction reaction of lactic acid [42]. For 8%K/HY100 zeolite catalyst, the acrylic acid selectivity decreased, indicating that the catalyst modified with high potassium loading is liable to cause damage of its structure and high coke deposition resulted in the blocking and packing of the micro channel, which is in agreement with XRD and TGA results. The catalytic results indicated that potassium modification could improve acrylic acid selectivity and reduce acetaldehyde selectivity.

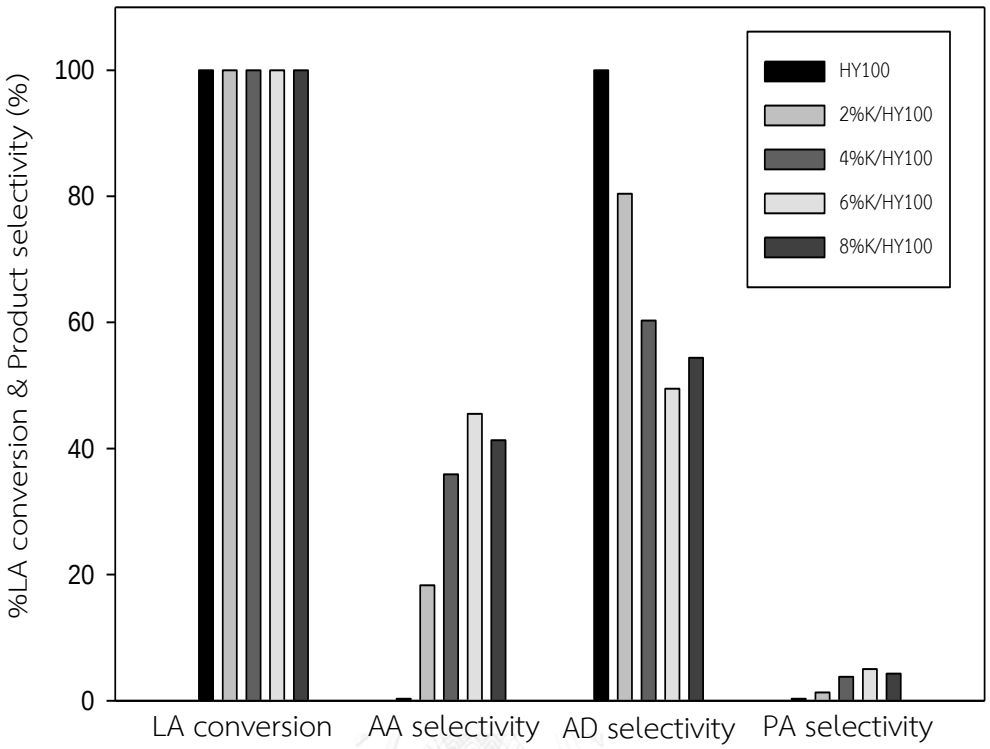

Figure 4.8 Lactic acid conversion and product selectivity of HY100 zeolite and HY100 zeolite modified with potassium at 2, 4, 6 and 8 wt.% at reaction temperature 340 ℃ and t = 90 min.

Table 4.5 The catalytic performance of HY100 zeolite and HY100 zeolite modified with potassium at 2, 4, 6 and 8 wt.%.

Catalysts	Lactic acid Conversion (%)	Product Selectivity [a] (%)		
		AA	AD	PA
HY100 zeolite	100	0.0	100	0.0
2%K/HY100 zeolite	100	18.3	80.4	1.3
4%K/HY100 zeolite	100	35.9	60.3	3.8
6%K/HY100 zeolite	100	45.5	49.5	5.0
8%K/HY100 zeolite	100	41.3	54.4	4.3

[a] AA-Acrylic acid, AD-acetaldehyde, PA-propionic acid. Reaction time 90 min, T=340℃

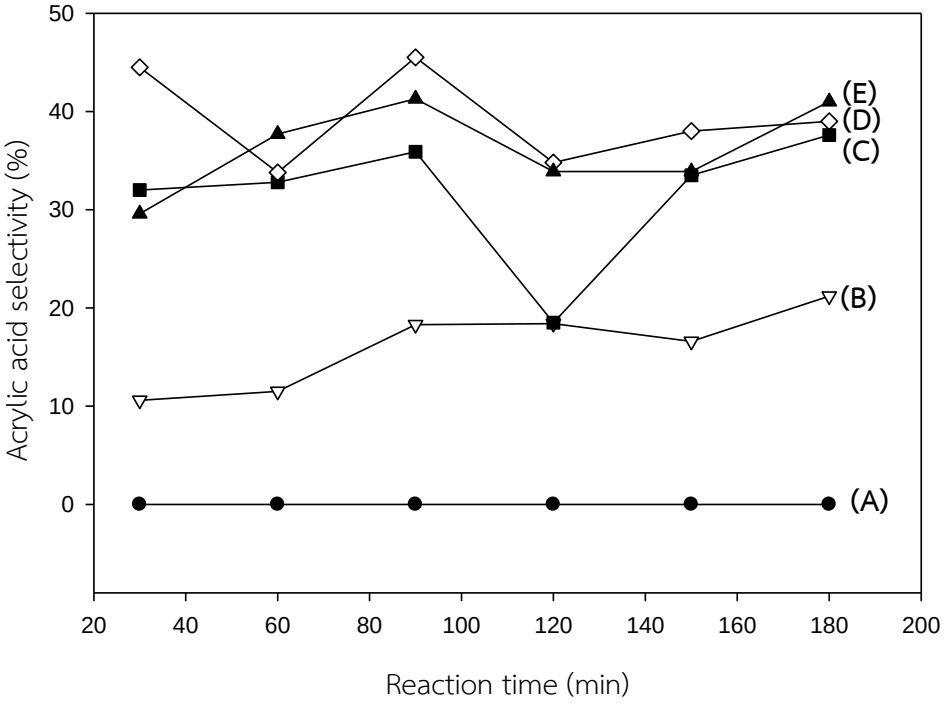

Figure 4.9 Acrylic acid selectivity of (A) HY100, (B) 2%K/HY100 zeolite, (C) 4%K/HY100 zeolite, (D) 6%K/HY100 zeolite and (E) 8%K/HY100 zeolite at T = 340 °C.

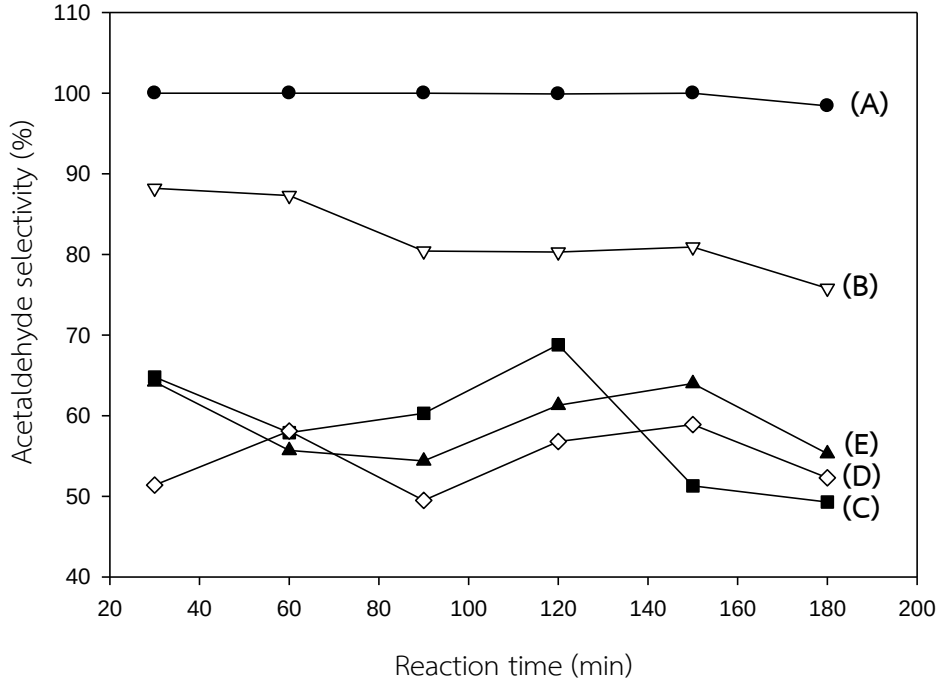

Figure 4.10 Acetaldehyde selectivity of (A) HY100, (B) 2%K/HY100 zeolite, (C) 4%K/HY100 zeolite, (D) 6%K/HY100 zeolite and (E) 8%K/HY100 zeolite at T = 340 °C.

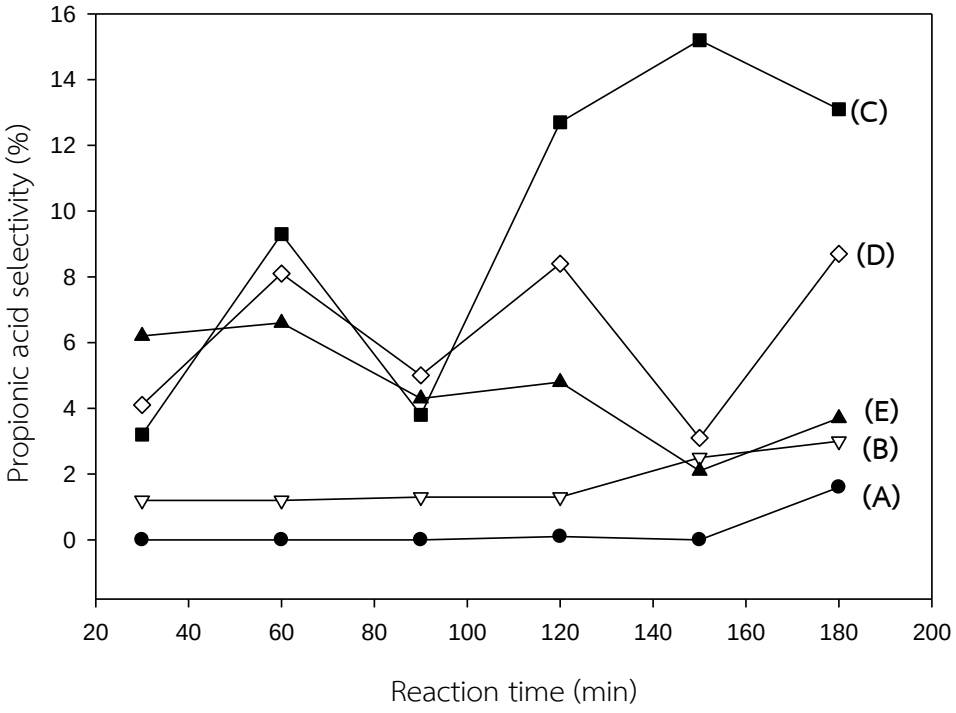

Figure 4.11 Propionic acid selectivity of (A) HY100, (B) 2%K/HY100 zeolite, (C) 4%K/HY100 zeolite, (D) 6%K/HY100 zeolite and (E) 8%K/HY100 zeolite at T = 340 °C.

4.2 The effect of different Si/Al molar ratios of HY zeolite (15, 100 and 500) in K over HY zeolite catalysts.

The catalyst nomenclatures are represent as below:

6**%K/HY15** represents the catalyst which have 6 wt.% K over HY zeolite with HY zeolite having Si/Al molar ratio of 15

6**%K/HY100** represents the catalyst which have 6 wt.% K over HY zeolite with HY zeolite having Si/Al molar ratio of 100

6**%K/HY500** represents the catalyst which have 6 wt.% K over HY zeolite with HY zeolite having Si/Al molar ratio of 500

4.2.1 Catalyst characterization

4.2.1.1 X-Ray diffraction pattern (XRD)

The X-ray diffraction (XRD) patterns of HY15 zeolite, HY100 zeolite and HY500 zeolite modified and unmodified with potassium at 6 wt.% are shown in Figure 4.12. The XRD patterns of all catalysts were observed at 2θ = 20.3°, 23.7°, 27.0°, 31.8°, 34.2°, 38.4° and 54.6° which are typical of zeolite faujasite [49]. Neither potassium nor any unidentified phase was observed on the XRD patterns of HY15 zeolite, HY100 zeolite and HY500 zeolite modified and unmodified with potassium. The identical XRD patterns of these samples and the parent zeolites indicated that the large surface area of the HY zeolites might contribute to good dispersion of potassium on the surface. For HY zeolite different Si/Al ratios, its is also obvious that the intensities of peaks decrease with loading of potassium at 6 wt.%. The result indicated that a potassium cations affect on the HY zeolite structure with different Si/Al molar ratios (HY15, HY100 and HY500).

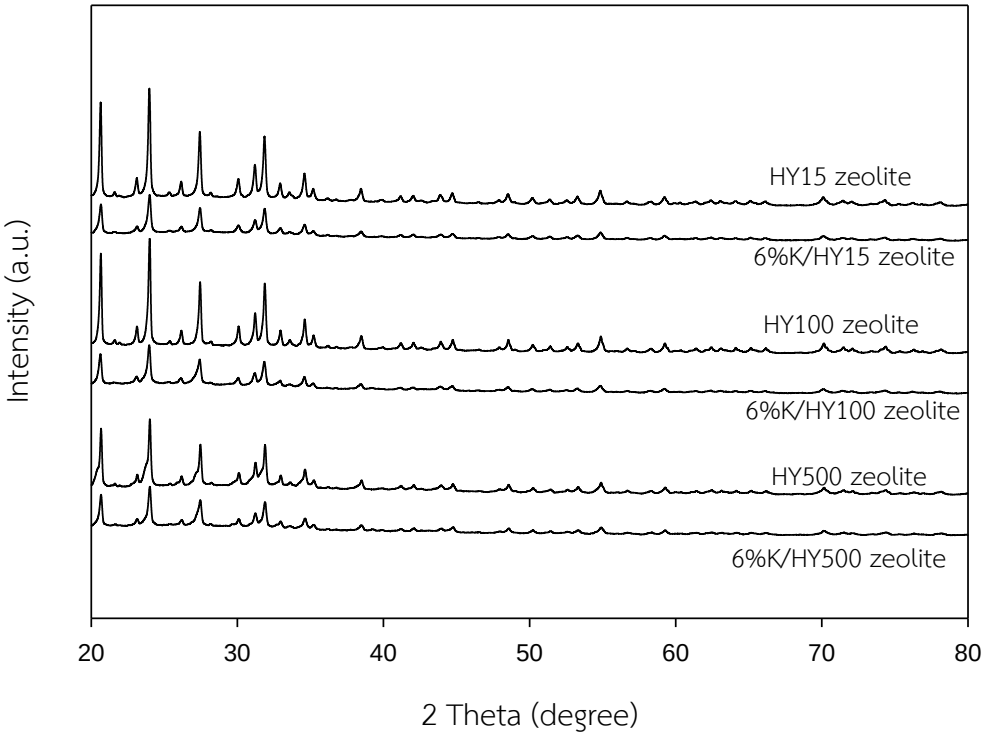

Figure 4.12 XRD patterns of HY15 zeolite, HY100 zeolite and HY500 zeolite modified and unmodified with potassium at 6 wt.%.

4.2.1.2 Nitrogen adsorption-desorption

The BET surface area, pore volume and pore size of catalysts were determined by nitrogen adsorption-desorption technique using Brunauer-Emmett-Teller (BET) method and Barret-Joyner-Halenda (BJH) method and there are given in Table 4.6. The BET surface area of HY zeolite for all Si/Al ratios were ranged between 617-717 m^2/g and increased with increasing Si/Al molar ratios, while the BET surface area of HY zeolite modified with potassium at 6 wt.% were ranged between 526-528 m^2/g that it had no significant change. The BET surface area of HY zeolite catalysts modified with potassium decreased compare to the HY zeolite for all Si/Al ratios. The pore volume of catalysts were range 0.16-0.23 cm^3/g. The decrease of BET surface area and pore volume may be due to the metal can access to the pores of HY zeolite, so that the pore may be blocked by the metal [8]. The pore size of HY15 zeolite, HY100 zeolite and HY500 zeolite modified with potassium at 6 wt.% were range 6.9-8.9 nm.

Table 4.6 The physiochemical properties of HY15 zeolite, HY100 zeolite and HY500 zeolite modified with potassium at 6 wt.%.

Catalysts	BET surface area (m^2/g)	Pore volume [a] (cm^3/g)	Pore size [a] (nm)
HY15 zeolite	617	0.19	9.4
HY100 zeolite	675	0.26	6.1
HY500 zeolite	717	0.26	7.5
6%K/HY15 zeolite	526	0.16	8.9
6%K/HY100 zeolite	527	0.23	6.9
6%K/HY500 zeolite	528	0.22	8.9

[a] Determined from the Barret-Joyner-Halenda (BJH) desorption method.

The N_2 adsorption-desorption isotherm of HY zeolite and 6%K/HY zeolite catalysts with different Si/Al molar ratios of HY zeolites are provided in Figure 4.13 and Figure 4.14, respectively. The isotherms of all catalyst can be classified as a type IV isotherm with H3-shaped hysteresis loops that are implied mesoporous structures [50].

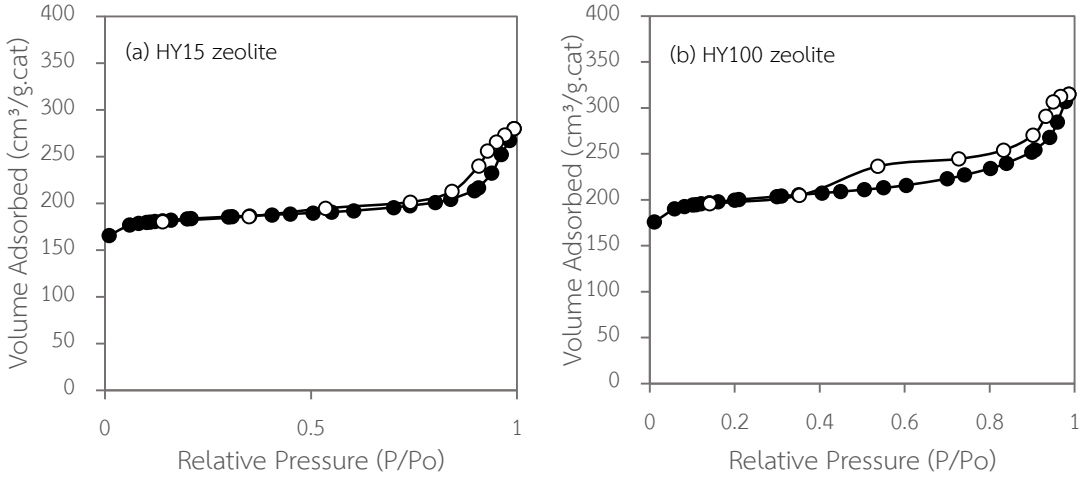

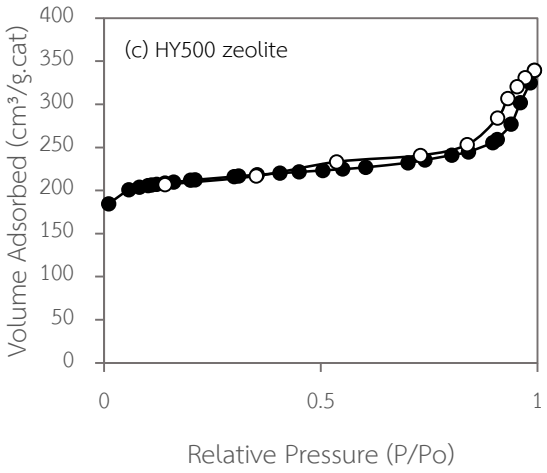

Figure 4.13 N_2 adsorption-desorption isotherm of HY15 zeolite, HY100 zeolite and HY500 zeolite.

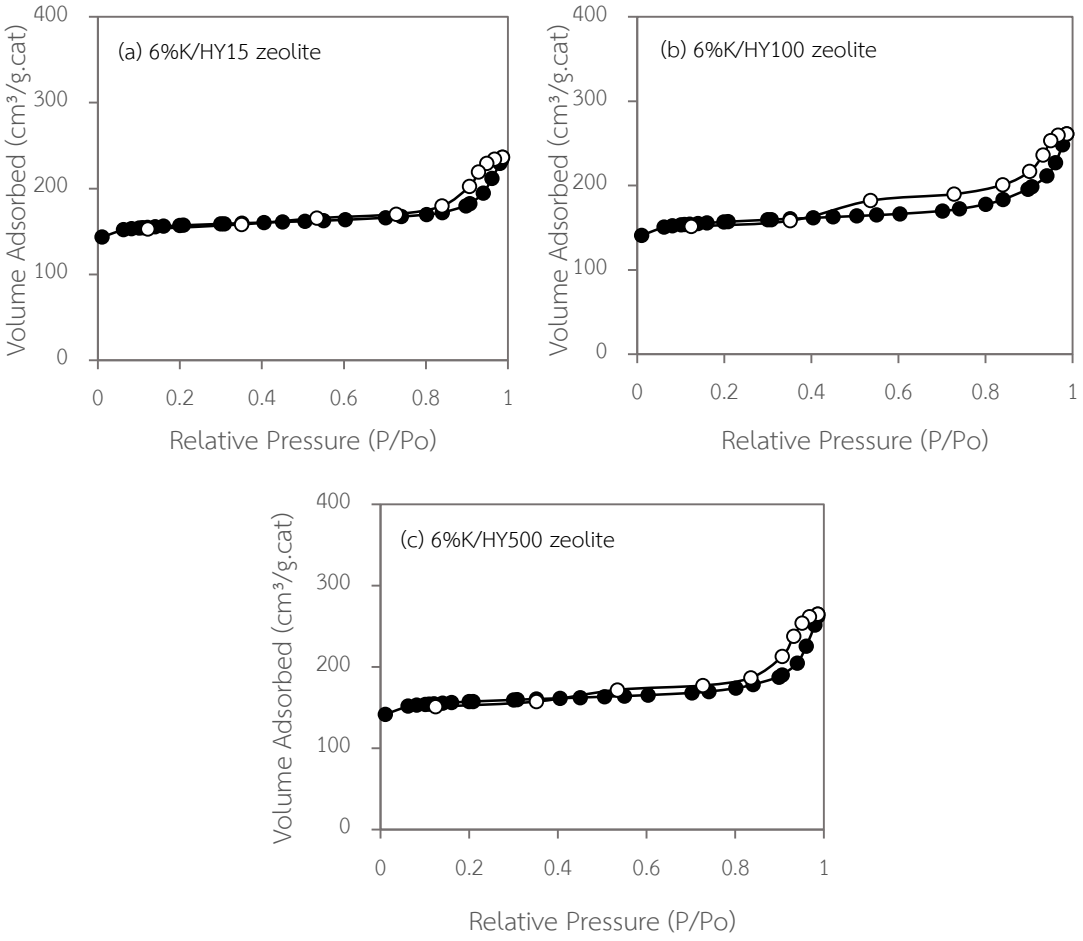

Figure 4.14 N_2 adsorption-desorption isotherm of HY15 zeolite, HY100 zeolite and HY500 zeolite modified with potassium at 6 wt.%.

4.2.1.3 Ammonia temperature program desorption (NH_3-TPD)

Ammonia temperature program desorption (NH_3-TPD) was used for evaluating the acidity on surface of HY15 zeolite, HY100 zeolite and HY500 zeolite modified with potassium at 6 wt.%. The amount of desorbed ammonia corresponds to the total surface acidity of the catalyst. In addition, the desorption temperature of desorbed ammonia corresponds to the acid strength on surface of the catalysts.

NH_3-TPD profiles of HY15 zeolite, HY100 zeolite and HY500 zeolite modified with potassium at 6 wt.% are shown in Figure 4.15. The temperature ranges of regions I (100-200 °C), II (200-400 °C) and III (400-600 °C) represent weak, medium and strong acid sites, respectively [36]. The 6%K/HY15 zeolite catalyst show higher acid strengths than 6%K/HY100 zeolite and 6%K/HY500 zeolite in view of the NH_3-desorption temperatures in Figure 4.15. There is a tendency that the surface acidity and the fractions of medium and strong acid sites were decreased with increasing Si/Al molar ratios of HY zeolite (from HY15 to HY500). The total acidity of 6%K/HY zeolite catalysts with different Si/Al molar ratios were quantified based on the area of NH_3 desorption peaks in the TPD profiles, and the results are shown in Table 4.7. The total acidity of catalysts decreased in the following order: 6%K/HY15 zeolite > 6%K/HY100 zeolite > 6%K/HY500 zeolite and it was ranged between 0.75-25.9 mmol NH_3/g.cat. The results shown that total acidity decreased with increasing of Si/Al molar ratio of HY zeolite. However, the catalysts with higher or lower acidity can catalyze lactic acid dehydration to acetaldehyde, and propionic acid, respectively.

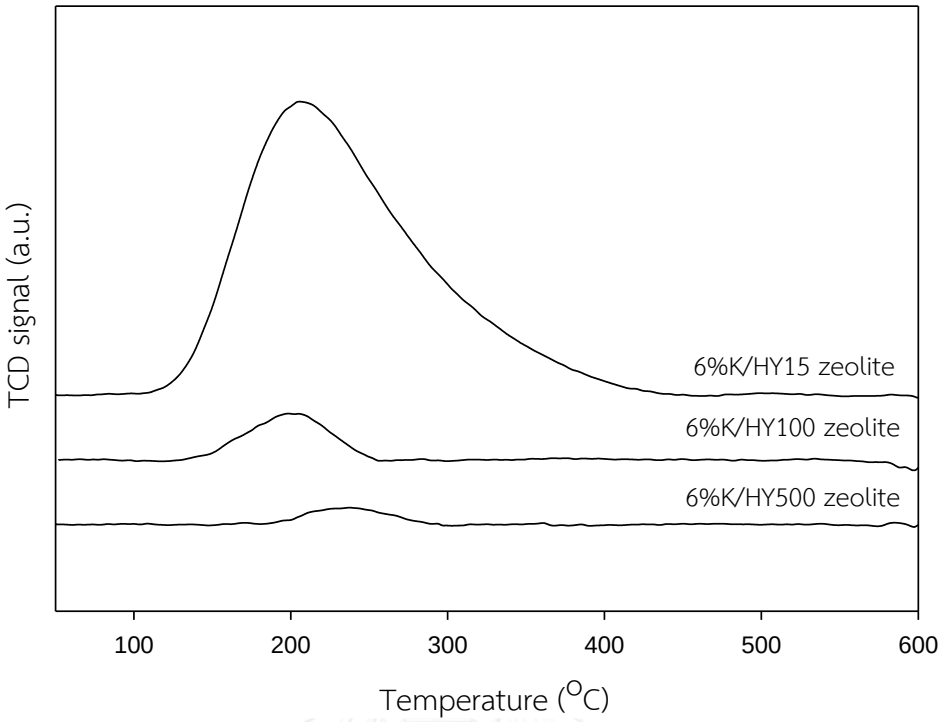

Figure 4.15 NH_3-TPD profiles of HY15 zeolite, HY100 zeolite and HY500 zeolite modified with potassium at 6 wt.%.

Table 4.7 Total acidity of HY15 zeolite, HY100 zeolite and HY500 zeolite modified with potassium at 6 wt.%.

Catalysts	Total acidity (mmol NH_3/g.cat)
6%K/HY15 zeolite	25.9
6%K/HY100 zeolite	2.01
6%K/HY500 zeolite	0.75

4.2.1.4 Carbon dioxide temperature program desorption (CO_2-TPD)

Carbon dioxide temperature program desorption (CO_2-TPD) was used for evaluating the basicity on surface of HY15 zeolite, HY100 zeolite and HY500 zeolite modified with potassium at 6 wt.%. The amount of desorbed carbon dioxide corresponds to the total surface basicity of the catalyst. In addition, the desorption temperature of desorbed carbon dioxide corresponds to the base strength on surface of the catalysts.

CO_2-TPD profiles of HY15 zeolite, HY100 zeolite and HY500 zeolite modified with potassium at 6 wt.% are shown in Figure 4.16. 6%K/HY100 zeolite and 6%K/HY100 zeolite have one large peak at around 100 $^{\circ}$C ascribed to the weak basic sites of the catalysts, while 6%K/HY15 zeolite have slightly part of peak at around 200-300 $^{\circ}$C ascribed to the medium basic sites of catalysts. The 6%K/HY500 zeolite show higher basic sites than 6%K/HY100 zeolite and 6%K/HY15 zeolite catalyst in view of the CO_2-desorption temperatures in Figure 4.16. There is a tendency that the surface basicity of HY zeolite increase with increasing Si/Al molar ratios from 15, 100 and 500, respectively. The total basicity of different samples were quantified based on the area of CO_2 desorption peaks in the TPD profiles, and the results are shown in Table 4.8. The total basicity of catalysts decreased in the following order: 6%K/HY500 zeolite > 6%K/HY100 zeolite > 6%K/HY15 zeolite. It is known that the catalysts with higher basicity can catalyze lactic acid dehydration to undesirable products such as propionic acid.

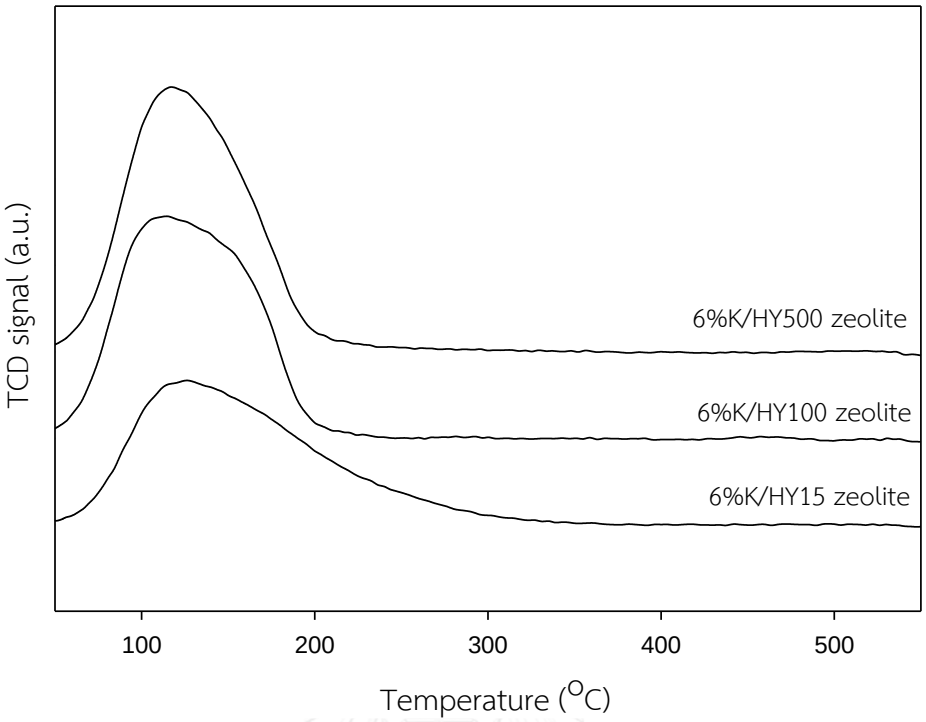

Figure 4.16 CO_2-TPD profiles of HY15 zeolite, HY100 zeolite and HY500 zeolite modified with potassium at 6 wt.%.

Table 4.8 Total basicity of HY15 zeolite, HY100 zeolite and HY500 zeolite modified with potassium at 6 wt.%.

Catalysts	Total basicity (μmol CO_2/g.cat)
6%K/HY15 zeolite	4.13
6%K/HY100 zeolite	5.18
6%K/HY500 zeolite	5.23

4.2.1.5 Scanning electron microscope and energy dispersive X-ray spectroscopy (SEM-EDX)

The morphology of HY15 zeolite, HY100 zeolite and HY500 zeolite modified with potassium at 6 wt.% studied by Scanning Electron Microscopy (SEM) are shown in Figure 4.17. All catalysts have similar surface morphology and uniform in size distribution. It was found that potassium over HY15 zeolite, HY100 zeolite and HY500 zeolite and Si/Al molar ratio of HY zeolites did not affect the morphology of catalysts.

The elements and potassium dispersion over the HY zeolite catalysts surface for all Si/Al molar ratios were determined by energy dispersive X-ray spectroscopy (EDX) in Table 4.9 and Figure 4.18. The results show that all catalyst have a good dispersion of potassium on the surface of HY zeolite catalyst, consistent with the XRD investigation. The HY15 zeolite, HY100 zeolite and HY500 zeolite modified with potassium at 6 wt.% from EDX results shown higher amount of potassium than initial loading because EDX can detect only the surface of catalysts.

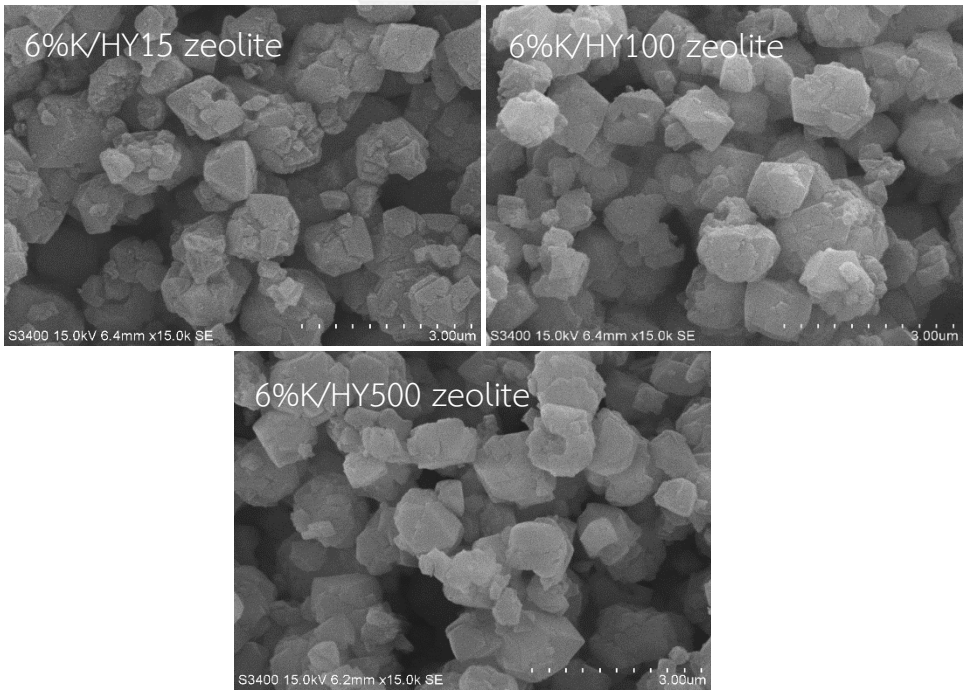

Figure 4.17 SEM images of HY15 zeolite, HY100 zeolite and HY500 zeolite modified with potassium at 6 wt.%.

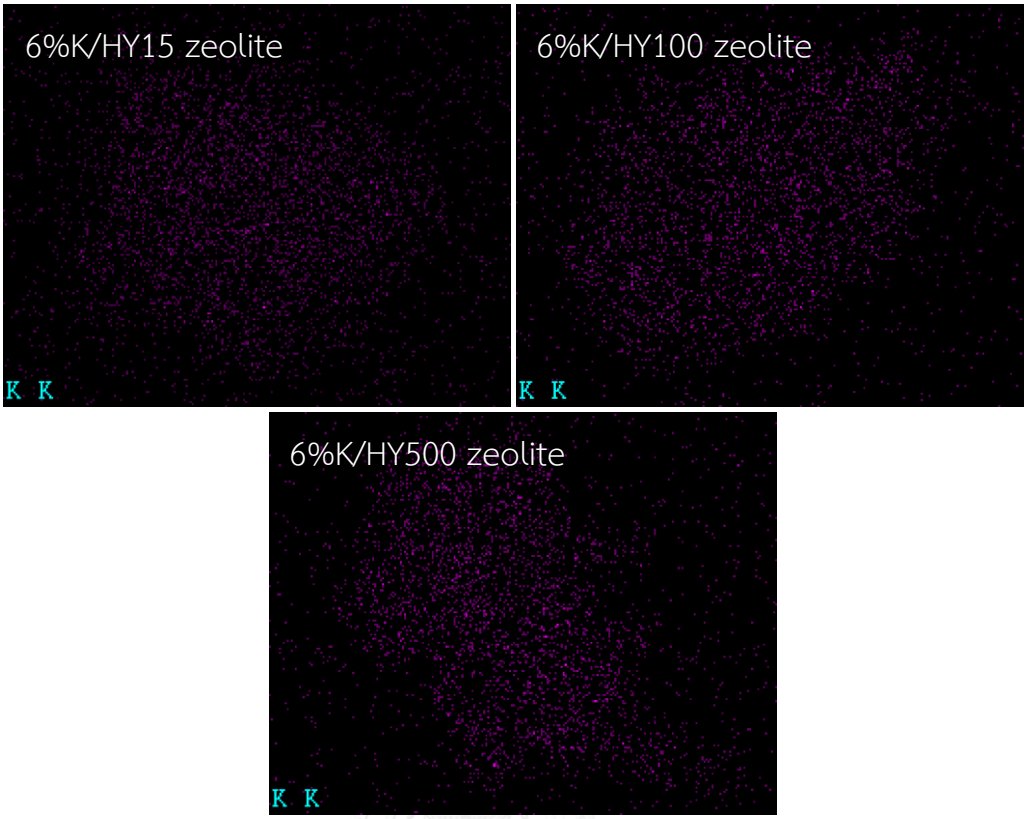

Figure 4.18 EDX images of potassium on the surface of HY15 zeolite, HY100 zeolite and HY500 zeolite modified with potassium at 6 wt.%.

Table 4.9 The elemental dispersion over the surface of HY15 zeolite, HY100 zeolite and HY500 zeolite modified with potassium at 6 wt.%.

Catalysts	Percent by weight (wt.%)			
	O	Al	Si	K
6%K/HY15 zeolite	45.29	6.22	42.16	6.34
6%K/HY100 zeolite	46.95	1.18	45.55	6.32
6%K/HY500 zeolite	43.67	0.18	49.17	6.97

4.2.1.6 Thermogravimetric analysis (TGA)

TGA analysis that was used for study carbon deposition of the spent catalysts are investigated in Figure 4.19. The slightly weight loss of all spent catalyst around 100 ℃ was occurred that was assigned to the evaporation of moisture in catalysts. Figure 4.19, the weight loss were observed at around 300-400 ℃ in the following order: 6%K/HY15 zeolite > 6%K/HY100 zeolite > 6%K/HY500 zeolite which should be attributed to the carbon deposits over spent catalyst [52]. Moreover, the 6%K/HY15 zeolite shown weight loss at around 600-700 ℃ that was assigned to two kinds of carbon deposit sites on the surface [42].

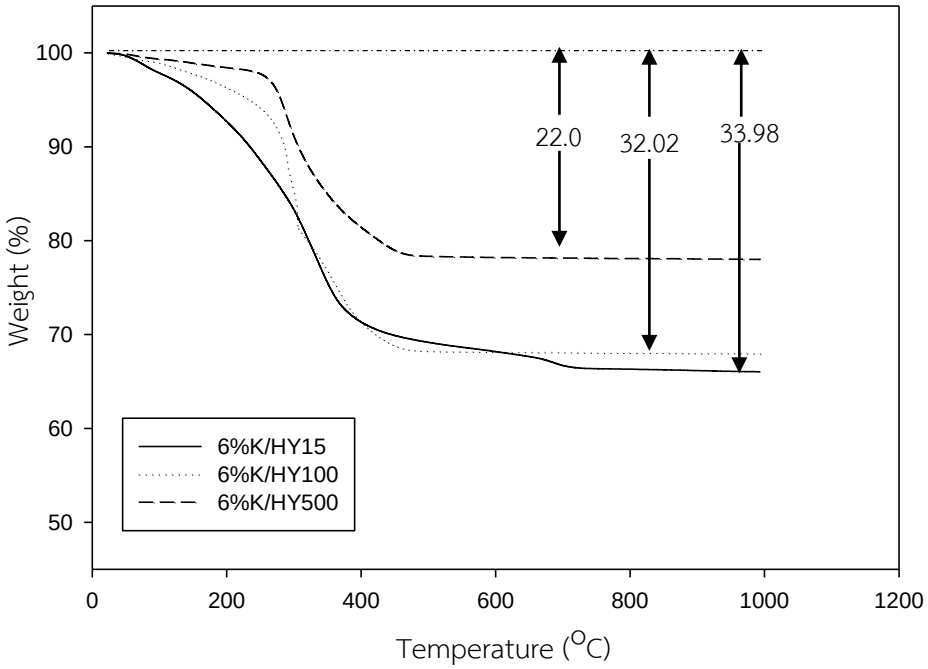

Figure 4.19 TGA results of spent HY15 zeolite, HY100 zeolite and HY500 zeolite modified with potassium at 6 wt.% after 180 min of reaction.

4.2.2 Activity in lactic acid dehydration reaction

The activity of HY15 zeolite, HY100 zeolite and HY500 zeolite modified with potassium at 6 wt.% were test in lactic acid dehydration reaction. The catalyst 0.1 g was packed in glass reactor with quartz wool and preheated at 340 °C for 30 min. After that, the lactic acid solution with concentration 34%volume were injected into the vaporizer at flow rate 1 ml/h and the vapor was carried through the catalyst bed by nitrogen. The gas products were analyzed by GC with a DB-WAX capillary column and FID detector.

The lactic acid conversion and product selectivity in lactic acid dehydration reaction at reaction temperature 340 °C and 90 min are shown in Figure 4.20 and Table 4.10. The lactic acid conversion of HY15 zeolite, HY100 zeolite and HY500 zeolite modified with potassium at 6 wt.% were shown 100% and acrylic acid selectivity were ranged between 4.7-45.5%. The 6%K/HY100 zeolite catalyst was the best for lactic acid dehydration with 100% conversion and 45.5% selectivity for acrylic acid. The acrylic acid selectivity of catalysts decreased in the following order: 6%K/HY100 zeolite > 6%K/HY500 zeolite > 6%K/HY15 zeolite catalyst. From table 4.10, it also seen that with increasing Si/Al molar ratio from 15 to 100, the formation of acetaldehyde is obviously suppressed with its selectivity decreasing from 90% to 49.5% and AA selectivity increasing from 4.7% to 45.5%. The decline of acetaldehyde selectivity should be ascribed to decrease of total acidity of 6%K/HY100 zeolite as shown in NH_3-TPD result since the formation of acetaldehyde from lactic acid reactant is preferred over acidic catalysts. The decrease of total acidity caused the suppression decarbonylation and decarboxylation reaction of lactic acid to acetaldehyde. The 6%K/HY500 zeolite higher propionic acid selectivity than 6%K/HY15 zeolite and 6%K/HY100 zeolite because the 6%K/HY500 zeolite with high surface basicity can catalyze lactic acid dehydration to propionic acid via reduction reaction of lactic acid [52]. The catalytic results indicated that the HY zeolite catalyst should suitable Si/Al molar ratio for catalyze lactic acid dehydration to acrylic acid.

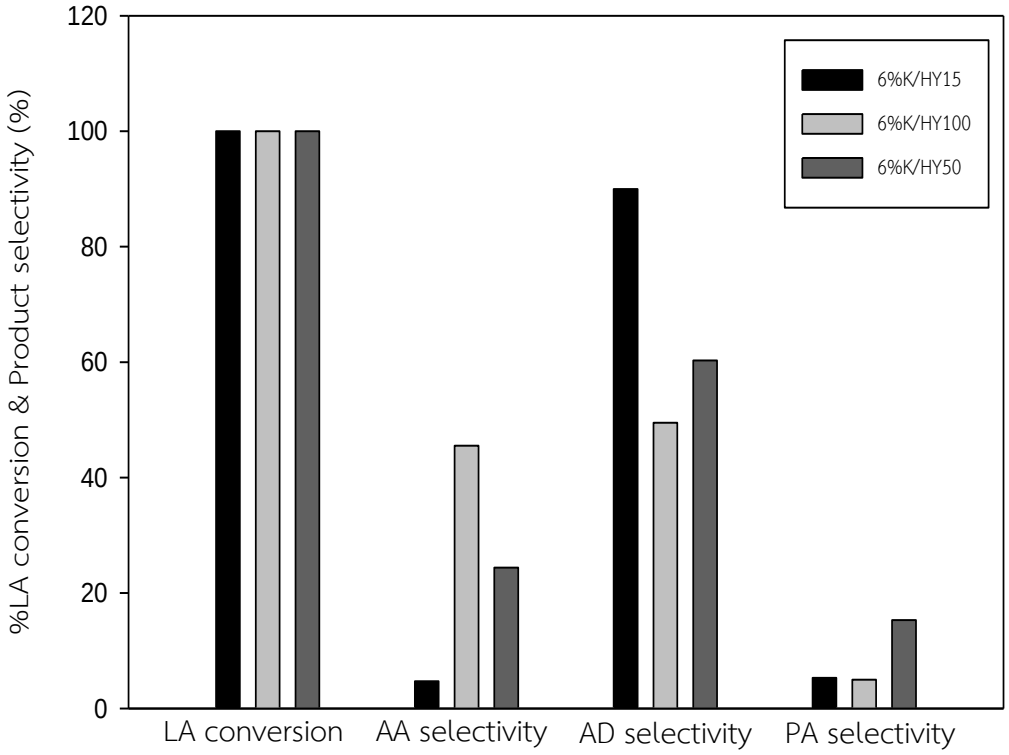

Figure 4.20 Lactic acid conversion and product selectivity of HY15 zeolite, HY100 zeolite and HY500 zeolite modified with potassium at 6 wt.% at reaction temperature 340 °C and t = 90 min.

Table 4.10 The catalytic performance of HY15 zeolite, HY100 zeolite and HY500 zeolite modified with potassium at 6 wt.%.

Catalysts	Lactic acid Conversion (%)	Product Selectivity [a] (%)		
		AA	AD	PA
6%K/HY15 zeolite	100	4.7	90.0	5.3
6%K/HY100 zeolite	100	45.5	49.5	5.0
6%K/HY500 zeolite	100	24.4	60.3	15.3

[a] AA-Acrylic acid, AD-acetaldehyde, PA-propionic acid. Reaction time 90 min, T=340 °C

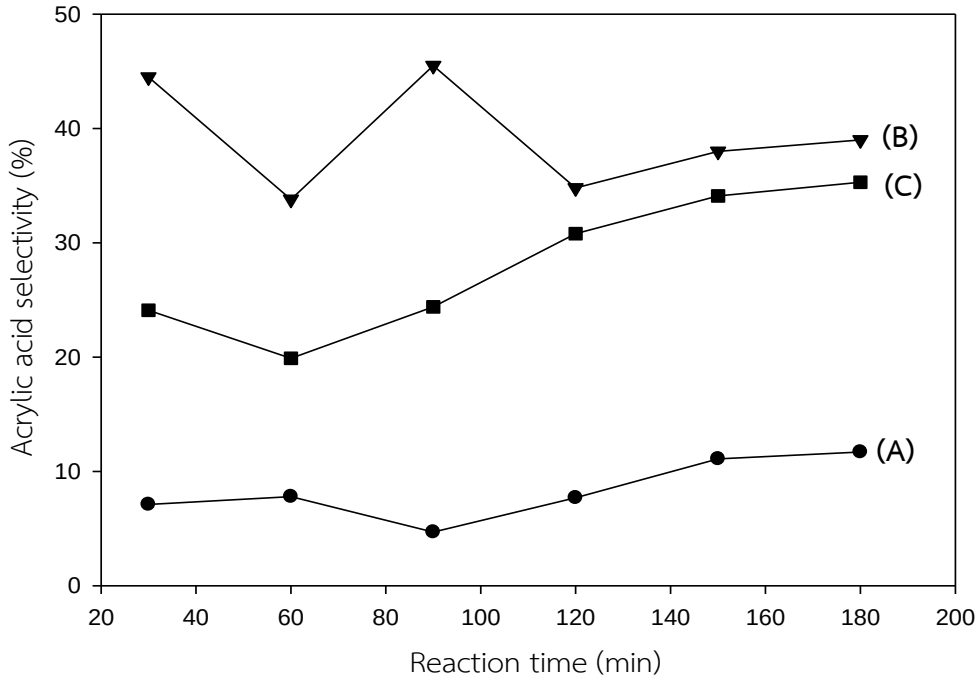

Figure 4.21 Acrylic acid selectivity of (A) 6%K/HY15 zeolite, (B) 6%K/HY100 zeolite, and (C) 6%K/HY500 zeolite at T = 340 °C.

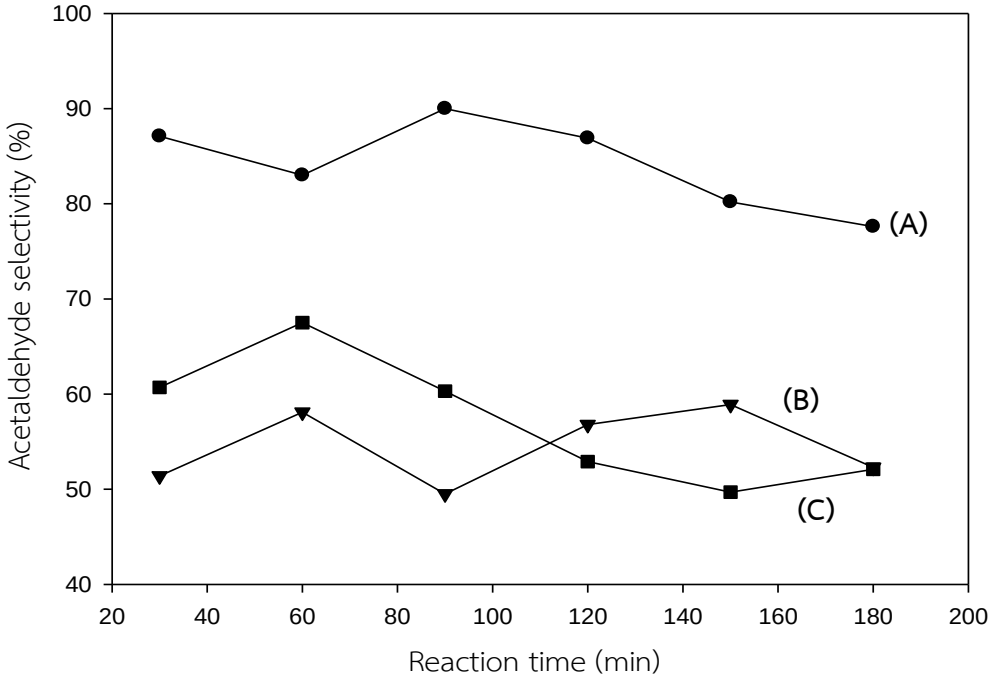

Figure 4.22 Acetaldehyde selectivity of (A) 6%K/HY15 zeolite, (B) 6%K/HY100 zeolite, and (C) 6%K/HY500 zeolite at T = 340 °C.

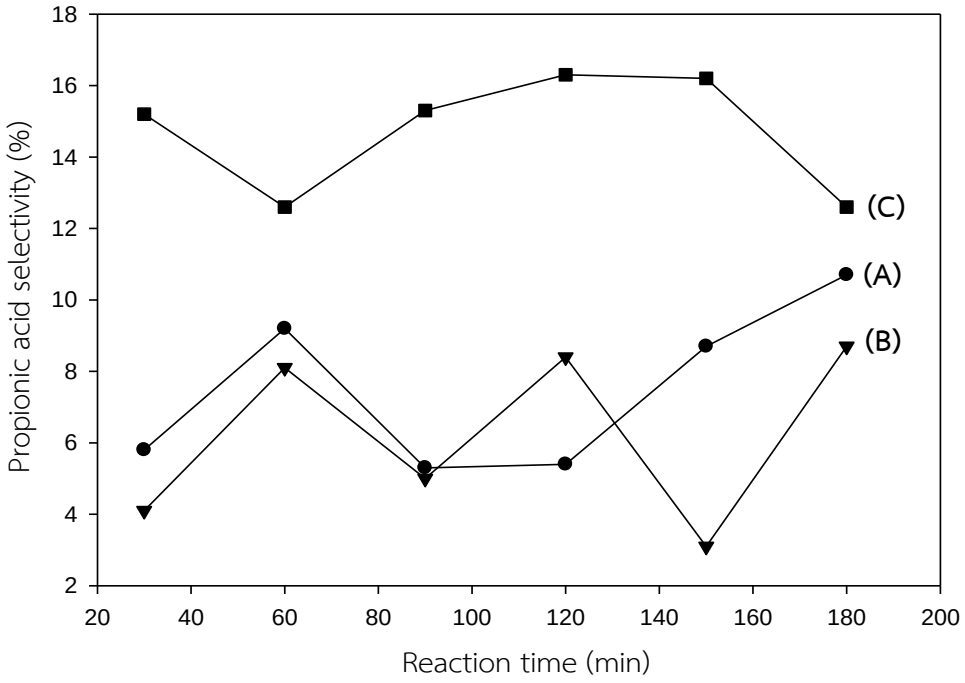

Figure 4.23 Propionic acid selectivity of (A) 6%K/HY15 zeolite, (B) 6%K/HY100 zeolite, and (C) 6%K/HY500 zeolite at T = 340 °C.

4.3 The effect of support Al_2O_3 and HY100 zeolite ratios from the second part modified with potassium at 6 wt.%.

The catalyst nomenclatures are represent as below:

6%K/3Al_2O_3-1HY100 represents the catalyst which have 6 wt.% K over Al_2O_3-HY100 zeolite with Al_2O_3 and HY100 zeolite ratio of 3:1

6%K/1Al_2O_3-1HY100 represents the catalyst which have 6 wt.% K over Al_2O_3-HY100 zeolite with Al_2O_3 and HY100 zeolite ratio of 1:1

6%K/1Al_2O_3-3HY100 represents the catalyst which have 6 wt.% K over Al_2O_3-HY100 zeolite with Al_2O_3 and HY100 zeolite ratio of 1:3

4.3.1 Catalyst characterization

4.3.1.1 X-Ray diffraction (XRD)

The X-ray diffraction (XRD) patterns of Al_2O_3, 6%K/HY100 zeolite and 6%K/Al_2O_3-HY100 zeolite with different Al_2O_3 and HY100 zeolite ratios (3:1, 1:1 and 1:3) are shown in Figure 4.24. The XRD patterns of Al_2O_3 shown two peaks at 2θ = 45.5° and 66.7°, which are ascribed to alumina crystalline phases. The XRD patterns of 6%K/HY100 zeolite catalysts were observed at 2θ = 20.3°, 23.7°, 27.0°, 31.8°, 34.2°, 38.4° and 54.6° which are typical of zeolite faujasite [49]. Neither potassium nor any unidentified phase was observed on the XRD patterns of HY100 zeolite modified with potassium. The identical XRD patterns of these samples and the parent zeolites indicated that the large surface area of the HY100 zeolites might contribute to good dispersion of potassium on HY100 zeolite. The mixed Al_2O_3 and HY100 zeolite had similar pattern alumina and zeolite faujasite except 6%K/3Al_2O_3-1HY100 zeolite catalyst. The intensities of peaks decrease with increasing of Al_2O_3 content, indicating that the higher of Al_2O_3 content and potassium modification affect to destroy the HY100 zeolite structure.

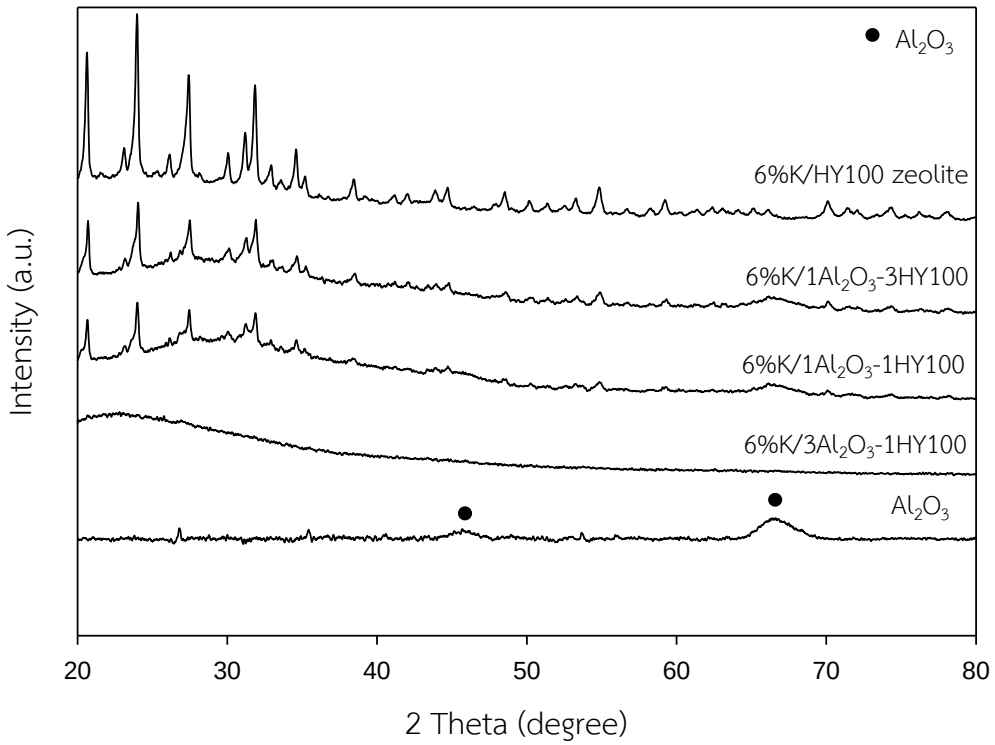

Figure 4.24 XRD patterns of Al_2O_3, 6%K/HY100 zeolite and 6%K/Al_2O_3-HY100 zeolite with different Al_2O_3 and HY100 zeolite ratios (3:1, 1:1 and 1:3).

4.3.1.2 Nitrogen adsorption-desorption

The textural properties of catalysts were investigated by nitrogen adsorption-desorption technique using Brunauer-Emmett-Teller (BET) method and Barret-Joyner-Halenda (BJH) method. The BET surface area, pore volume and pore size were summarized in Table 4.11. The BET surface area of 6%K/Al_2O_3-HY100 zeolite with different Al_2O_3 and HY100 zeolite ratios (3:1, 1:1 and 1:3) were ranged between 75-447 m^2/g. The BET surface area of mixed Al_2O_3 and HY100 zeolite modified with potassium at 6 wt.% decreased significantly with increasing Al_2O_3 content. The pore volume of catalysts were range 0.18-0.24 cm^3/g. The decrease of BET surface area and pore volume may be due to the pores of Al_2O_3-HY100 zeolite filled with potassium species, so that the pore may be blocked by the metal [42] and the higher Al_2O_3 content that

cause seriously destroys HY100 zeolite structure by dealumination [53], consistent with the XRD investigation. The pore size of 6%K/Al_2O_3-HY100 zeolite with different Al_2O_3 and HY100 zeolite ratios (3:1, 1:1 and 1:3) were range 4.6-7.0 nm.

Table 4.11 The physiochemical properties of 6%K/Al_2O_3-HY100 zeolite with different Al_2O_3 and HY100 zeolite ratios (3:1, 1:1 and 1:3).

Catalysts	BET surface area (m^2/g)	Pore volume [a] (cm^3/g)	Pore size [a] (nm)
6%K/3Al_2O_3-1HY100	75	0.18	7.0
6%K/1Al_2O_3-1HY100	321	0.21	4.6
6%K/1Al_2O_3-3HY100	447	0.24	5.9

[a] Determined from the Barret-Joyner-Halenda (BJH) desorption method.

The N_2 adsorption-desorption isotherm of 6%K/Al_2O_3-HY100 zeolite with different Al_2O_3 and HY100 zeolite ratios (3:1, 1:1 and 1:3) are provided in Figure 4.25. The isotherms of all catalyst can be classified as a type IV isotherm with H3-shaped hysteresis loops that are implied the mesoporous structures [50].

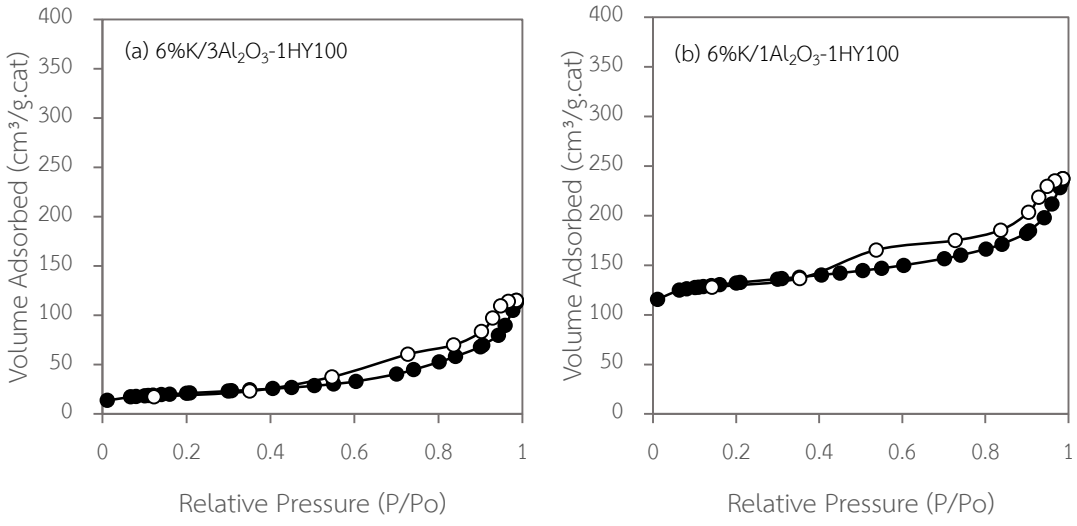

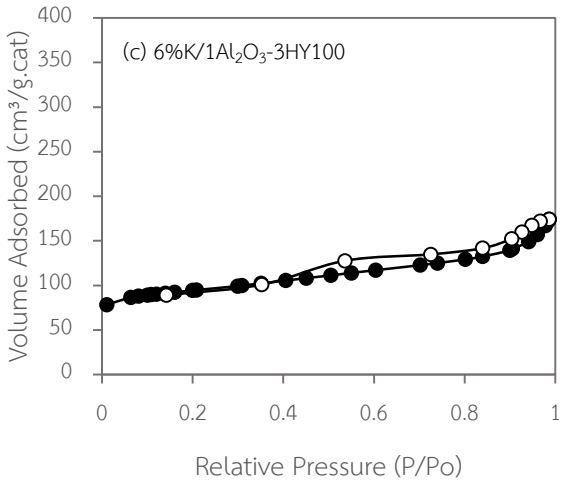

Figure 4.25 N_2 adsorption-desorption isotherm of 6%K/Al_2O_3-HY100 zeolite with different Al_2O_3 and HY100 zeolite ratios (3:1, 1:1 and 1:3).

4.3.1.3 Ammonia temperature program desorption (NH_3-TPD)

Ammonia temperature program desorption (NH_3-TPD) was used for evaluating the acidity on surface of 6%K/Al_2O_3-HY100 zeolite with different Al_2O_3 and HY100 zeolite ratios (3:1, 1:1 and 1:3). The amount of desorbed ammonia corresponds to the total surface acidity of the catalyst. In addition, the desorption temperature of desorbed ammonia corresponds to the acid strength on surface of the catalysts.

NH_3-TPD profiles of 6%K/Al_2O_3-HY100 zeolite with different Al_2O_3 and HY100 zeolite ratios (3:1, 1:1 and 1:3) are shown in Figure 4.26. The temperature ranges of regions I (100-200 ℃), II (200-400 ℃) and III (400-600 ℃) represent weak, medium and strong acid sites, respectively [36]. The 6%K/1Al_2O_3-3HY100 zeolite catalyst shown only one peak around 100-300 ℃ indicating the presence of weak and medium acid sites, whereas 6%K/1Al_2O_3-1HY100 and 6%K/3Al_2O_3-1HY100 zeolite catalyst exhibited two desorption peaks at low temperature represent weak acid site and high temperature indicating the presence of medium and strong acid sites for 6%K/1Al_2O_3-1HY100 and 6%K/3Al_2O_3-1HY100, respectively. There is a tendency that the fractions of medium and strong acid sites decrease with decreasing Al_2O_3 content in 6%K/Al_2O_3-HY100 zeolite catalyst. The total acidity of different samples were quantified based on the area of NH_3 desorption peaks in the TPD profiles, and the results are shown in Table

4.12. The total acidity of catalysts decreased in the following order: 6%K/1Al_2O_3-3HY100 zeolite > 6%K/1Al_2O_3-1HY100 zeolite > 6%K/3Al_2O_3-1HY100 zeolite but the 6%K/3Al_2O_3-1HY100 had more strong acid sites than other catalyst. The results shown that total acidity decreased with increasing Al_2O_3 content due to the Al_2O_3 have more weak and medium acid sites than strong acid sites which can reduce the total acidity by potassium addition. However, it is known that the catalysts with high strong acid sites can catalyze lactic acid dehydration to undesirable products such as acetaldehyde.

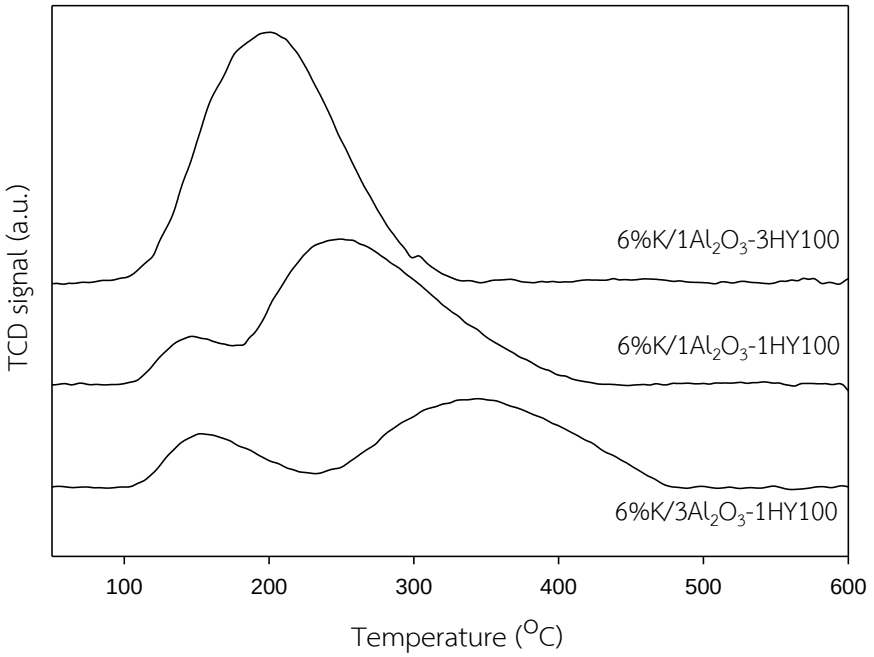

Figure 4.26 NH_3-TPD profiles of 6%K/Al_2O_3-HY100 zeolite with different Al_2O_3 and HY100 zeolite ratios (3:1, 1:1 and 1:3).

Table 4.12 Total acidity of 6%K/Al_2O_3-HY100 zeolite with different Al_2O_3 and HY100 zeolite ratios (3:1, 1:1 and 1:3).

Catalysts	Total acidity (mmol NH_3/g.cat)
6%K/1Al_2O_3-3HY100	11.82
6%K/1Al_2O_3-1HY100	9.10
6%K/3Al_2O_3-1HY100	7.25

4.3.1.4 Carbon dioxide temperature program desorption (CO_2-TPD)

Carbon dioxide temperature program desorption (CO_2-TPD) was used for evaluating the basicity on surface of 6%K/Al_2O_3-HY100 zeolite with different Al_2O_3 and HY100 zeolite ratios (3:1, 1:1 and 1:3). The amount of desorbed carbon dioxide corresponds to the total surface basicity of the catalyst. In addition, the desorption temperature of desorbed carbon dioxide corresponds to the base strength on surface of the catalysts.

CO_2-TPD profiles of 6%K/Al_2O_3-HY100 zeolite with different Al_2O_3 and HY100 zeolite ratios (3:1, 1:1 and 1:3) are shown in Figure 4.27. All catalysts have one large peak at around 50-250 $^{\circ}$C ascribed to the weak basic sites of the catalysts. The 6%K/3Al_2O_3-1HY100 zeolite show higher basic sites than 6%K/1Al_2O_3-3HY100 zeolite catalyst in view of the CO_2-desorption temperatures in Figure 4.27. There is a tendency that the surface basicity of 6%K/Al_2O_3-HY100 zeolite with different Al_2O_3 and HY100 zeolite ratios (3:1, 1:1 and 1:3) increase with increasing Al_2O_3 content. The total basicity of different samples were quantified based on the area of CO_2 desorption peaks in the TPD profiles, and the results are shown in Table 4.13. The total basicity of catalysts decreased in the following order: 6%K/3Al_2O_3-1HY100 zeolite > 6%K/1Al_2O_3-1HY100 zeolite > 6%K/1Al_2O_3-3HY100 zeolite. The 6%K/3Al_2O_3-1HY100 zeolite catalyst had a higher total basicity than the other catalysts due to it high Al_2O_3 content affect to increase interaction between potassium and Al_2O_3.

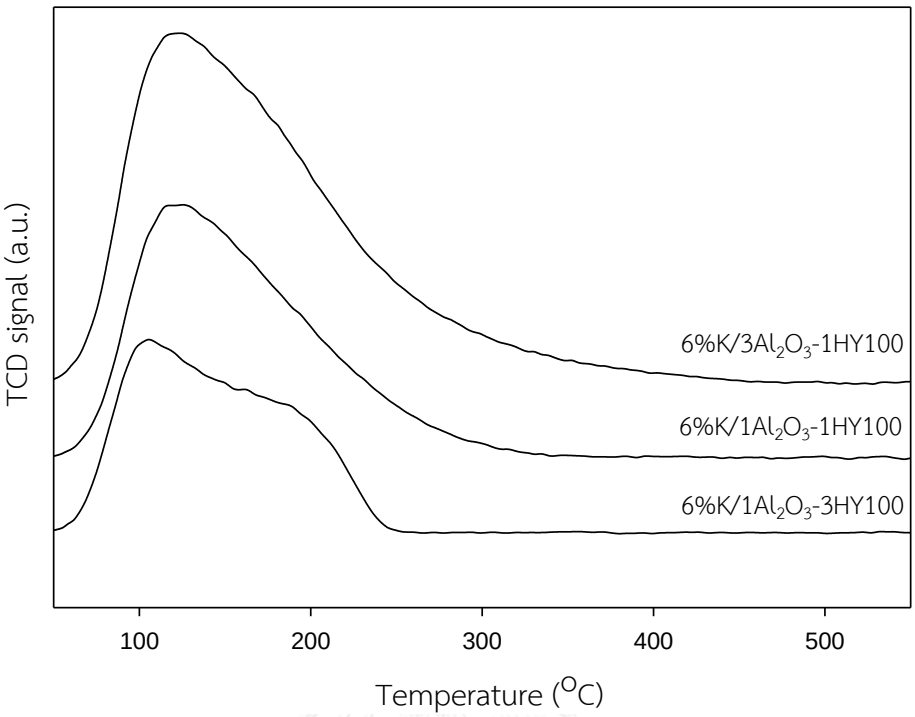

Figure 4.27 CO_2-TPD profiles of 6%K/Al_2O_3-HY100 zeolite with different Al_2O_3 and HY100 zeolite ratios (3:1, 1:1 and 1:3).

Table 4.13 Total basicity of 6%K/Al_2O_3-HY100 zeolite with different Al_2O_3 and HY100 zeolite ratios (3:1, 1:1 and 1:3).

Catalysts	Total basicity (μmol CO_2/g.cat)
6%K/3Al_2O_3-1HY100	13.01
6%K/1Al_2O_3-1HY100	8.05
6%K/1Al_2O_3-3HY100	5.80

4.3.1.5 Scanning electron microscope and energy dispersive X-ray spectroscopy (SEM-EDX)

The morphology of 6%K/Al_2O_3-HY100 zeolite with different Al_2O_3 and HY100 zeolite ratios (3:1, 1:1 and 1:3) studied by Scanning Electron Microscopy (SEM) are shown in Figure 4.28. All catalysts have similar surface morphology and uniform in size distribution. It was found that potassium over Al_2O_3-HY100 zeolite with different Al_2O_3 and HY100 zeolite ratios (3:1, 1:1 and 1:3) did not affect the morphology of catalysts. The elements and potassium dispersion over Al_2O_3-HY100 zeolite with different Al_2O_3 and HY100 zeolite ratios (3:1, 1:1 and 1:3) were determined by energy dispersive X-ray spectroscopy (EDX) in Table 4.14 and Figure 4.29. All catalyst have a good dispersion of potassium on the surface of Al_2O_3-HY100 zeolite, consistent with the XRD investigation. The catalyst modified with potassium from EDX results shown higher amount of potassium than initial loading because EDX can detect only the surface of catalysts.

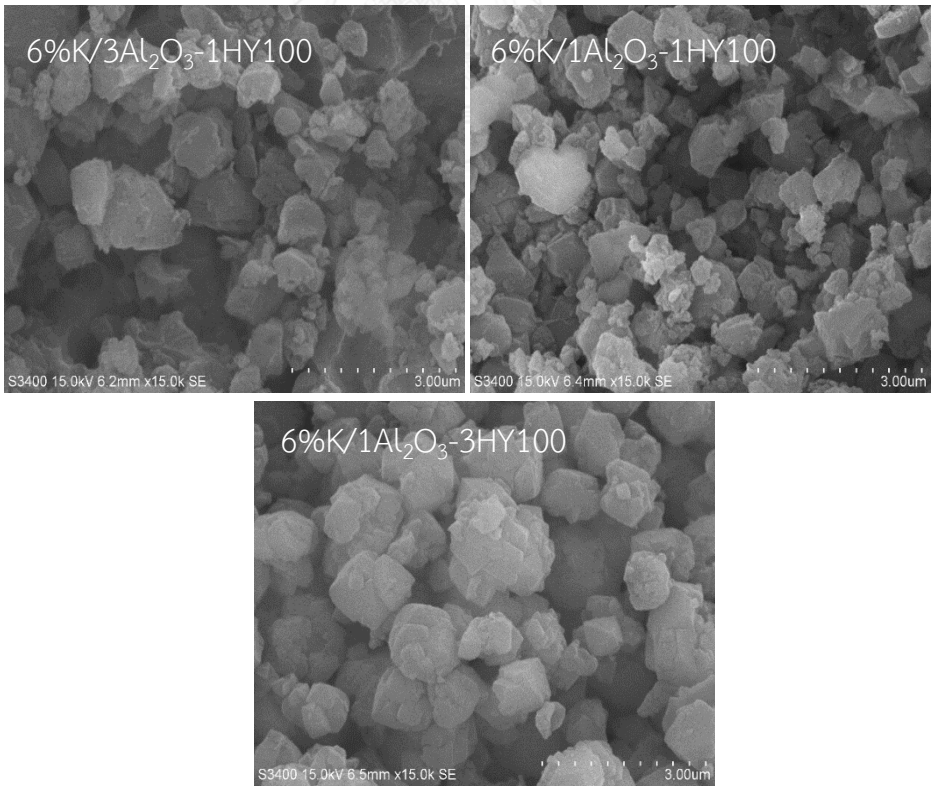

Figure 4.28 SEM images of 6%K/Al_2O_3-HY100 zeolite with different Al_2O_3 and HY100 zeolite ratios (3:1, 1:1 and 1:3).

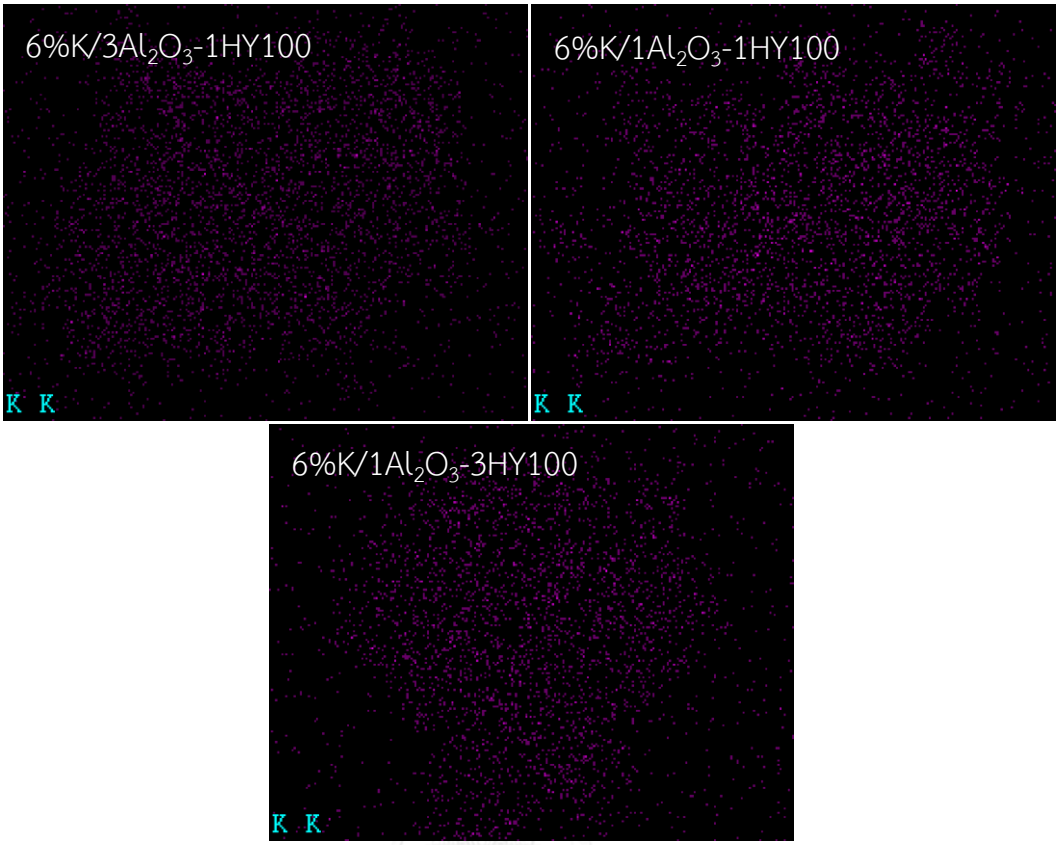

Figure 4.29 EDX images of potassium on the surface of 6%K/Al_2O_3-HY100 zeolite with different Al_2O_3 and HY100 zeolite ratios (3:1, 1:1 and 1:3).

Table 4.14 The elemental dispersion over the surface of 6%K/Al_2O_3-HY100 zeolite with different Al_2O_3 and HY100 zeolite ratios (3:1, 1:1 and 1:3).

Catalysts	Percent by weight (wt.%)			
	O	Al	Si	K
6%K/3Al_2O_3-1HY100	43.96	24.15	25.6	6.29
6%K/1Al_2O_3-1HY100	43.56	11.96	37.65	6.83
6%K/1Al_2O_3-3HY100	46.66	1.94	45.31	6.09

4.3.1.6 Thermogravimetric analysis (TGA)

Thermogravimetric analysis (TGA) was used for study carbon deposition of the spent 6%K/Al_2O_3-HY100 zeolite with different Al_2O_3 and HY100 zeolite ratios (3:1, 1:1 and 1:3) after 180 min of reaction are investigated in Figure 4.30. The slightly weight loss of all spent catalyst around 100 ℃ could be assigned to the evaporation of moisture in catalysts. The weight loss were observed at around 300-400 ℃ in the following order: 6%K/3Al_2O_3-1HY100 zeolite > 6%K/1Al_2O_3-1HY100 zeolite > 6%K/1Al_2O_3-3HY100 zeolite which should be attributed to the carbon deposits over spent catalyst [52].

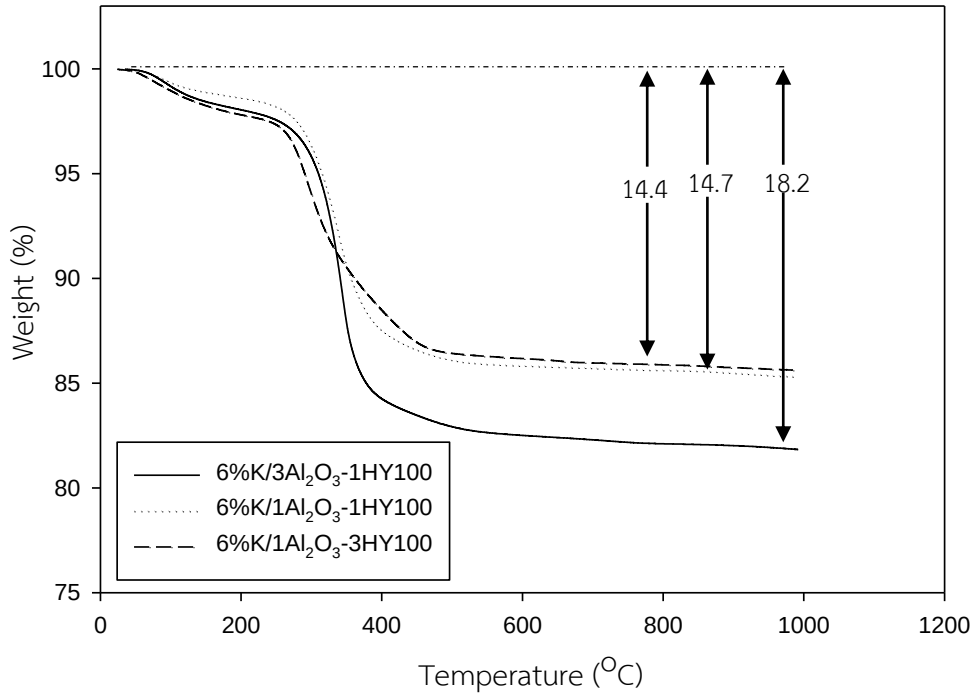

Figure 4.30 TGA results of spent 6%K/Al_2O_3-HY100 zeolite with different Al_2O_3 and HY100 zeolite ratios (3:1, 1:1 and 1:3) after 180 min of reaction.

4.3.2 Activity in lactic acid dehydration reaction

The activity of 6%K/Al_2O_3-HY100 zeolite with different Al_2O_3 and HY100 zeolite ratios (3:1, 1:1 and 1:3) were test in lactic acid dehydration reaction. The catalyst 0.1 g was packed in glass reactor with quartz wool and preheated at 340 °C for 30 min. After that, the lactic acid solution with concentration 34%volume were injected into the vaporizer at flow rate 1 ml/h and the vapor was carried through the catalyst bed by nitrogen. The gas products were analyzed by GC with a DB-WAX capillary column and FID detector.

The lactic acid conversion and product selectivity in lactic acid dehydration reaction at reaction temperature 340 °C and 90 min are shown in Figure 4.31 and Table 4.15. The lactic acid conversion of 6%K/Al_2O_3-HY100 zeolite with different Al_2O_3 and HY100 zeolite ratios (3:1, 1:1 and 1:3) were shown 100% and acrylic acid selectivity were ranged between 6.4-22.7%, in the following order: 6%K/1Al_2O_3-3HY100 zeolite > 6%K/1Al_2O_3-1HY100 zeolite > 6%K/3Al_2O_3-1HY100 zeolite. The 6%K/1Al_2O_3-3HY100 zeolite catalyst was the best for lactic acid dehydration with 100% conversion and 22.7% selectivity for acrylic acid to compare with 6%K/1Al_2O_3-1HY100 zeolite and 6%K/3Al_2O_3-1HY100 zeolite catalyst. From table 4.15, it also seen that with decreasing the Al_2O_3 content, the formation of acetaldehyde is obviously suppressed with its selectivity decreasing from 84.3% to 67.6% and AA selectivity increasing from 6.4% to 22.7%. From NH_3-TPD result, there is a tendency that the fractions of medium and strong acid sites increase with increasing Al_2O_3 content in 6%K/Al_2O_3-HY100 zeolite catalyst. The decline of acetaldehyde selectivity should be ascribed to decrease strong acid site of 6%K/Al_2O_3-HY100 zeolite as shown in NH_3-TPD result. For 6%K/3Al_2O_3-1HY100 zeolite catalyst, the acrylic acid selectivity decreased, indicating that the catalyst with high Al_2O_3 content is liable to cause damage of its structure, high strong acid site and high coke deposition resulted in the blocking and packing of the micro channel, which is in agreement with XRD, NH_3-TPD and TGA results. The catalytic results indicated that 6%K/Al_2O_3-HY100 zeolite with high Al_2O_3 content had increased strong acid site. Also, the catalysts with high strong acid sites can catalyze lactic acid dehydration to undesirable products such as acetaldehyde.

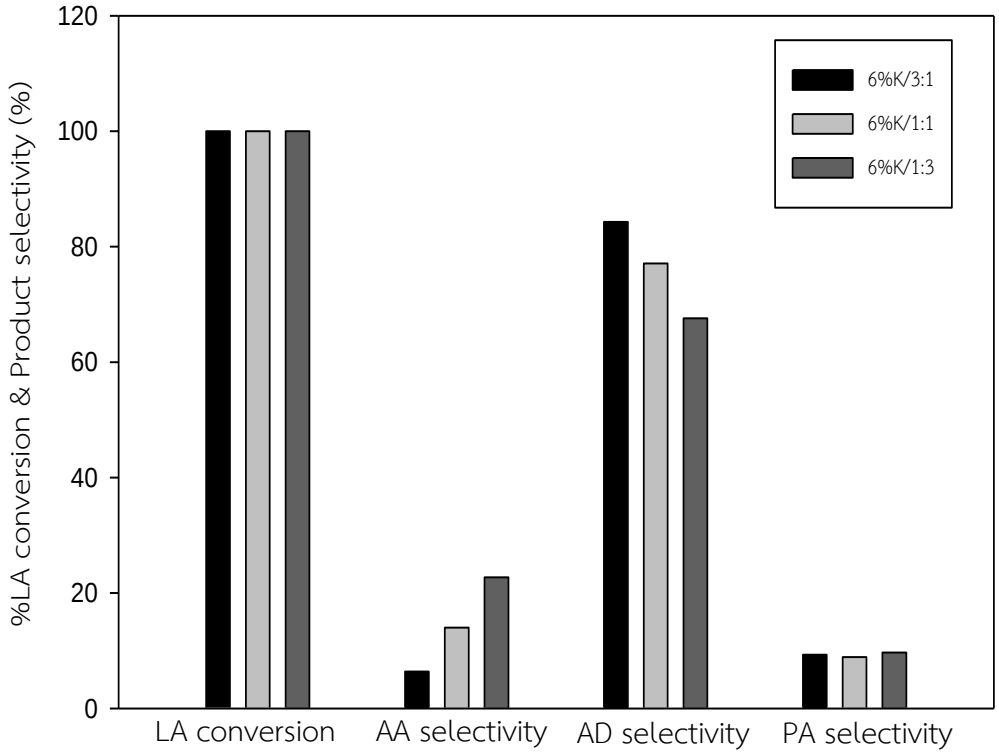

Figure 4.31 Lactic acid conversion and product selectivity of 6%K/Al_2O_3-HY100 zeolite with different Al_2O_3 and HY100 zeolite ratios (3:1, 1:1 and 1:3) at reaction temperature 340 ℃ and t = 90 min.

Table 4.15 The catalytic performance of 6%K/Al_2O_3-HY100 zeolite with different Al_2O_3 and HY100 zeolite ratios (3:1, 1:1 and 1:3).

Catalysts	Lactic acid Conversion (%)	Product Selectivity [a] (%)		
		AA	AD	PA
6%K/3Al_2O_3-1HY100	100	6.4	84.3	9.3
6%K/1Al_2O_3-1HY100	100	14.0	77.1	8.9
6%K/1Al_2O_3-3HY100	100	22.7	67.6	9.7

[a] AA-Acrylic acid, AD-acetaldehyde, PA-propionic acid. Reaction time 90 min, T=340℃

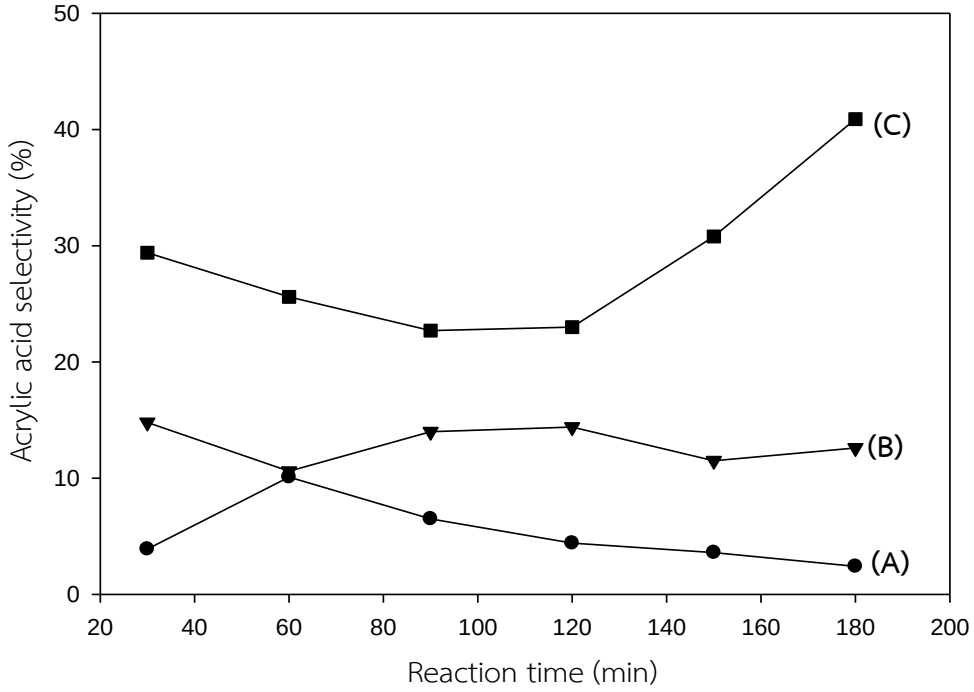

Figure 4.32 Acrylic acid selectivity of (A) 6%K/3Al_2O_3-1HY100, (B) 6%K/1Al_2O_3-1HY100, and (C) 6%K/1Al_2O_3-3HY100 at T = 340 °C.

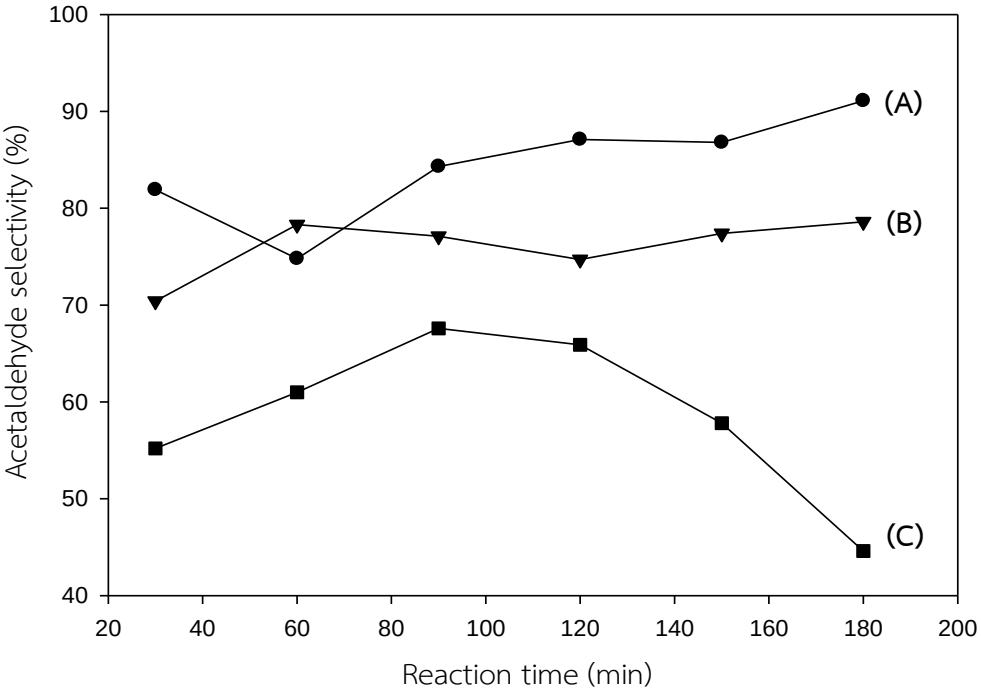

Figure 4.33 Acetaldehyde selectivity of (A) 6%K/3Al_2O_3-1HY100, (B) 6%K/1Al_2O_3-1HY100, and (C) 6%K/1Al_2O_3-3HY100 at T = 340 °C.

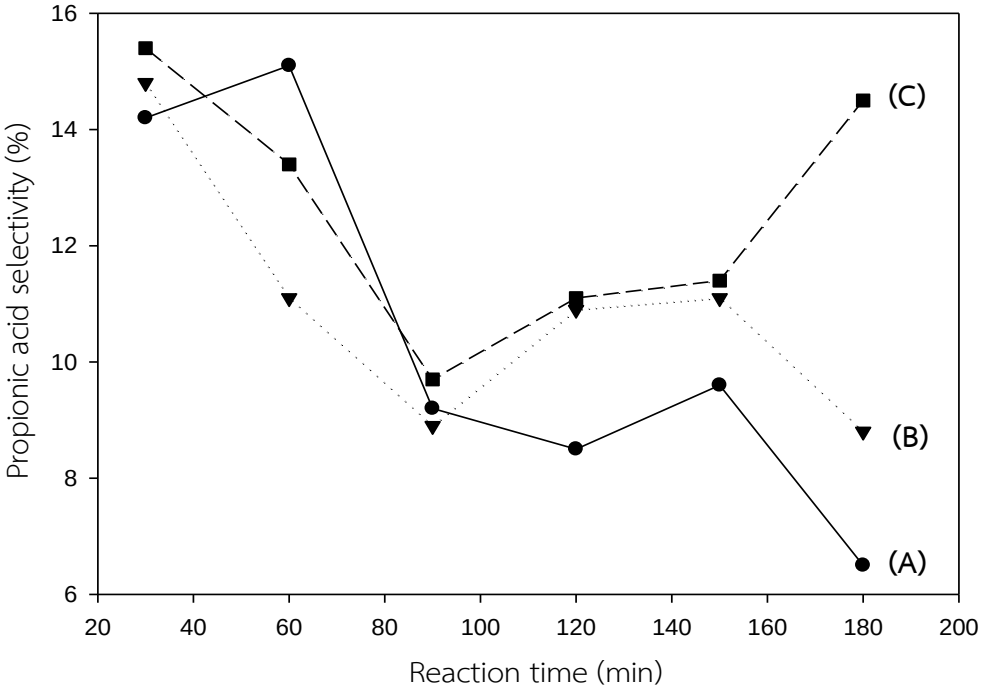

Figure 4.34 Propionic acid selectivity of (A) 6%K/3Al_2O_3-1HY100, (B) 6%K/1Al_2O_3-1HY100, and (C) 6%K/1Al_2O_3-3HY100 at T = 340 °C.

CHAPTER V
CONCLUSIONS AND RECOMMENDATION

5.1 Conclusion

In this study, the effect of different percent loading of K over HY100 zeolite catalysts at 0, 2, 4, 6 and 8 wt.%. Among these catalysts, HY zeolite modified with potassium at 6 wt.% was selected to study the effect of different Si/Al molar ratio of HY zeolite (15, 100 and 500) in 6 wt.% of K over HY zeolite catalysts were investigated. After that, HY zeolite with Si/Al molar ratio of 100 was selected to study effect of Al_2O_3-HY100 zeolite with different Al_2O_3 and HY100 zeolite ratios (3:1, 1:1 and 1:3) modified with potassium 6 wt.%. The results can be concluded as follows:

1. The catalytic results indicated that potassium modification could improve acrylic acid selectivity and reduce acetaldehyde selectivity. The catalyst modified with high potassium loading is liable to cause damage of its structure and high carbon deposition resulted in the decreasing selectivity of acrylic acid. The 6%K/HY100 zeolite catalyst was the best for lactic acid dehydration with 100% conversion and 45.5% selectivity for acrylic acid.
2. The 6%K/HY15 zeolite catalyst has more formation of acetaldehyde than other catalyst because the catalyst with lower the Si/Al molar ratio should be ascribed to high total acidity. On the other hand, the 6%K/HY500 zeolite catalyst affected the decrease selectivity of acrylic acid and increase selectivity to propionic acid due to the catalyst have highest total basicity and very low acidity on surface. The catalytic results indicated that the HY100 zeolite catalyst should suitable Si/Al molar ratio for catalyze lactic acid dehydration to acrylic acid.

3. The catalyst with high Al_2O_3 content is liable to cause damage of its structure, high coke deposition and high amount of strong acid sites. The catalysts with high strong acid sites can catalyze lactic acid dehydration to undesirable products such as acetaldehyde.

5.2 Recommendations

1. Study stability in long term of catalysts for lactic acid dehydration reaction.
2. Study the catalytic performance in different calcination temperature of catalyst that is the one factors of influence the activity of reaction.
3. Study the catalytic performance in different preparation of catalyst.

REFERENCES

[1] Lin, M.M. Selective oxidation of propane to acrylic acid with molecular oxygen. Applied Catalysis A: General 207(1) (2001): 1-16.

[2] Boesel, L.F. and Reis, R.L. A review on the polymer properties of Hydrophilic, partially Degradable and Bioactive acrylic Cements (HDBC). Progress in Polymer Science 33(2) (2008): 180-190.

[3] Bernkop-Schnürch, A. Thiomers: a new generation of mucoadhesive polymers. Advanced drug delivery reviews 57(11) (2005): 1569-1582.

[4] Mizuno, N., Tateishi, M., and Iwamoto, M. Pronounced catalytic activity of $Fe_{0.08}Cs_{2.5}H_{1.26}PVMo_{11}O_{40}$ for direct oxidation of propane into acrylic acid. Applied Catalysis A: General 128(2) (1995): L165-L170.

[5] Shiju, N.R., Liang, X., Weimer, A.W., Liang, C., Dai, S., and Guliants, V.V. The role of surface basal planes of layered mixed metal oxides in selective transformation of lower alkanes: Propane ammoxidation over surface ab planes of Mo– V– Te– Nb– O M1 phase. Journal of the American Chemical Society 130(18) (2008): 5850-5851.

[6] Lin, M.M. Complex metal-oxide catalysts for selective oxidation of propane and derivatives: I. Catalysts preparation and application in propane selective oxidation to acrylic acid. Applied Catalysis A: General 250(2) (2003): 305-318.

[7] Botella, P., Nieto, J.L., Solsona, B., Mifsud, A., and Márquez, F. The preparation, characterization, and catalytic behavior of MoVTeNbO catalysts prepared by hydrothermal synthesis. Journal of Catalysis 209(2) (2002): 445-455.

[8] Zhang, J., Zhao, Y., Pan, M., Feng, X., Ji, W., and Au, C.-T. Efficient Acrylic Acid Production through Bio Lactic Acid Dehydration over NaY Zeolite Modified by Alkali Phosphates. ACS Catalysis 1(1) (2011): 32-41.

[9] Gunter, G.C., Langford, R.H., Jackson, J.E., and Miller, D.J. Catalysts and supports for conversion of lactic acid to acrylic acid and 2,3-pentanedione. Industrial & engineering chemistry research 34(3) (1995): 974-980.

[10] Tam, M.S., Gunter, G.C., Craciun, R., Miller, D.J., and Jackson, J.E. Reaction and spectroscopic studies of sodium salt catalysts for lactic acid conversion. Industrial & engineering chemistry research 36(9) (1997): 3505-3512.

[11] Varadarajan, S. and Miller, D.J. Catalytic Upgrading of Fermentation-Derived Organic Acids. Biotechnology progress 15(5) (1999): 845-854.

[12] Corma, A. Inorganic solid acids and their use in acid-catalyzed hydrocarbon reactions. Chemical Reviews 95(3) (1995): 559-614.

[13] Maher, K. and Bressler, D. Pyrolysis of triglyceride materials for the production of renewable fuels and chemicals. Bioresource Technology 98(12) (2007): 2351-2368.

[14] Helwani, Z., Othman, M., Aziz, N., Fernando, W., and Kim, J. Technologies for production of biodiesel focusing on green catalytic techniques: a review. Fuel Processing Technology 90(12) (2009): 1502-1514.

[15] Williams, B., Babitz, S., Miller, J., Snurr, R., and Kung, H. The roles of acid strength and pore diffusion in the enhanced cracking activity of steamed Y zeolites. Applied Catalysis A: General 177(2) (1999): 161-175.

[16] Weitkamp, J. Zeolites and catalysis. Solid State Ionics 131(1) (2000): 175-188.

[17] Kim, S.D., Baek, S.C., Lee, Y.-J., Jun, K.-W., Kim, M.J., and Yoo, I.S. Effect of γ-alumina content on catalytic performance of modified ZSM-5 for dehydration of crude methanol to dimethyl ether. Applied Catalysis A: General 309(1) (2006): 139-143.

[18] Serrano-Ruiz, J.C. and Dumesic, J.A. Catalytic upgrading of lactic acid to fuels and chemicals by dehydration/hydrogenation and C–C coupling reactions. Green Chemistry 11(8) (2009): 1101-1104.

[19] Culp, A., Holmes, K., Nagrath, R., and Nessenson, D. Propane to Acrylic Acid. (2013).

[20] Holmen, R.E. Production of acrylates by catalytic dehydration of lactic acid and alkyl lactates. 1958, Google Patents.

[21] Fan, Y., Zhou, C., and Zhu, X. Selective Catalysis of Lactic Acid to Produce Commodity Chemicals. Catalysis Reviews 51(3) (2009): 293-324.

[22] Mok, W.S.L., Antal Jr, M.J., and Jones Jr, M. Formation of acrylic acid from lactic acid in supercritical water. The Journal of Organic Chemistry 54(19) (1989): 4596-4602.

[23] Sugiyama, S., et al. Vapor-Phase Oxidation of Ethyl Lactate to Pyruvate over Various Oxide Catalysts. Bulletin of the Chemical Society of Japan 66(5) (1993): 1542-1547.

[24] Gunter, G.C., Miller, D.J., and Jackson, J.E. Formation of 2, 3-pentanedione from lactic acid over supported phosphate catalysts. Journal of Catalysis 148(1) (1994): 252-260.

[25] Benjelloun, H., Rochex, A., Lecouturier, D., Dechemi, S., and Lebeault, J.-M. An on-line technique for monitoring propionic acid fermentation. Applied microbiology and biotechnology 68(3) (2005): 316-321.

[26] Cortright, R., Sanchez-Castillo, M., and Dumesic, J. Conversion of biomass to 1, 2-propanediol by selective catalytic hydrogenation of lactic acid over silica-supported copper. Applied Catalysis B: Environmental 39(4) (2002): 353-359.

[27] Katryniok, B., Paul, S., and Dumeignil, F. Highly efficient catalyst for the decarbonylation of lactic acid to acetaldehyde. Green Chemistry 12(11) (2010): 1910-1913.

[28] Cicero, J.A., Dorgan, J.R., Garrett, J., Runt, J., and Lin, J. Effects of molecular architecture on two-step, melt-spun poly (lactic acid) fibers. Journal of Applied Polymer Science 86(11) (2002): 2839-2846.

[29] Cho, J.-Y., Iverson, C.N., and Smith, M.R. Steric and chelate directing effects in aromatic borylation. Journal of the American Chemical Society 122(51) (2000): 12868-12869.

[30] Davis, K. Material Review: Alumina (Al_2O_3). School of Doctoral Studies European Union Journal (2) (2010).

[31] Santos, P.S., Santos, H.S., and Toledo, S. Standard transition aluminas. Electron microscopy studies. Materials Research 3(4) (2000): 104-114.

[32] Virta, R.L. Zeolites. US Geological Survey Minerals Yearbook-2002 (2002): 84.1-84.4.

[33] Hriljac, J., Eddy, M., Cheetham, A., Donohue, J., and Ray, G. Powder neutron diffraction and 29 Si MAS NMR studies of siliceous zeolite-Y. Journal of Solid State Chemistry 106(1) (1993): 66-72.

[34] Park, C. and Keane, M.A. Gas phase dehydration of C 6 alcohols promoted by Y zeolite and supported nafion catalysts. Journal of Molecular Catalysis A: Chemical 166(2) (2001): 303-322.

[35] Wells, R.P., et al. Dehydration of butan-2-ol using modified zeolite crystals. Applied Catalysis A: General 182(1) (1999): 75-84.

[36] Yan, J., Yu, D., Sun, P., and Huang, H. Alkaline Earth Metal Modified NaY for Lactic Acid Dehydration to Acrylic Acid: Effect of Basic Sites on the Catalytic Performance. Chinese Journal of Catalysis 32(3-4) (2011): 405-411.

[37] Teas, J., Pino, S., Critchley, A., and Braverman, L.E. Variability of iodine content in common commercially available edible seaweeds. Thyroid 14(10) (2004): 836-841.

[38] Sun, P., Yu, D., Tang, Z., Li, H., and Huang, H. NaY zeolites catalyze dehydration of lactic acid to acrylic acid: studies on the effects of anions in potassium salts. Industrial & engineering chemistry research 49(19) (2010): 9082-9087.

[39] Korotcenkov, G. Handbook of Gas Sensor Materials: Properties, Advantages and Shortcomings for Applications Volume 2: New Trends and Technologies. Springer Science & Business Media, 2013.

[40] Innocenzi, P., Zub, Y.L., and Kessler, V.G. Sol-gel methods for materials processing. Vol. 1, 2008.

[41] Wang, H., Yu, D., Sun, P., Yan, J., Wang, Y., and Huang, H. Rare earth metal modified NaY: Structure and catalytic performance for lactic acid dehydration to acrylic acid. Catalysis Communications 9(9) (2008): 1799-1803.

[42] Sun, P., et al. Potassium modified NaY: A selective and durable catalyst for dehydration of lactic acid to acrylic acid. Catalysis Communications 10(9) (2009): 1345-1349.

[43] Yan, J., Yu, D., Li, H., Sun, P., and Huang, H. NaY zeolites modified by La^{3+} and Ba^{2+}: the effect of synthesis details on surface structure and catalytic

performance for lactic acid to acrylic acid. Journal of Rare Earths 28(5) (2010): 803-806.

[44] Zhang, J., Feng, X., Zhao, Y., Ji, W., and Au, C.-T. Sodium nitrate modified SBA-15 and fumed silica for efficient production of acrylic acid and 2,3-pentanedione from lactic acid. Journal of Industrial and Engineering Chemistry 20(4) (2014): 1353-1358.

[45] Tang, C., Peng, J., Fan, G., Li, X., Pu, X., and Bai, W. Catalytic dehydration of lactic acid to acrylic acid over dibarium pyrophosphate. Catalysis Communications 43 (2014): 231-234.

[46] Blanco, E., Delichere, P., Millet, J.M.M., and Loridant, S. Gas phase dehydration of lactic acid to acrylic acid over alkaline-earth phosphates catalysts. Catalysis Today 226 (2014): 185-191.

[47] Matsuura, Y., Onda, A., Ogo, S., and Yanagisawa, K. Acrylic acid synthesis from lactic acid over hydroxyapatite catalysts with various cations and anions. Catalysis Today 226 (2014): 192-197.

[48] Yuan, C., Liu, H., Zhang, Z., Lu, H., Zhu, Q., and Chen, Y. Alkali-metal-modified ZSM-5 zeolites for improvement of catalytic dehydration of lactic acid to acrylic acid. Chinese Journal of Catalysis 36(11) (2015): 1861-1866.

[49] Echeandia, S., et al. Enhancement of phenol hydrodeoxygenation over Pd catalysts supported on mixed HY zeolite and Al_2O_3. An approach to O-removal from bio-oils. Fuel 117 (2014): 1061-1073.

[50] Storck, S., Bretinger, H., and Maier, W.F. Characterization of micro-and mesoporous solids by physisorption methods and pore-size analysis. Applied Catalysis A: General 174(1) (1998): 137-146.

[51] Yan, B., Tao, L.Z., Liang, Y., and Xu, B.Q. Sustainable production of acrylic acid: alkali‐ion exchanged beta zeolite for gas‐phase dehydration of lactic acid. ChemSusChem 7(6) (2014): 1568-1578.

[52] Zhang, X., Lin, L., Zhang, T., Liu, H., and Zhang, X. Catalytic dehydration of lactic acid to acrylic acid over modified ZSM-5 catalysts. Chemical Engineering Journal 284 (2016): 934-941.

[53] Groen, J., Peffer, L.A., Moulijn, J., and Pérez-Ramí, J. On the introduction of intracrystalline mesoporosity in zeolites upon desilication in alkaline medium. Microporous and Mesoporous Materials 69(1) (2004): 29-34.

APPENDIX

APPENDIX A

CALCULATION FOR CATALYST PREPARATION

A.1 Preparation of the mixed Al_2O_3 and HY zeolite by sol-gel method

The preparation of Al_2O_3-HY100 zeolite with different Al_2O_3 and HY100 zeolite ratios (3:1, 1:1 and 1:3) by sol-gel method are shown as follow:

Example The calculation for the preparation of $3Al_2O_3$-1HY100 zeolite by sol-gel method are shown as follow:

Reagent:	HY zeolite	Si/Al molar ratio = 100
	Aluminum isoproproxide (>98%)	Molecular weight = 204.24 g/mol
	Ethanol (99%)	Molecular weight = 46 g/mol
	Deionized water	Molecular weight = 18 g/mol
	Hydrochloric acid (37.7%)	Molecular weight = 36.46 g/mol

Calculation: For Al_2O_3-HY100 zeolite ratio 3:1

Based on 15 g of Aluminum isoproproxide

So, HY100 = 15 g / 3

= 5 g

For molar ratio of Al_2O_3:H_2O = 0.1:15

Aluminum isoproproxide = 0.1 mol

= 0.1 mol x 204.24 g/mol

= 20.424 g

H_2O = 15 mol

= 15 mol x 18 g/mol

= 270 g

Required aluminum isoproproxide = 15 g

So required H_2O = (15 g x 270 g)/20.424 g

= 198.3 g

For volume ratio of H_2O:Ethanol = 1:1

Density of H_2O = 1 g/cm^3

H_2O = 198.3 g x 1 g/cm^3

So required ethanol = 198.3 cm^3

In case of Al_2O_3-HY100 zeolite with different Al_2O_3 and HY100 zeolite ratios (3:1, 1:1 and 1:3), the method of preparing uses the same calculation.

A.2 Preparation of HY zeolite and Al_2O_3-HY100 zeolite modified with potassium by incipient wetness impregnation method

Example The preparation of 6%K/HY100 zeolite catalyst by incipient wetness impregnation method are shown as follow:

Reagent: Potassium nitrate Molecular weight = 101.10 g/mol

Potassium Molecular weight = 39 g/mol

Calculation: Based on 1 g of catalyst, 6%K/HY100 zeolite catalyst contains 10 wt.% metal.

So, K = 0.06 g

HY100 zeolite required = 1-0.06 g = 0.94 g

6%K/HY100 zeolite catalyst were prepared using KNO_3 as metal precursors.

$$KNO_3 \text{ required} = \frac{\text{K required x MW of } KNO_3}{\text{MW of K x 0.99}}$$

$$= \frac{0.06 \text{ g x } 101.1 \text{ g/mol}}{39 \text{ g/mol x } 0.99}$$

$$= 0.157 \text{ g of } KNO_3$$

A.3 Calculation of lactic acid concentration before driven through the reactor

- Mole of N_2: n_{N2} = PV/RT = (2 bar x 0.04 L/min) / (0.08314 L.bar/K.mol x 303 K)

n_{N2} = 0.0032 mol/min

- Mole of LA: n_{LA} = (0.34 ml/h x 1.209 g/ml) / (60 min/h x 90.08 g/mol)

n_{LA} = 0.000076 mol/min

- Mole of H_2O: n_{H2O} = (0.66 ml/h x 1 g/ml) / (60 min/h x 18 g/mol)

n_{H2O} = 0.00061 mol/min

So, Concentration of lactic acid before and after vaporization are (0.000076 / 0.000686) = 0.11 = 11 mol.% and (0.000076 / 0.003886) = 0.02 = 2.0 mol.%, respectively.

APPENDIX B
CALIBRATION CURVES

The calibration curves are used for calculation the mole of lactic acid reactant, and acrylic acid as main product and byproduct include acetaldehyde, propionic acid in lactic acid dehydration reaction.

The reactant and all product gas were analyzed by gas chromatography Shimudzu, GC-14B with flame ionization detector (FID) and DB-WAX UI column.

The calibration curves exhibit area and mole of gas in x-axis and y-axis, respectively. The curves of lactic acid, acrylic acid, acetaldehyde and propionic acid are illustrated in Figure B1-B4.

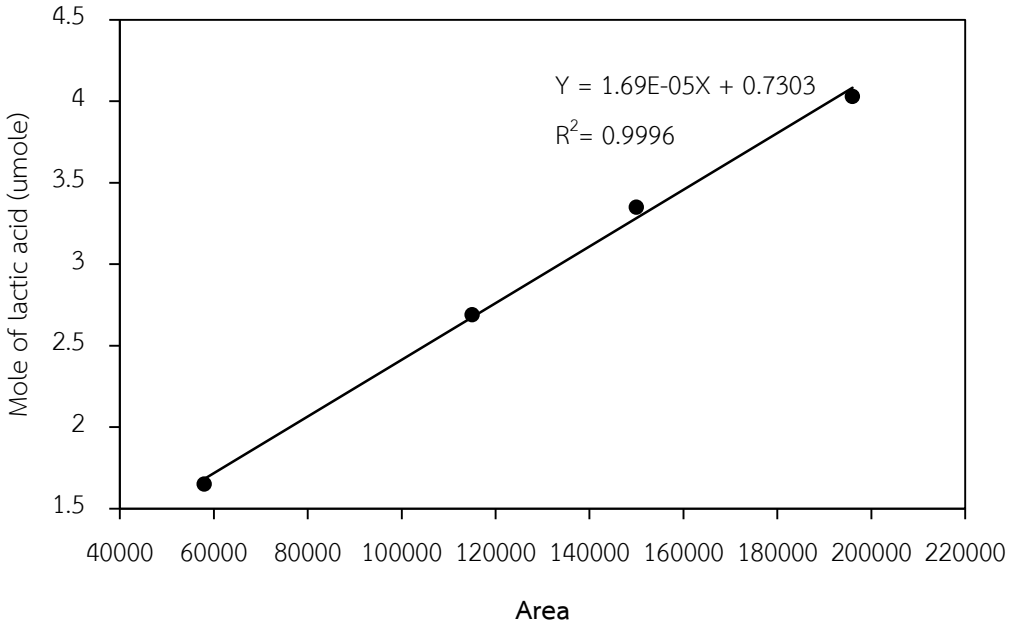

Figure B.1 The calibration curve of lactic acid

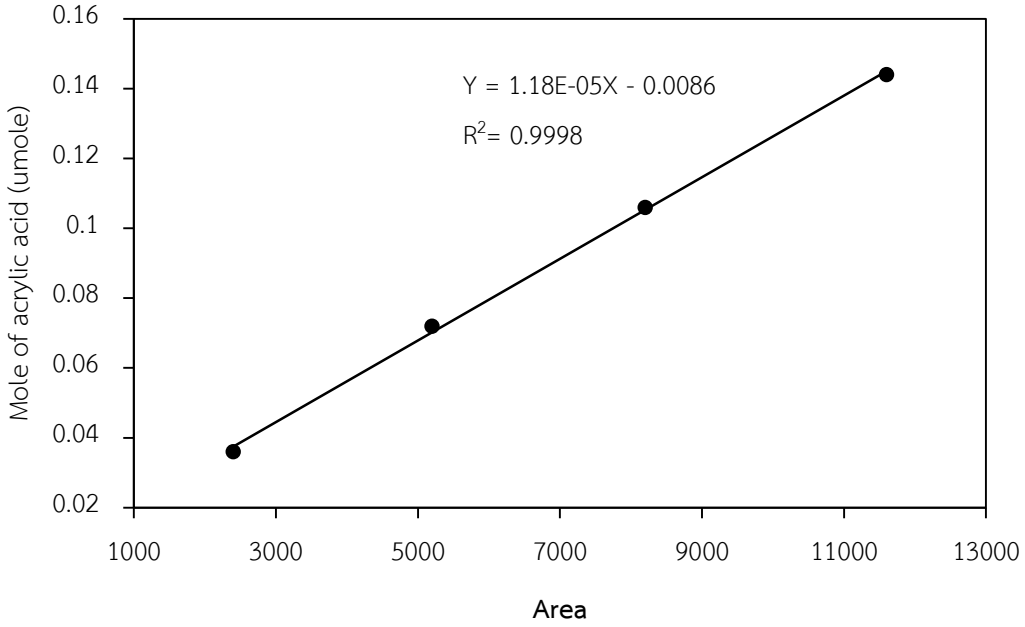

Figure B.2 The calibration curve of acrylic acid

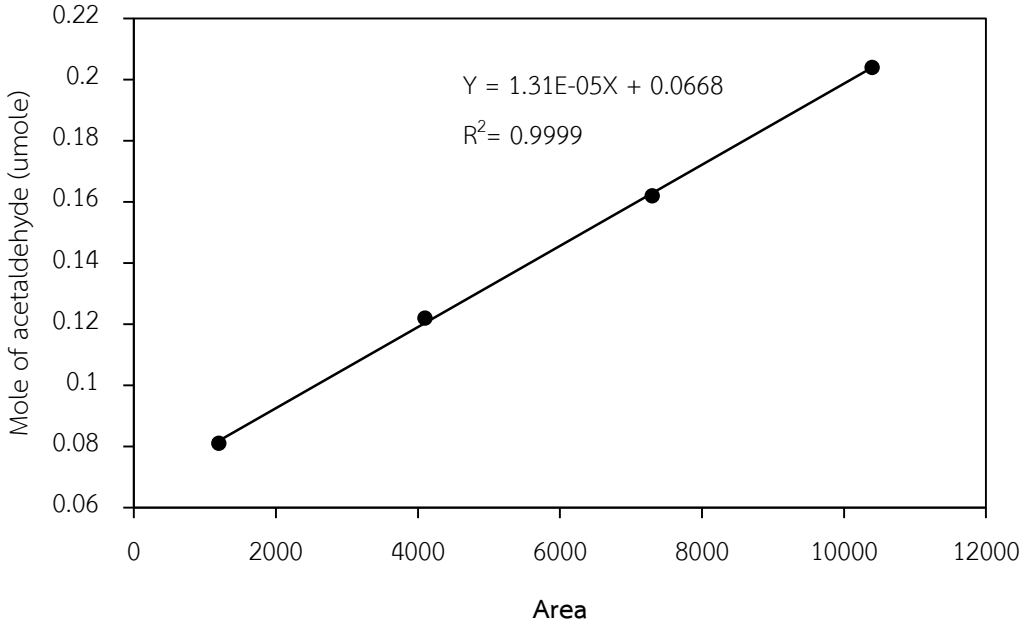

Figure B.3 The calibration curve of acetaldehyde

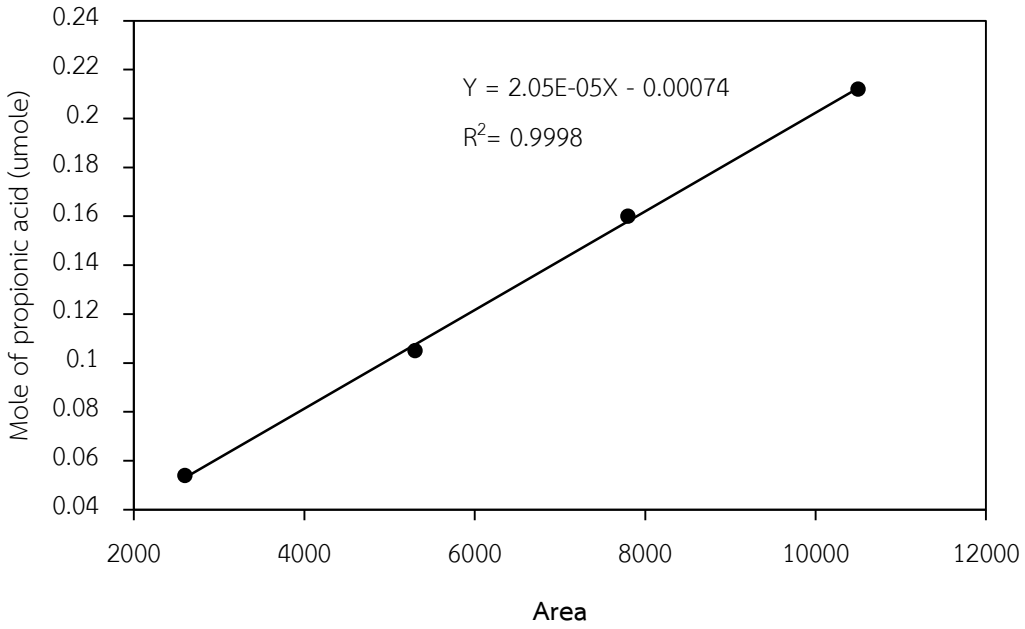

Figure B.4 The calibration curve of propionic acid

APPENDIX C

CALCULATION OF TOTAL ACID SITES OF CATALYST

Calculation of total acid sites of catalyst which were measured by Ammonia Temperature Programmed Desorption (NH_3-TPD) is shown as follows:

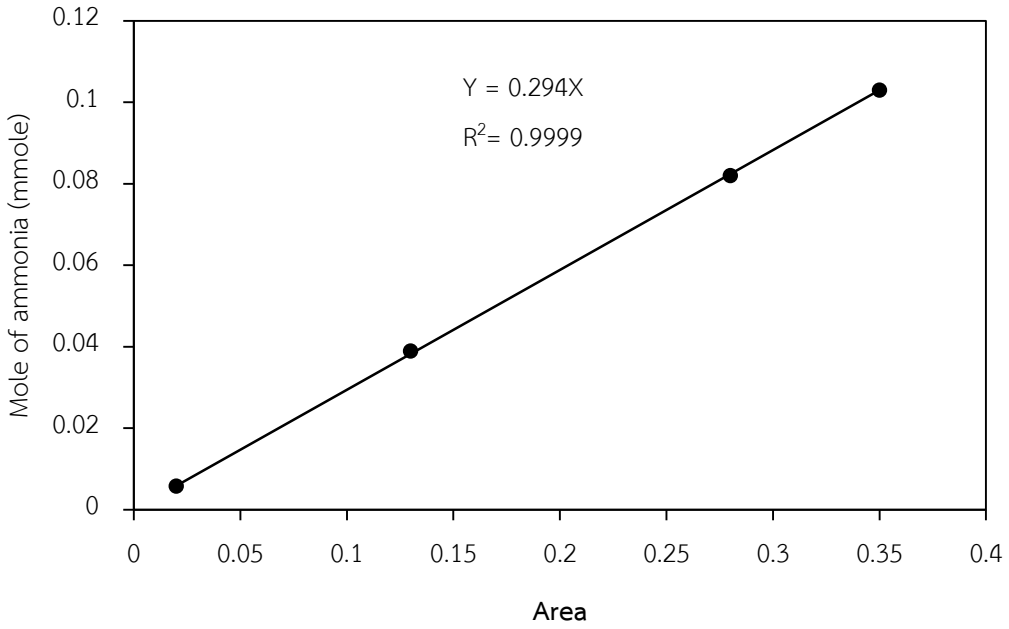

Figure C.1 The calibration curve of ammonia from Micromeritics Chemisorp 2750.

The acidity of all catalysts can be calculated from

$$\text{The acidity of catalyst} = \frac{0.294 \times \text{Area of } NH_3\text{-TPD profile}}{\text{Weight of catalyst (g)}} \quad ; \text{mmol}NH_3/\text{g catalyst}$$

APPENDIX D

CALCULATION OF TOTAL BASIC SITES OF CATALYST

Calculation of total basic sites of catalyst which were measured by Carbondioxide Temperature Programmed Desorption (CO_2-TPD) is shown as follows:

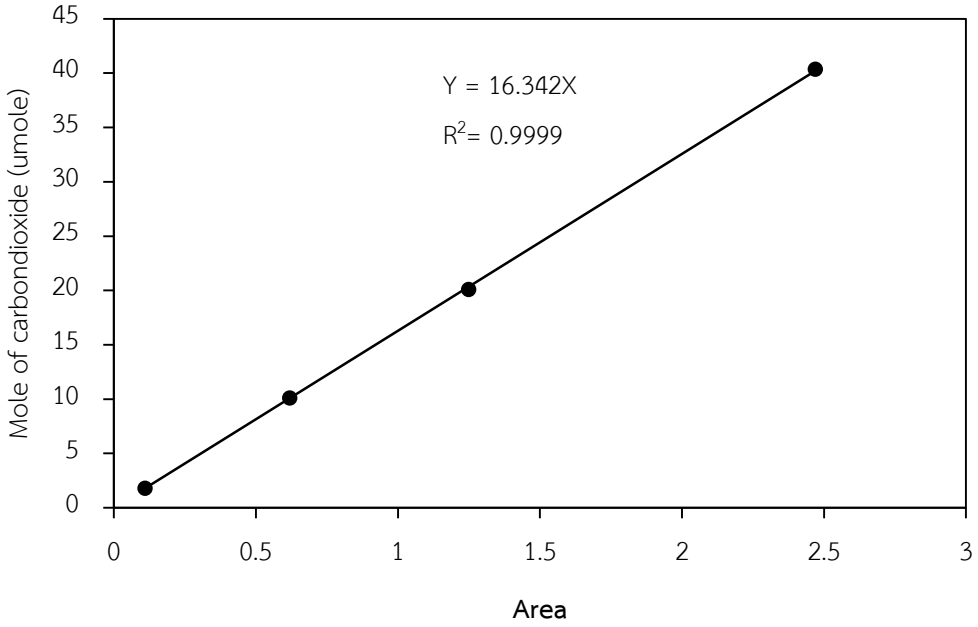

Figure D.1 The calibration curve of carbondioxide from Micromeritics Chemisorp 2750.

The basicity of all catalysts can be calculated from

$$\text{The basicity of catalyst} = \frac{16.342 \times \text{Area of } CO_2\text{-TPD profile}}{\text{Weight of catalyst (g)}} \quad ; \mu mol CO_2/g \text{ catalyst}$$

APPENDIX E

CALCULATION OF CONVERSION AND SELECTIVITY

The lactic acid conversion was calculated as defined equations as follows:

Lactic acid conversion

$$X_{LA}\,(\%) = \frac{\text{Area of lactic acid in feed - Area of lactic acid in product}}{\text{Area of lactic acid in feed}} \times 100$$

The product selectivity based on mole of acrylic acid, mole of acetaldehyde, and mole of propionic acid were calculated as defined equations as follows:

Acrylic acid selectivity

$$S_{AA}\,(\%) = \frac{\text{Mole of acrylic acid in product}}{\text{Total mole of product}} \times 100$$

Acetaldehyde selectivity

$$S_{AD}\,(\%) = \frac{\text{Mole of acetaldehyde in product}}{\text{Total mole of product}} \times 100$$

Propionic acid selectivity

$$S_{AA}\,(\%) = \frac{\text{Mole of propionic acid in product}}{\text{Total mole of product}} \times 100$$

Total mole of product are the summation of mole of acrylic acid, mole of acetaldehyde, and mole of propionic acid.

VITA

Mr. Natthapong Satitpoom was born on November 18, 1991 in Trang province, Thailand. He finished high school from Ayutthaya Witthayalai School in 2010, and graduated in bachelor's degree from Faculty of Engineering and Industrial Technology in Petrochemical and Polymeric Material, Silpakorn University of Sanam Chandra Palac Campus, Nakornpathom province, Thailand in April 2014. He continued to study in Master's degree of Chemical Engineering, faculty of Engineering, Chulalongkorn University, Thailand in August 2014.

List of publication:

Natthapong Satitpoom, and Suphot Phatanasri, "The effect of potassium addition on acidity of Y-zeolite catalysts", proceeding of the Pure and Applied Chemistry International Conference 2017 (PACCON), Bangkok, Thailand, Feb. 2-3, 2017.